Rheological Properties of Peanut Paste and Characterization of Fat Bloom Formation in Peanut-Chocolate Confectionery

Vinodini Immanuela Buck

Dissertation submitted to the faculty of the Virginia Polytechnic Institute and State University in partial fulfillment of the requirements for the degree of

Doctor of Philosophy
in
Food Science & Technology

Sean F. O'Keefe (Chairman)
Richey M. Davis
Susan E. Duncan
Kequan Zhou

April 12, 2010
Blacksburg, Virginia

Keywords: triacylglycerols, peanuts, squeeze flow rheology, fat bloom, chocolate, sensory tests

Rheological properties of peanut paste and characterization of fat bloom formation in peanut-chocolate confectionery

Vinodini Immanuela Buck

ABSTRACT

Fat bloom in chocolates is the gray-white discoloration and dullness that can occur on the surface of the confectionery. Fat bloom is a common quality defect that can result from temperature fluctuations during storage. Chocolates candies with peanuts or other nut fillings are more prone to fat bloom compared to plain chocolates, due to a release of incompatible nut oils into the chocolate matrix. The overall goal of this study was to determine if differences in triacylglycerol (TAG) composition and rheological properties of high, medium, and normal oleic peanuts influence fat bloom formation. All three peanut varieties showed high concentrations of triolein. Normal oleic peanuts had a slightly higher trilinolein than high and medium oleic peanuts, which contained trilinolein in trace amounts. Peanut pastes from the three peanut varieties all had a minimum apparent yield stress, and all pastes showed varying degrees of shear thinning. The apparent yield stress of high and normal oleic pastes was higher than the apparent yield stress of medium oleic paste. The absolute value of the flow index behavior was 1 for the high oleic peanut paste, suggesting friction in the experimental apparatus, even with use of Teflon plates. The peanut chocolate candies took around 45 days for significant dulling of the chocolates with temperature cycling between 26-29 °C approximately every 26 hours. Optical microscopy scans showed differences in glossiness and surface textural attributes of the unbloomed and bloomed peanut chocolate confectionery. Consumer evaluation showed some differences in the glossiness and significant differences in surface texture of unbloomed and bloomed

chocolates. A majority (62%) of the survey respondents had seen whitish discoloration in chocolates and 40% of the respondents thought this is because the chocolate had grown old.

Dedicated to My Family: Vijay and Malcolm Buck (parents), Sam Buck (brother)
For their unconditional love, encouragement, and support

ACKNOWLEDGEMENTS

I would like to thank God for his guiding grace. I would like to thank my advisor Dr. Sean O'Keefe for his support and encouragement. Thank you for all that you have taught me both as a student and as a friend. Thank you to Dr. Richey Davis for all his support and encouragement and especially for teaching me about the seemingly simple, yet highly complex field of squeeze flow rheology. I would like to thank Dr. Susan Duncan for her support, encouragement, and the opportunity to be a part of the MILES program. Thank you to Dr. Kevin Zhou for his support, encouragement and commitment to the completion of my degree. Thank you to Harriet Williams for learning with me how to fix instruments and also teaching me how to use so many instruments. Thank you to Dr. W. Keith Ray for his assistance with MALDI-TOF/MS analysis. Thank you to all my friends in the MILES program and Food Science department, especially to Robert Moore, for all the good times. Best of luck to all of you in your future endeavors. Thank you to the entire faculty and staff at the Virginia Tech Food Science department for their support and for always making me feel warm and welcomed. Thank you to Pastor Reggie Tuck and Blacksburg United Methodist Church for making me feel at home in Blacksburg. I will always treasure the happy memories I have of Virginia Tech.

And finally a big thank you to my dear family, especially my parents, my brother, and my Leela (dog) for believing in me and always being there for me day and night. I would like to thank Dr. Sheryl Barringer who was my Masters advisor at the Ohio State University, for inspiring me to pursue my career in food science. A special thank you to all my friends especially; Najmus Abdullah, Pradeep Gnanaprakasam, Anisha Gorty,

Sanjay Sarang, Rishi Prasad, and Swati Kanaujia for all your love, support, meaningful conversations, fun and good laughs.

TABLE OF CONTENTS

LIST OF TABLES

LIST OF FIGURES

CHAPTER 1: INTRODUCTION

1.1 Significance of fat bloom in chocolates

Chocolate has been around for ages and is undoubtedly one of the most popular confectionary products in the world. The satisfaction that the rich creamy sweet taste of chocolate gives to consumers is often considered irreplaceable by other sweets. More recently, scientific evidence suggests that moderate consumption of dark chocolate that contains flavonoids with antioxidant properties can provide numerous health benefits such as reducing the risk of inflammation and coronary heart disease (Jan Wollgast, 2000). However chocolates also contain large amounts of cocoa butter, and milk fat solids making the product very susceptible to fat bloom formation. Fat bloom is the gray-whitish discoloration on the surface of chocolates due to the formation of large imperfect fat crystals. The chocolate discoloration often leads to consumer disappointments and raises questions about the safety and quality of the products.

Cocoa butter, which constitutes a minimum 18% of the chocolate, is a mostly saturated fat that is responsible for providing the chocolate with a good texture, shine and viscosity (Lonchampt and Hartel, 2004). Cocoa butter is a well studied fat that is rich in [1,3-palmitoyl-2-oleoylglycerol (POP)], [1,3-palmitoyl-2-oleoyl-3-stearoylglycerol (POS)] and [1,3-stearoyl-2-oleoylglycerol (SOS)] triacylglycerols. The polymorphic behavior of the cocoa butter triacylglycerols was first identified by Wille and Lutton in 1966. Previous studies have shown that chocolates containing nuts are more prone to fat bloom than plain chocolates because the nuts release oil into the chocolate matrix (McCarthy and McCarthy, 2008; Khan and Rousseau, 2006). The studies conducted by McCarthy and McCarthy (2008) and Khan and Rousseau

(2006) studied the kinetics of oil release in the chocolates. A practical solution to better understanding fat bloom would be to identify differences in triacylglycerols between cocoa butter and the nut oils released.

The three different causes of fat bloom are temperature variation, incompatible fats, and improper tempering during processing (Lonchampt and Hartel, 2004; Hodge and Rousseau, 2002). Increasing temperatures to 20 °C or warmer can cause liquid triacylglycerols with solubilized high melting fractions to migrate to the surface and recrystallize upon cooling (Hodge and Rousseau, 2002). The two main theories explaining fat migration mechanisms are capillary action and simple diffusion (Aguilera and others 2004; Rousseau and Smith, 2008; Loisel and others 1997). Regardless of how the triacylglycerol migration occurs studies have not focused on how different fillings may affect the kinetics of fat bloom formation. Fillings with a high saturated fat content or fillings made with polyunsaturated fats may exhibit different rheological characteristics. Thus, it is appropriate to determine the rheological properties of peanut fillings as they can affect the kinetics of triacylglycerol migration from the center of the chocolate to the surface.

The extensive studies on fat bloom have primarily focused on fat bloom formation especially in dark chocolates because the gray discoloration associated with bloom is much more prominent in the dark chocolates than in other chocolates. Fat bloom exists in all chocolate varieties and especially those with nuts. The overwhelming popularity of milk chocolates and lack of sensory studies in determining flavor and texture quality of bloomed milk chocolates is an area still to be addressed.

1.2 Rationale and Justification

The overall goal of this study is to better understand fat bloom formation in peanut chocolates by determining the triacylglycerol composition of peanut oils, the rheological properties of peanut pastes for fillings and the consumer response to fat bloomed chocolates. By determining the triacylglycerol composition of peanut oil the role of triacylglycerols from peanut oils effect on fat bloom may be better understood. Our understanding of the rheological properties of peanut paste may allow development of fillings that may inhibit bloom formation. And lastly, determining consumer response to fat bloomed chocolates is critical to addressing why research needs to continue in this area.

1.3 Specific Objectives

1) Determine triacylglycerols profiles of high, medium and normal oleic peanut oils.

Peanut will be roasted and the oil will be extracted and analyzed using gas chromatography and mass spectrometry methods.

Null hypothesis: There are no differences in triacylglycerols composition and triacylglycerol concentration of high, medium, and normal oleic peanut oils and no differences between peanut oil triacylglycerols and cocoa butter triacylglycerols.

Alternate hypothesis: There are differences in triacylglycerol composition and triacylglycerol concentration of high, medium, and normal oleic peanut oils and differences between peanut oil triacylglycerols and cocoa butter triacylglycerols.

2) Determine the flow index and yield stress of peanut pastes using squeezing flow rheology.

Peanuts pastes will be made from high, medium and normal oleic pastes and squeezing flow rheology will be performed with the use of a lubricated system.

Null hypothesis: There are no differences in the yield stress and flow index behavior of high, medium and normal oleic peanut pastes

Alternate hypothesis: There are differences in the yield stress and flow index behavior of high, medium and normal oleic peanut pastes.

3. Determine glossiness and surface texture differences between unbloomed and bloomed commercial peanut chocolate candy bars by sensory analysis and optical microscopy. Determine the number of temperature cycling between 26 and 29 °C needed for significant bloom coverage of the chocolates.

Null hypothesis: There are no differences in the glossiness and surface texture attributes of unbloomed and bloomed commercial peanut chocolate candy bars.

Alternate hypothesis: There are differences in the glossiness and surface texture attributes of unbloomed and bloomed commercial peanut chocolate candy bars.

References

Aguilera JM, Michel M & Mayor G. 2004. Fat migration in chocolate: diffusion or capillary flow in particulate solid?-a hypothesis paper. Journal of Food Science 69(7):R167-R174.

Hodge S & Rousseau D. 2002. Fat bloom formation and characterization in milk chocolate observed by atomic force microscopy. Journal of the American Oil Chemists' Society 79(11):1115-1121.

Jan Wollgast EA. 2000. Polyphenols in chocolate: is there a contribution to human health? Food Research International 33(2000):449-459.

Khan RS & Rousseau D. 2006. Hazelnut oil migration in dark chocolate - kinetic, thermodynamic and structural considerations. European Journal of Lipid Science and Technology 108(5):434-443.

Loisel C, G GL, G P & Ollivon KM. 1997. Fat Bloom and Chocolate Structure Studied by Mercury Porosimetry. Journal of Food Science 62(4):781-788.

Lonchampt P & Hartel RW. 2004. Fat bloom in chocolate and compound coatings. European Journal of Lipid Science and Technology 106(4):241-274.

McCarthy KL & McCarthy MJ. 2008. Oil Migration in chocolate-peanut butter paste confectionary as a function of chocolate formulation. Journal of Food Science 73(6):E266-273.

Rousseau D & Smith P. 2008. Microstructure of fat bloom development in plain and filled chocolate confections. The Royal Society of Chemistry Soft Matter 4:1706-1712.

Wille R & Lutton E. 1966. Polymorphism of cocoa butter. Journal of the American Oil Chemists' Society 43(8):491-496.

CHAPTER 2: LITERATURE REVIEW

2. 1 Chocolate production and composition

Chocolates are a complex food product composed of cocoa butter, chocolate liquor, sugar, milk solids, and many more constituents. Chocolate is processed from cocoa beans. The beans are harvested from cocoa pods that grow on cocoa trees in regions near the equator (Tannenbaum, 2004). Fermentation of the pods involves harvesting of the pods, cleaning and removal of the beans, followed by storage at around 50 °C for 5-6 days (Tannenbaum, 2004). The fermentation step allows activation of the enzyme polyphenoloxidase, which reacts with oxygen to produce browning in the beans. The enzyme activation reaction releases certain sugars and acids that contribute to the flavor of chocolate (Bruinsma and Taren, 1999; Beckett, 2000). Following the fermentation step, the beans are allowed to dry and care is taken to prevent mold. Next, the beans are roasted at high temperatures for periods of thirty minutes (Tannenbaum, 2004). The roasting step allows for flavor development, loss of moisture and loosening of the husks (winnowing). The winnowing step separates the central cotyledons commonly referred to as the nib from the shell. The nib is dense and spherical in shape. Beckett discusses three types of roasting; whole bean roasting, nib roasting and liquor roasting where the steps of roasting, winnowing, and grinding are in different order. The roasting method to follow depends on factors such as the bean size, desired flavor, and the overall desired end products (cocoa butter and cocoa liquor). The grinding of the nibs produces cocoa liquor, also known as unsweetened chocolate (Tannenbaum, 2004). Applying hydraulic pressure (6,000-12,000 psi) removes cocoa butter from the cocoa liquor. The remaining portion of the cocoa liquor is referred to as cocoa powder (Chen and Mackley, 2006; Tannenbaum, 2004).

Based on the desired product, other ingredients such as milk fat, milk powder (for milk chocolate), emulsifiers, spices, sweeteners, and fat substitutes are added to the product. Conching is a two step process that first improves flavor by removing acetic acid and other volatile fatty acids from the chocolate. The second step in conching turns powdered chocolate into liquid chocolate (Beckett, 2000). Chocolates are then tempered to form βV fat crystals from cocoa butter (Lonchampt and Hartel, 2006). Tempering involves pre-crystallization of the chocolate to promote the formation of a small batch of seeds which are then added to a large batch of chocolate to promote the right crystal form βV (Beckett, 2000; Lonchampt and Hartel, 2006). The steps of tempering include erasing the temperature history of any pre-existing crystals in the chocolates by heating to 50 °C followed by cooling between 26-28 °C to induce pre-crystallization seeds and finally heating to 31-32 °C (just below the melting temperature of the βV form) to allow nucleation of the βV form (Lonchampt and Hartel, 2006). The tempering temperature is determined based on achieving the formation of proper crystallization of triacylglycerols from cocoa butter. If the chocolate are tempered improperly (lack of tempering, over tempering, or use of improper temperature) the results is fat bloom formation (Rousseau and Smith, 2008; Kinta and Hattia, 2005; Lonchampt and Hartel, 2006). Lack of tempering or over tempering involves not having the right concentration of seed crystals for nucleation of the entire chocolate mass (Lonchampt and Hartel, 2006).

Generally, chocolate does not contain butter fat due to the liquid state of the fat at room temperature. White Chocolate contains no dark cocoa. It is made simply from sugar, milk powder and cocoa butter (Beckett, 2000). Milk chocolate is the most consumed chocolate in much of the world due to the softer texture and creamy taste. According to the code of federal regulations, Title 21, section 163.30, milk chocolate cannot contain less than 12 % of those

ingredients specified as milk solids (FDA, 2005). The process of producing chocolate is complicated. The relationship between time and temperature are critical factors that can affect the polymorphic characteristics of the fat present in the product.

Chocolate is an extremely popular product. Maintaining the product quality is essential for chocolate manufacturers to continue to compete for consumer loyalty. The average consumer may lack sufficient knowledge to know the cause behind fat bloom that results in discoloration of the product. The gray discoloration or whitish haze that results from fat bloom can lead to questions regarding the safety and quality of the product.

2.2 Peanuts

Peanuts (*Arachis hypgaea L*) come in four main varieties: Runner, Virginia, Spanish, and Valencia (Horn and others 1999; Knauft and others 1987). Peanuts are used in many products such as snacks, peanut butter, cooking oil and confectionaries. Runners are the most common nuts used in products such as peanut butter (Knauft et al., 1987). Besides being a popular snack peanuts are also considered to be beneficial to human health due to their low levels of saturated fatty acids (Isanga and Zhang, 2007). Peanut seeds contain about 40-50% oil (Davis and others 2008; Isanga and Zhang, 2007). Peanut oil contains bioactive compounds such as tocopherols and phytosterols (Isanga and Zhang, 2007). It is estimated that half of all peanuts produced are crushed for peanut oil (Isanga and Zhang, 2007). The high oleic acid content of some varieties improves the oxidative stability of peanuts and their products (Isleib and others 2006; O'Keefe and others 1993; Knauft et al., 1987; Patterson and others 1996).

Peanuts that are termed high oleic are composed of 74-84% oleic fatty acid as compared to peanuts that are termed normal oleic peanuts, which have approximately 50% oleic fatty acids

(Knauft et al., 1987). Davis and Sanders (2007) found that high oleic peanut oils have lower crystallization temperature than normal oleic peanut oil. Davis (2007) describes this finding as being caused by the increased viscosity which limits structural formation of the crystal network (Davis and Sanders, 2007). However, there is not much difference in the structure of the two fatty acids, and this crystallization difference would most likely arise due to positioning of the fatty acids on the triacylglycerol molecule and stacking arrangement of the triacylglycerols. Little research has looked at the triacylglycerol composition of peanut oils. Singleton and Pattee (1987) identified the major triacylglycerols (without stereospecific analysis) in normal oleic peanuts as being OLL, OOL, POL and PLL with P=palmitic acid, O=oleic acid, and L=linoleic acid.

Peanut butter is a popular filling used in confectionary products. Peanut butter naturally separates by gravity into an oil phase and a solid phase. During storage, temperature affects the separation and texture of peanut butter. Hinds (1994) was able to reduce separation of oil from peanut butter with addition of un-hydrogenated palm oil, although hydrogenated or partially hydrogenated oils are commonly used commercially for this purpose (Hinds and others 1994).

2.3 Triacylglycerols

Triacylglycerols complex together to form crystal structures. They compose 95-98% of most oils (Wiesman and Chapagain, 2009). Triacylglycerol analysis provides information about the physical properties of fats and oils. Figure 2.1 shows the structure of a triacylglycerol which consists of 3 fatty acids that are attached to a glycerol compound via esters. The complex nature of triacylglycerol is the result of a combination of fatty acids arrangement differing in chain length, degree of unsaturation, *cis* and *trans* arrangement of the fatty acid bonds, and distribution

between the sn-1, sn-2, sn-3 (sn=stereospecific numbering) position on the glycerol backbone (K.Sato, 2001; Lawler and Dimick, 2008). The structure of triacylglycerols is in the shape of a tuning fork and the packing arrangement of one triacylglycerol with another triacylglycerol is what determines the overall properties of the fat (Lawler and Dimick, 2008). The bilayer arrangement of the triacylglycerol is the most common arrangement for monoacidic triacylglycerols. The trilayer arrangement is a complex arrangement that arises due to differences in fatty acids in the sn-2 position. The fatty acid in the sn-2 position can be a *cis*-unsaturated fatty acid ester, or a fatty acid that is different by four or more units in length, or it can be a saturated acyl ester with unsaturated fatty acids in the sn-1 and sn-3 position (Lawler and Dimick, 2008). Predicting the fatty acid distribution in the triacylglycerol is complicated especially since animal and plants lipids differ. Determining the fatty acids in the different positions can be done using pancreatic lipase to hydrolyze the fatty acid at the sn-2 position followed by gas chromatography and Grignard degradation to determine distribution at the sn-1 and sn-3 positions (Lawler and Dimick, 2008). Figure 2.2 is reprinted from Chemical Engineering Science, Vol. 56/Issue 7, K. Sato, Crystallization behaviour of fats and lipids -- a review, 2255-2265, 2001 with permission from Elsevier. Figure 2.2 shows the tuning fork structure of triacylglycerols and the bilayer and trilayer arrangement of the triacylglycerols. The more saturated the fat the more solid the fat is at room temperature and thus is termed as having a high melting fraction, the reverse is true of unsaturated fats with are generally liquid at room temperature and are termed as low melting fractions. The subshell of the packing arrangement gives useful information about the crystallization properties of fats, adulteration of oils, and compatibility among fats. Three main triacylglycerol crystal structures have been identified; α, β', and β (Larsson, 1966; Lutton, 1972). Larrson (1966) describes the three packing

arrangements of the subshell according to spacing lines as determined by X-ray diffraction. X ray diffraction still remains one of the most popular instruments of choice for characterization of the different crystal arrangements. Triacylglycerol compositions have been linked to numerous different melting behaviors within a crystal networks (Narine and Marangoni, 1999; Loisel and others 1998).

2.3.1 Triacylglycerol analysis

Current methods of triacylglycerol analysis include the use of chromatography instruments such as high pressure liquid chromatography (HPLC) and gas chromatography (GC). Both instruments can be coupled with a mass spectrometer (MS). Chromatographic techniques can separate triacylglycerols according their molecular size and/or degree of unsaturation (Laakso, 2002). Mass spectrometry is a powerful technique that can provide structural information such as the connectivity of atoms in a molecule (Glish and Vachet, 2003).

2.3.2 Gas chromatography (GC)

A very high temperature is required to make the triacylglycerols volatile to pass through the GC. Capillary columns coated with a very polar stationary phase such as cyanopropyl polysiloxane, which are often used for fatty analysis, cannot withstand the high temperature needed for triacylglycerol analysis (Buchgraber and others 2004). The type of injection can be cold on column or vaporized (split/splitless). The injection type can be applied and modified as need to get the best peak separation. The drawback of a cold on column injection means a lower column temperature which can affect separation, but this can be resolved by cooling the fist few centimeters of the column with compressed air and later shutting of the air supply to rapidly

increase the column temperature. A DB5-HT (5%-phenyl 95%-dimethylpolysiloxane high temperature) capillary non polar column equipped with a flame ionization detector can be used. The use of a more polar column with 50-65% phenyl groups addition can create even better separation (Buchgraber et al., 2004). The flame ionization detector is a universal detector for most GC analysis. GC on a polar stationary phase allows separation according to increasing acyl carbon number (ACN) and degree of unsaturation (Buchgraber and others 2000; Andrikopoulos and others 2001; Laakso, 2002). As the degree of unsaturation increases, the polarity of the triacylglycerols also increase. Separation of triacylglycerols by GC may be difficult because many triacylglycerols can have the same ACN. Gas chromatography identification relies on retention time matching. GC-MS generally utilizes electron ionization mass spectrometry which can help identify fatty acids, but not their positional distribution (Laakso, 2002). There are many GC parameters such as column type (polarity, length, age) injection mode, and air flow that can affect the separation of triacylglycerols.

2.3.3 Reversed phase high performance liquid chromatography

Generally reversed phase high performance liquid chromatography (RP-HPLC) with a nonpolar stationary phase and polar mobile phase is used for separation of triacylglycerols. HPLC separates triacylglycerols according to equivalent carbon number (ECN) (Buchgraber et al., 2004). ECN is calculated according to the following equation:

$$ECN=CN-2(DB)$$

where CN is the carbon number and DB is the number of double bonds.

However, in a mixture of triacylglycerols this can lead to co-elution. A bonded C18 silica column is known to show high separation and acetone/acetonitrile are considered good solvents

for the mobile phase (Buchgraber et al., 2004). The acetone assists in separation of crucial triacylglycerols and acetonitrile interacts with *pi* bonds of the double bonds of unsaturated species (Buchgraber et al., 2004). Reversed phase HPLC has disadvantages over GC because triacylglycerol do not have strong chromophoric components (Buchgraber et al., 2000). HPLC equipped with a refractive index detector or an evaporative light scattering detector would be preferred (Buchgraber et al., 2000). The refractive index detectors measures change in the refractive index of the mobile phase due to dissolve analytes (Rounds and Gregory, 2003). The evaporative light scattering detector detects beams of scattered light from non-volatile analytes (after the solvent is evaporated by spraying the mobile phase into a heated air stream)(Rounds and Gregory, 2003).

2.3.4 Mass spectrometry

Mass spectrometry generates ions that can be used to determine structure. Mass spectrometers consists of three parts: the ionization source, the mass analyzer and the detector (Glish and Vachet, 2003). New mass spectrometry technologies used for triacylglycerol analysis include electrospray ionization, matrix assisted time of flight (MALDI-TOF/MS), and tandem mass spectrometry (MS/MS) (Glish and Vachet, 2003).

Electrospray ionization generates vaporized charged droplets. The charged droplets consist of both solvent and analyte molecules with positive or negative charges. When the ion become free of the solvent they make their way to the mass analyzer (Glish and Vachet, 2003).

Matrix assisted laser desorption/ionization time of flight mass spectrometry (MALDI-TOF/MS) is a soft ionization technique allowing analysis of intact biomolecules and synthetic polymers that have an extremely broad mass range. MALDI-TOF/MS allows for rapid data

acquisition, and easy instrument maintenance (Glish and Vachet, 2003). Limitations of MALDI-TOF/MS include analysis of volatile and low molecular weight compounds. The matrix used for MALDI produces a lot of low mass peaks often masking the signal of the molecules of interest. This however is not an issue with triacylglycerols, which are the main molecules of interest in fats and oils. The MALDI-TOF/MS requires the sample to be mixed with a highly absorbing matrix compound and spotted onto a special MALDI plate. The matrix is selected based on type of the sample (Ex: proteins, carbohydrates, polymers). Once the solvent has evaporated, the matrix and sample mix produce a crystalline structure. The ionization mechanism involves the laser being pulsed onto the sample and the transfer of energy (protons) from the matrix causing desorption and ionization of the analyte molecules (Duncan and others 2008). The vaporized molecules travel down a flight tube to the detector. The detector records the time of flight (TOF) which separates based on differences in velocities of ions which are then used to calculate the *(m/z)* ratio according to the following equation:

$$(m/z) = 2t^2K/L^2$$

t is the drift time, L is the drift length, K is the kinetic energy of ion, m is the mass of ion, z is number of charges on ion

In reflectron TOF mode, the ions travel down one flight tube and are then reflected by a mirror down a second flight distance to compensate for differences in velocities of ions with the same *(m/z)* ratio.

Tandem mass spectrometry utilizes MS/MS techniques. MS/MS is a multi stage process, the first step results in isolation of parent ions with specific mass to charge ratio. The parent ions are then involved in a chemical reaction that changes the parent ions mass or charge to make product ions (Glish and Vachet, 2003).

2.4 Fat crystal structure and mechanical properties

The fat crystal structure is determined by triacylglycerol composition and is critical to sensory attributes such as mouthfeel, texture, and spreadability (Narine and Marangoni, 1999). Crystallinity of fats is affected by chain length and degree of saturation. Predicting the crystal structure that will form from triacylglycerol packing is difficult and complicated. Three main triacylglycerol crystal structures have been identified; α, β', and β (Larsson, 1966; Lutton, 1972). The difference between these structures lies in the difference in the subcell structure which determines cross-sectional packing of the hydrocarbon chains. In α, the chain axes are randomly aggregated, in the β' the pattern is perpendicular with one row of axes facing in the opposite direction of the subsequent row (orthorhombic) and in β all axes are in the same direction (triclinic, parallel) (Lutton, 1972). Figure 2.3 is reprinted from Chemical Engineering Science, Vol. 56/Issue 7, K. Sato, Crystallization behaviour of fats and lipids -- a review, 2255-2265, 2001 with permission from Elsevier. The figure shows that the subshell which undergoes polymorphism is a cross section of the aliphatic chains. As mentioned earlier, the structure of triacylglycerols is in the shape of a tuning fork and the packing of one triacylglycerol with another triacylglycerol is what determines the overall properties of the fat. When triacylglycerol molecules come together with different crystalline packing different polymorphs form (Narine and Marangoni, 1999). Triacylglycerol compositions have been linked to numerous different melting behaviors within a crystal networks (Narine and Marangoni, 1999). It is a theory that fat crystal networks grow as liquid triacylglycerols melt and re-crystallize into particular polymorphic states (Sonwai and Rousseau, 2010; Loisel et al., 1998). Heat transfer can cause growth aggregation of the crystal networks from microscopic to macromolecule size (Narine and

Marangoni, 1999). This growth known as polymorphism can occur during the tempering steps of the chocolate manufacturing or during the storage of chocolates.

2.5 Cocoa butter

Cocoa butter is a yellow color vegetable fat extracted from cocoa liquor after high pressure processing. Cocoa butter is the main ingredient in chocolate that gives the confectionary a rich and creamy texture (Chen and Mackley, 2006). Cocoa butter is composed mainly of monounsaturated triacylglycerides (Loisel et al., 1998). The TAGs are composed of 26 % palmitate (C16:0), 34 % stearate (C18:0), and 35 % oleate (C18:1ω9), fatty acid arrangements (Hodge and Rousseau, 2002; Beckett, 2000). Specifically [1,3-palmitoyl-2-oleoylglycerol (POP)], [1,3-palmitoyl-2-oleoyl-3-stearoylglycerol (POS)] and [1,3-stearoyl-2-oleoylglycerol (SOS)] (Loisel et al., 1998). Polyunsaturated TAG correspond to about 13 % TAG content and trisaturated TAG correspond to approximately 3% TAG content in cocoa butter (Loisel et al., 1998).

Polymorphism of cocoa butter is due to the different lateral packing of the fatty acid chains and longitudinal stacking of molecules in the lamellae (Narine and Marangoni, 1999; Loisel et al., 1998; Beckett, 2000). The cocoa butter used in chocolates are polymorphic with six basic forms I , II, III, IV, V, VI with three different crystal packing arrangements α, β', and β (Loisel et al., 1998). The melting temperature (t_m) of the different forms influences the tempering temperature during chocolate processing. The melting temperature of the forms were determined by Wille and Lutton (1966). Generally forms I (t_m=16.5 °C), II (t_m=20.4 °C) have α arrangement, and forms III (t_m=22.5 °C) and IV (t_m=25.6 °C) are β' (Wille and Lutton, 1966). Forms V (t_m=37.0 °C) and VI (t_m=37.0 °C) have β arrangements and are considered to be more

stable as they take longer to form (Wille and Lutton, 1966). Of the two β structures, the most stable crystal structure is the β-VI form. However, the β-V crystals are the desired form in chocolate as their size is generally less than 5 μm in size (Rousseau and Smith, 2008).

2.6 Fat bloom and causes

A chocolate that undergoes fat bloom is marked with loss of glossiness and appearance of white discoloration. The visible discoloration associated with bloom formation is due to the larger crystal spiky structure that can reflect light. There are several different theories that attempt to explain the cause of fat bloom. These theories include improper tempering of the chocolate during processing, addition of incompatible fats to cocoa butter and incorrect storage at warm temperature (Minifie, 1989).

Tempering of chocolate as discussed earlier is a process of using mechanical manipulation and temperature control to force chocolate into one particular crystalline form so that when it is molded it forms a smooth shiny surface. The β-V form is the desired crystal structure of cocoa butter in properly tempered chocolates but fat bloom can cause formation of the β-VI form. It is important to address that the β-VI form is associated with bloom formation, but not necessarily a factor causing the gray discoloration characteristic of bloom (Bricknell and Hartel, 1998). When poor tempering of chocolates occurs the cocoa butter crystallizes in β-IV form. Upon cooling during storage the crystals polymorph into the β-V form but are visible as bloom (Hodge and Rousseau, 2002).

Addition of incompatible fats can cause separation due to a difference in melting points between the fats. Fats are composed of a combination of triacylglycerols and many of these triacylglycerols have different melting profiles. Some triacylglycerols have more saturated fatty

acids and have higher melting temperatures than unsaturated fats. Fats that are can cause bloom formation due to limited compatibility with cocoa butter include coconut and palm kern oil which are high in lauric (C12:0) acyl esters in their triacylglycerols (Lawler and Dimick, 2008).

Several studies have shown that incorrect storage of chocolates at warm temperatures causes lipid segregation to occur in CB on cooling and/or during storage (Ali and others 2001; Loisel et al., 1998). At warm temperatures oil viscosities decrease resulting in faster migration ((McCarthy, 2008). Slight temperature changes of ($\pm$ 1 to 3 ^{o}C) can initiate fat bloom.

2.6.1 Evaluation of fat bloomed chocolates

Common techniques that have been applied to study crystallization events include differential scanning calorimetry (DSC), x-ray diffraction (XRD), and various forms of microscopy such as atomic force (AFM), scanning electron (SEM), and environmental scanning electron (ESEM). Other novel techniques include magnetic resonance imaging (MRI), nuclear magnetic resonance (NMR), and mercury porosity. Differential scanning calorimetry (DSC) is a popular thermal analysis technique that is used to measure endothermic and exothermic transitions of a material as a function of temperature. DSC compares the difference in heat flow rate of the sample of interest to that of an inert reference as a function of time and temperature. Possible measurements include endothermic processes due to heating, such as T_g (glass transition temperature), melting and evaporation, or exothermic processes due to cooling, such as material crystallization, curing (cross-linking), oxidation, etc (Lopez and others 2006). From the melting curve the solid fat index at a particular temperature can also be analyzed (Lopez et al., 2006).

X-ray diffraction of a crystalline material results in coherent x ray scattering. Coherent scattering is determined by diffraction patterns of light by wide angle measurements and

incoherent scattering by small angle measurements (Stevens, 1999). Wide angles consist of a concentric cone created by crystal planes and small angle scatter patterns are diffused (Stevens, 1999). This is a particularly popular instrument for measuring crystals growth in relation with fat bloom.

AFM is a microscopy technique that uses a sharp vibrating probe with a tip size of <50 nm to scan a sample surface at a distance over which atomic forces act. The forces between the tip and sample cause a cantilever to deflect from its intense range of oscillation. A photo detector measures this deflection, and from this information a 3-dimensional map of the sample topography can be created (Hodge and Rousseau, 2002).

In SEM, a very fine electron incident beam scans across the surface of a sample in synchronization with the beam in a cathode-ray tube. Scattered electrons are used to produce a signal that modulates the beam in the cathode ray tube and produces an almost 3-dimensional image (Stevens, 1999). SEM studies are limited to surface topography. ESEM is used to image samples that are difficult to impossible to image in high vacuum SEMs; in situ experiments such as hydrating, dehydrating and heating samples are possible with the ESEM (Rousseau and Smith, 2008). ESEM can have up to 2 nm resolution and samples can be heated up to 1000 °C (Rousseau and Smith, 2008). The general characteristics evaluated in fat bloomed chocolates include information on surface roughness, color, and recording the number of temperature cycles needs for visible bloom formation.

Studies that have evaluated fat bloom in chocolate have focused on the effects of altering the fat composition by the use of different milk fractions and alternate fats. Lohman and Hartel (1994) studied the effects of partial replacement of cocoa butter with milk fat and slowing the growth of bloom. The examination technique employed included DSC to show how

increasing milk fat fractions shifted the melting temperature of the fat and the use of an Instron texture analyzer to determine hardness. Sonwai and Rousseau (2010) also examined the effects of adding milk fat fractions to partially replace cocoa butter by AFM microscopy. AFM was used to study surface roughness and detection of cone protrusions as bloomed advanced. Sonwai and Rousseau (2001) concluded that an optimal concentration of milk fat must be used as replacement to cocoa butter, below which concentration fat bloom is promoted due to increased cocoa butter triacylglycerol mobility.

Very few studies have evaluated sensory properties associated with fat bloom using a human panel. Ali (2001) showed that chocolates filled with palm mid fraction and desiccated coconut blend showed changes in the softness with storage temperature. Sensory evaluation showed significant dislike of color and texture of chocolates stored at 30 °C as compared to chocolates stored at 18 °C (Ali et al., 2001). The visual appearance of chocolates is the most important characteristic that influences purchases of the product. Visual appearance can be described by both color and gloss (Voltz and Beckett, 1997). Textural properties of cohesiveness, chewiness and guminess of bloomed chocolates correlated well with human sensory evaluation of hardness (Andrae-Nightingale and others 2009).

2.7 Rheology

The rheological properties of foods are very important to study, due to the significant impact on texture and quality of the foods (Fellows, 2003). Foods are considered complex systems that contain many additives such as sweeteners, gums, starches, flavor enhancers, preservatives, etc. By understanding the rheological properties of food, predicting how the food will behave during processing at different temperatures and under pressure can be simplified. For

example, homogenization in milk leads to creamier texture by reducing the size of fat globules from 4 μm to less than 1 μm (Fellows, 2003). The standard definition for rheology is the science of deformation of objects under the influence of applied forces (Fellows, 2003). A rheometer measures the response of a material to a given stress or strain. Shear is a force applied to one side of a surface in a direction parallel to the surface (Stevens, 1999). The resistance to shear is denoted as *G*, the shear modulus (Stevens, 1999). Measuring the values of *G'* (elasticity) and *G''* (viscosity) and tan sigma=*G''/G'* (a value of zero would be perfect elastic substance) the material can be termed as being more liquid or solid state. The forces are vectors characterized by both size and a direction and are calculated per unit area (ex: stress) (Vliet, 1999). When shear stress σ is applied the object will deform in shear. The shear strain rate γ will be determined by tan α, which is equal to ΔX/ΔY due to the applied stress (Vliet, 1999). Rheological behaviors can be divided into two categories viscous and elastic. Under stress, a viscous material starts to flow at a certain rate, and upon removal of the stress, the material will retain the deformed shape (Vliet, 1999). An elastic material will deform under the stress, and upon removal of the stress will return to its original shape (Vliet, 1999). A linear viscous fluid is called Newtonian and is mostly independent of shear rate. Apparent viscosity is viscosity that is dependent on the shear rate (Vliet, 1999). Non-Newtonian liquids have non linear relationship between shear stress, σ, and shear rate γ (Vliet, 1999). Foods that are classified as shear thinning such as applesauce and tomato puree, have a decrease in viscosity as shear rate increases. Shear thickening foods such as liquid chocolate and corn starch have a increase in viscosity as shear rate increases (Vliet, 1999). Yield stress is also an important parameter in rheological measurements used to define the behavior of foods. Yield stress is the applied stress required to

initiate shear flow (Campanella and Peleg, 1987a). The shear stress and strain relationship of the different semi liquid foods is showed in Figure 2.4.

A cone and plate rotation viscometer can be used to determine the behavior or liquids. In this set up, the liquid is contained between a bottom plate and cone. The cone is rotated at a constant velocity (Ω) and sheer stress and rate are calculated (Stevens, 1999). Davis and Sanders (2007) found that small differences in rheological data between high and normal oleic peanut oils was due to differences in crystallization behaviors. As previously discussed, this may be attributed to differences in arrangements of fatty acids in the TAGs of the oil. Davis and Sanders (2007) also found that high oleic oils had the highest dynamic and kinematic viscosities of oils tested at high temperatures. There has been positive correlation between the mass fraction of polyunsaturated or monounsaturated fatty acids in the oil and the melting characteristics and viscosities of vegetable oils (Fasina and others 2006).

A parallel plate set up can also be used where the material is placed between two plates. The motor applies a torque to turn the top plate at an angular frequency (radiants/second) at a constant shear or stress to generate the curves for the loss and storage moduli from which viscosity can be calculated. However, for foods that are high in fat, the rheometer is difficult to use due to problems of the specimen slipping. To overcome specimen slipping, the use of deliberately roughened plates is suggested. This can be done by applying sand paper to the plates such as done by Citerne and other (2001) to determine the rheological properties of peanut butter (Citerne and others 2001). Another method to determine rheological parameters is to use squeezing flow rheology to determine the elongational viscosity and then calculate the shear viscosity.

2.7.1 Squeezing flow viscometry

Squeezing flow viscometry can be applied to measure rheological properties of foods that are spreadable in nature. These products include tomato ketchup, mustards, mayonnaise and fruit purees. Squeezing flow viscometry produces lateral flow as a result of uniaxial compression between parallel plates (Campanella and Peleg, 2002; Campanella and Peleg, 1987a; Campanella and Peleg, 1987b). There are two main types of squeezing flow tests. The first being a constant displacement rate with the generation of force vs. height curves and the second being constant load (creep) tests with the generation of height vs. time curves (Campanella and Peleg, 2002; Campanella and Peleg, 1987b). It is important that prior to beginning the test the researcher be aware of the type of fluid (Newtonain or NonNewtonian) being tested. This information is crucial in determining the appropriate equations to be applied in order to calculate rheological properties (Campanella and Peleg, 2002; Campanella and Peleg, 1987b; Terpstra and others 2007). There are two types of flows that can be generated by squeezing flow viscosity; lubricated and frictional flow. The equations applied to determine rheological properties depends on behavior of the sample (Newtonian or NonNewtonian) as well as the finish of the plate. A smooth plate does not necessarily mean the flow is lubricated (Terpstra et al., 2007). Figure 2.5 is reprinted from Journal of Texture Studies, Vol. 28, E. Damrau and M. Peleg, Imperfect squeezing flow viscosimetry of newtonian liquids-theoretical and practical considerations, pg 187-204, 1997 with permission from John Wiley and sons. In Figure 2.5 the squeeze flow apparatus and the boundary effects of using a lubricated plates as compared to frictional plates is shown. The flow pattern can be distinguished based on the shape of the flow of the fluid upon compression (Figure 2.5). Lubricated flow can be generated when plates are lubricated with oil or are composed of Teflon material which is extremely low in viscosity.

Flow between parallel plates for Newtonian fluids is calculated by the Stefan's Equation when the diameter to height ratio is greater than 10. Newtonian fluids do not exhibit slip. The biaxial elongational visocity for Newtonian fluids is six times the Newtonian viscosity in shear (Terpstra et al., 2007). For Newtonian fluids, during non-lubricated frictional compression, the force vs. height relationship with a constant displacement rate is governed by the following equation (Campanella and Peleg, 2002; Terpstra et al., 2007; Damrau and Peleg, 1997):

$$F(t)=\frac{3\pi R^4 V(t)\mu}{2H(t)^3}$$

Equation (1)

F is the momentary force, *H* is the specimen's momentary height, R is the radius of the plate, V is compression speed and μ is the fluid shear viscosity

For Newtonian fluids, during lubricated compression, the force vs. height relationship with a constant displacement rate is governed by the following equation (Damrau and Peleg, 1997):

$$F(t)=\frac{3\pi R^2 V(t)\mu}{H(t)}$$

Equation (2)

F is the momentary force, *H* is the specimen's momentary height, R is the radius of the plate, V is compression speed, and μ is the fluid shear viscosity

For Newtonian fluids during the lubricated conditions, the absolute value of the slope is equal to 1 and for the non lubricated condition the absolute value of the slope is equal to 3 (Hoffner and others 1997; Terpstra et al., 2007; Damrau and Peleg, 1997; Suwonsichon and Peleg, 1998).

For Non-Newtonian fluids, during non-lubricated frictional flow the force height relationship with a constant displacement rate is governed by the following equation (Campanella and Peleg, 2002; Terpstra et al., 2007):

$$F(t)=[2\pi KR^{(n+3)}/\ (n+3)][(2n+1)/n)^n V^n/H(t)^{2n+1}]$$

Equation (3)

F is the momentary force, *H* is the specimen's momentary height, *K* and n are the specimen's consistency and flow index, respectively, R is the radius of the upper plate *V* is the compression speed

For Non-Newtonian fluids during lubricated flow, the force vs. height relationship with a constant displacement rate is governed by the following equation (Campanella and Peleg, 2002; Terpstra et al., 2007):

$$F(t)=3^{(n+1/2)}\pi KR^2(V/H(t))^n$$

Equation (4)

F is the momentary force, *H* is the specimen's momentary height, *K* and n are the specimen's consistency and flow index, respectively, R is the radius of the upper plate *V* is the linear velocity

For Non-Newtonian fluids in a non-lubricated set up, the slope is equal to -(2*n*+1) and for the lubricated condition the slope is equal to –*n*. The absolute value of the slope should be greater than 1 for non-lubricated flow and less than 1 for lubricated flow. Lubrication of the plates intentionally produces slip, and slip is calculated in the results (Campanella and Peleg, 1987b; Suwonsichon and Peleg, 1998). Damrau and Peleg (1997) state that irrespective of the fluid's viscosity or testing speed, the forces in lubricated flow are 50 times smaller than those in non-lubricated flow in which case slip can have a considerable impact on the measured forces. Slip can only occur during non-lubricated conditions. Some foods also exhibit self lubrication and can produce plug flow even with the use of grooved plates (frictional flow). Lorenzo and others (1998) demonstrated the self lubricating properties of tomato products using metal grooved plates and finding similar rheological properties to the similar tests done using smooth metal plates.(Lorenzo and others 1997)

For a power law fluid under lubricated conditions when the behavior of the fluid is unknown, then if the absolute slope of the log F(t) and log H (t) is less than one, the conclusion

can be the flow is lubricated and the fluid is shear thinning. If the absolute slope of the log F(t) and log H (t) is between 1.0 and 3.0 the flow can be pseudoplastic or slip (Campanella and Peleg, 2002; Damrau and Peleg, 1997). Campanella and Peleg (1987) used lubricated squeezing flow viscometry to determine the rheological characteristics of commercial peanut butter.

Imperfect squeezing flow viscometry differs from perfect squeezing flow viscometry due to the specimen being place in a shallow container such as a petri dish (Campanella and Peleg, 2002; Damrau and Peleg, 1997; Suwonsichon and Peleg, 1998). An important point to note is in imperfect squeezing flow the measured forces of squeezing flow are influenced by buoyancy. Buoyancy is measured according to the following equation:

$$B(t)= \frac{[H_{ini-} H_{(t)}]\, R^2_{container}\, R^2_{plate}\, \pi\rho g}{R^2_{container} - R^2_{plate}}$$

Equation (5)

H_{ini} is the specimen's initial height, $H_{(t)}$ is the specimen's momentary height, $R_{container}$ is the radius of the container, R_{plate} is the radius of the top plate ρ is the density of the fluid, and g is the gravitational acceleration

However, this error can be reduced if the specimen is pressed to a very small height using a large wide plate (Damrau and Peleg, 1997).

The apparent yield stress, τ_o, can be determined from squeezing flow viscometry performed at constant displacement from the residual apparent stress of the fluid at a given after it has been allowed to relax for a given time (Suwonsichon and Peleg, 1998). For a Newtonian fluid, the residual stress level would reduce to the level of the buoyancy effect. Apparent stress is calculated with the following equation:

$$\tau_o = F_{@time(t)}/\pi R^2$$

Equation (6)

F is the momentary force at time (t), R is the radius of the upper plate

Apparent yield stress is considered as a measure of consistency (Corradini and Peleg, 2005).

Lubricated flow can also be used to calculate a fluid's elongational viscosity also known as biaxial viscosity according to the following equation (Corradini and Peleg, 2005; Lorenzo et al., 1997).

$$\mu_b(t) = \frac{2F(t)H(t)}{(\pi R^2 V)}$$

Equation (7)

F is the momentary force, *H* is the specimen's momentary height, R is the radius of the upper plate *V* is the linear velocity

The elongational viscosity is dependent on the biaxial strain rate [Velocity/2Height (t)]. For Newtonian fluids the elongational viscosity is three times the shear viscosity.

Under fully lubricated conditions, squeezing flow rheology can give very useful information on the yield stress and flow behavior of power law fluids. Previous studies using lubricated squeezing flow rheology have suggested that the ideal conditions for imperfect lubricated squeeze flow include using a large diameter container and shallow amount of liquid on the bottom (Damrau and Peleg, 1997).

References

Aguilera JM, Michel M & Mayor G. 2004. Fat migration in chocolate: diffusion or capillary flow in particulate solid?-a hypothesis paper. Journal of Food Science 69(7):R167-R174.

Ali A, Selamat J, CheMan YB & Suria AM. 2001. Effect of storage temperature on texture, polymorphic structure, bloom formation and sensory attributes of filled dark chocolate. Food Chemistry 72(4):491-497.

Andrae-Nightingale LM, Lee S-Y & Engeseth NJ. 2009. Textural changes in chocolate characterized by instrumental and sensory techniques. Journal of Texture Studies 40:427-444.

Andrikopoulos NK, Giannakis IG & Tzamtzis V. 2001. Analysis of olive oil and seed oil triacylglycerols by capillary gas chromatography as a tool for the detection of the adulteration of olive oil. Journal of Chromatographic Science 39:137-144.

Beckett ST. 2000. The Science of Chocolate. Cambridge, UK: The Royal Society of Chemistry.

Bricknell J & Hartel R. 1998. Relation of fat bloom in chocolate to polymorphic transition of cocoa butter. Journal of the American Oil Chemists' Society 75(11):1609-1615.

Bruinsma K & Taren DL. 1999. Chocolate: Food or Drug? Journal of the American Dietetic Association 99(10):1249-1256.

Buchgraber M, Ulberth F & Anklam E. 2000. Comparison of HPLC and GLC techniques for the determination of the triglyceride profile of cocoa butter. Journal of Agricultural and Food Chemistry 2000(48):3359-3363.

Buchgraber M, Ulberth F, Emons H & Anklam E. 2004. Triglyceride profiling by using chromatographic techniques. European Journal of Lipid Science and Technology 106(9):621-648.

Campanella OH & Peleg M. 1987a. Determination of the yield Stress of semi-liquid foods from squeezing flow data. Journal of Food Science 52(1):214-215.

Campanella OH & Peleg M. 1987b. Squeezing flow viscosimetry of peanut butter. Journal of Food Science 52(1):180-184.

Campanella OH & Peleg M. 2002. Squeezing flow viscometry for nonelastic semiliquid foods-theory and application. Critical Reviews in Food Science and Nutrition 42(3):241-264.

Chen YW & Mackley MR. 2006. Flexible chocolate. The Royal Society of Chemistry Soft Matter 2:304-309.

Citerne GP, Carreau PJ & Moan M. 2001. Rheological properties of peanut butter. Rheologica Acta 40(1):86-96.

Corradini MG & Peleg M. 2005. Consistency of dispersed food systems and its evaluation by squeezing flow viscometry Journal of Texture Studies 36(5-6):605-629.

Davis JP, Dean LO, Faircloth WH & Sanders TH. 2008. Physical and chemical characterizations of normal and high oleic oils from nine commercial cultivars of peanuts. Journal of The American Oil Chemist Society 85:235-243.

Davis JP & Sanders TH. 2007. Liquid to semisolid rheological transitions of normal and high-oleic peanut oils upon cooling to refrigeration temperatures. Journal of American Oil Chemist Society 84:979-987.

Damrau E & Peleg M. 1997a. Imperfect squeezing flow of viscosimetry of Newtonian liquids-theoretical and practical considerations. Journal of Texture Studies 28(1997):187-204.

Duncan MW, Roder H & Hunscuker SW. 2008. Quantitative matrix-assisted laser/desorption/ionization mass spectrometry. Briefings in Functional Genomics and Proteomics 7(5):355-370.

Fasina O, Hallman H, Craig-Schmidt M & Clements C. 2006. Predicting temperature-dependence viscosity of vegetable oils from fatty acid composition. Journal of the American Oil Chemists' Society 83(10):899-903.

FDA. 2005. Code of Federal Regulations 21 Parts 100-169. In: Administration, F. a. D., editor). Washington DC: Office of the Federal Register National Archvies and Records Administration

Fellows PJ. 2003. Food Processing Technology Principles and Technology,2 ed. Boca Raton: CRC Press LLC. pg 14.

Glish GL & Vachet RW. 2003. The basics of mass spectrometry in the twenty-first century. Nature 2(1 February):140-150.

Hinds MJ, Chinnan MS & Beuchat LR. 1994. Unhydrogenated palm oil as a stabilizer for peanut butter. Journal of Food Science 59(4):816-820.

Hodge S & Rousseau D. 2002. Fat bloom formation and characterization in milk chocolate observed by atomic force microscopy. Journal of the American Oil Chemists' Society 79(11):1115-1121.

Hoffner B, Gerhards C & Peleg M. 1997. Imperfect lubricated squeezing flow viscometry for foods. Rheologica Acta 36(6):686-693.

Horn ME, Eikenberry EJ, Lanuza JER & Sutton JD, inventors. 1999. High Stability Peanut Oil. USA patent.

Isanga J & Zhang G-n. 2007. Biologically active components and nutraceuitcals in peanuts and related products: review. Food Reviews International 23:123-140.

James BJ & Smith BG. 2009. Surface structure and composition of fresh and bloomed chocolate analysed using X-ray photoelectron spectroscopy, cryo-scanning electron microscopy and environmental scanning electron microscopy. LWT - Food Science and Technology 42(5):929-937.

Jan Wollgast EA. 2000. Polyphenols in chocolate: is there a contribution to human health? Food Research International 33(2000):449-459.

K.Sato. 2001. Crystallization behaviour of fats and lipids - a review. Chemical Engineering Science 56(7):2255-2265

Kampf N & Peleg M. 2002. Characterization of chick pea (Cicer arietum L) pastes using squeezing flow viscometry. Rheologica Acta 41(6):549-556.

Khan RS & Rousseau D. 2006. Hazelnut oil migration in dark chocolate - kinetic, thermodynamic and structural considerations. European Journal of Lipid Science and Technology 108(5):434-443.

Kinta Y & Hattia T. 2005. Composition and structure of fat bloom in untempered chocolate. Journal of Food Science 70(7):S450-S452.

Knauft DA, Gorbet DW, Norden AJ & Norden CK, inventors; University of Florida Research Foundation, Inc., Gainsville, Fla., assignee. 1987. Peanut Oil From Enhanced Peanut Products. USA patent.

Laakso P. 2002. Mass spectrometry of triacylglycerols. European Journal of Lipid Science and Technology 104(1):43-49.

Larsson K. 1966. Classification of glyceride crystal forms. Acta Chemica Scandinavia 20:2255–2260

Lawler PJ & Dimick PS. 2008. Food Lipids, chemistry, Nutrition and Biotechnology. In: Akoh, C. C. & Min, D. B., editors. 3 ed. Boca Raton: CRC Press. p. 245-263.

Lipp M, Simoneau C, Ulberth F, Anklam E, Crews C, Brereton P, de Greyt W, Schwack W & Wiedmaier C. 2001. Composition of genuine cocoa butter and cocoa butter equivalents. Journal of Food Composition and Analysis 14(4):399-408.

Lohman M & Hartel R. 1994. Effect of milk fat fractions on fat bloom in dark chocolate. Journal of the American Oil Chemists' Society 71(3):267-276.

Lopez C, Briard-Bion V, Camier B & Gassi JY. 2006. Milk Fat Thermal Properties and Solid Fat Content in Emmental Cheese: A Differential Scanning Calorimetry Study. Journal of Dairy Science 89(8):2894-2910.

Loisel C, Lecq G, Ponchel G & Ollivon KM. 1997. Fat Bloom and chocolate structure studied by mercury porosimetry. Journal of Food Science 62(4):781-788.

Loisel C, Keller G, Lecq G, Bourgaux C & Ollivon M. 1998. Phase transitions and polymorphism of cocoa butter. Journal of the American Oil Chemists' Society 75(4):425-439.

Lonchampt P & Hartel RW. 2004. Fat bloom in chocolate and compound coatings. European Journal of Lipid Science and Technology 106(4):241-274.

Lonchampt P & Hartel RW. 2006. Surface bloom on improperly tempered chocolates. European Journal of Lipid Science and Technology 108(2006):159-168.

Lorenzo MA, Gerhards C & Peleg M. 1997. Imperfect squeezing Flow viscosimetry of selected tomato products. Journal of Texture Studies 28:543-567.

Lutton E. 1972. Lipid structures. Journal of the American Oil Chemists' Society 49(1): 1-9.

McCarthy KL & McCarthy MJ. 2008b. Oil Migration in chocolate-peanut butter paste confectionary as a function of chocolate formulation. Journal of Food Science 73(6):E266-273.

Meilgaard MC, Civille GV & Carr BT. 2007. Sensory Evaluation Techniques. Boca Raton: CRC press. pg 9-10.

Minifie BW. 1989. Chocolate, Cocoa, and Confectionary. 3 ed. New York: AVI. p. 904.

Narine SS & Marangoni AG. 1999. Relating structure of fat crystal networks to mechanical properties : a review. Food Research International 32:227-248.

O'Keefe S, Wiley V & Knauft D. 1993. Comparison of oxidative stability of high- and normal-oleic peanut oils. Journal of the American Oil Chemists' Society 70(5):489-492.

Patterson G, Stuart DA, Thomas P & Lehrian DW, inventors. 1996. Method for extending the shelf-life of chocolate confectionery products containing peanuts and the product produced therefrom USA patent.

Reed K, Gorbet D & O'Keefe S. 2000. Effect of chocolate coating on oxidative stability of normal and high oleic peanuts. Journal of Food Lipids 7(1):31-38.

Rounds MA & Gregory JF. 2003. Food Analysis. In: Nielsen, S., editor). New York: Kluwer Academic /Plenum Publishers. p. 468.

Rousseau D. 2006. On the porous mesostructure of milk chocolate viewed with atomic force microscopy. LWT 39:852–860.

Rousseau D & Smith P. 2008. Microstructure of fat bloom development in plain and filled chocolate confections. The Royal Society of Chemistry Soft Matter 4:1706-1712.

Sato K. 2001. Crystallization behaviour of fats and lipids -- a review. Chemical Engineering Science 56(7):2255-2265.

Singleton J & Pattee H. 1987. Characterization of peanut oil tricacyglycerols by HPLC, GLC and EIMS. Journal of the American Oil Chemists' Society 64(4):534-538.

Sonwai S & Rousseau D. 2010. Controlling fat bloom formation in chocolate - Impact of milk fat on microstructure and fat phase crystallization. Food Chemistry 119(1):286-297.

Stevens MP. 1999. Polymer Chemistry and Introduction,63-70 ed.: Oxford University Press.

Suwonsichon T & Peleg M. 1999. Rheological characterization of almost intact and stirred yogurt by imperfect squeezing flow viscometry. Journal of the Science of Food and Agriculture 79(6):911-921.

Suwonsichon T & Peleg M. 1998. Imperfect squeezing flow viscometry of mustards with suspended particulates. Journal of Food Engineering 39:217-226.

Tannenbaum G. 2004. Chocolate: a marvelous natural product of chemistry. Journal of Chemical Education 81(8):1131.

Terpstra MEJ, Janssen AM & Linden Evd. 2007. Exploring imperfect squeezing flow measurements in a Teflon geometry for semisolid foods. Journal of Food Science 72(9):E492-E502.

Isleib TG, Pattee HE, Sanders TH, Hendrix KW & Dean LO. 2006. Compositional and sensory comparisons between normal- and high-oleic peanuts. Journal of Agricultural and Food Chemistry 2006(54):1759-1763.

Vliet Tv. 1999. Rheological Classification of Foods and Instrumental Techniques for Their Study. In: Rosenthal, A. J., editor). Food Texture Measurement and Perception. Gaithersburg: Aspen Publications.

Voltz M & Beckett ST. 1997. Sensory of chocolate. The Manufacturing Confectioner February 49.

Wiesman Z & Chapagain BP. 2009. Determination of fatty acid profiles and TAGs in vegetable oils by MALDI-TOF/MS fingerprinting. p. 315-336.

Wille R & Lutton E. 1966. Polymorphism of cocoa butter. Journal of the American Oil Chemists' Society 43(8):491-496.

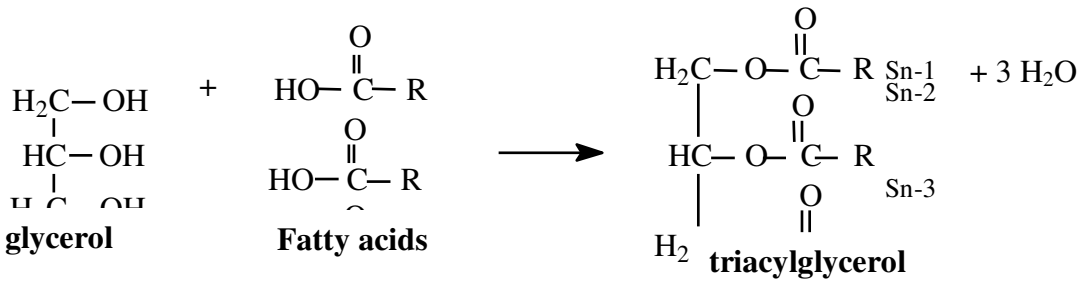

Figure 2.1: Triacylglycerol structure. A triacylglycerol forms when a glycerol molecule reacts with a fatty acid molecule (esterification reaction). Sn indicates stereospecific numbering of the position.

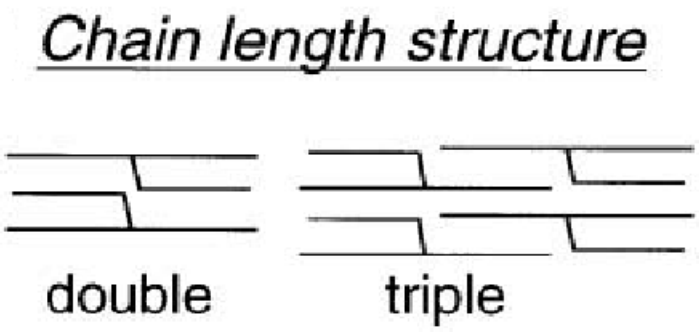

Figure 2.2: Tuning fork structure of triacylglycerols. This figure shows the bilayer and trilayer arrangement of the triacylglycerols. Bilayer structure is predominant when all the fatty are of similar chain structure where as in the trilayer structure the fatty acid located in the sn-2 position is different. Reprinted from Chemical Engineering Science, Vol. 56/Issue 7, K. Sato, Crystallization behaviour of fats and lipids -- a review, pg 2255-2265, 2001 with permission from Elsevier.

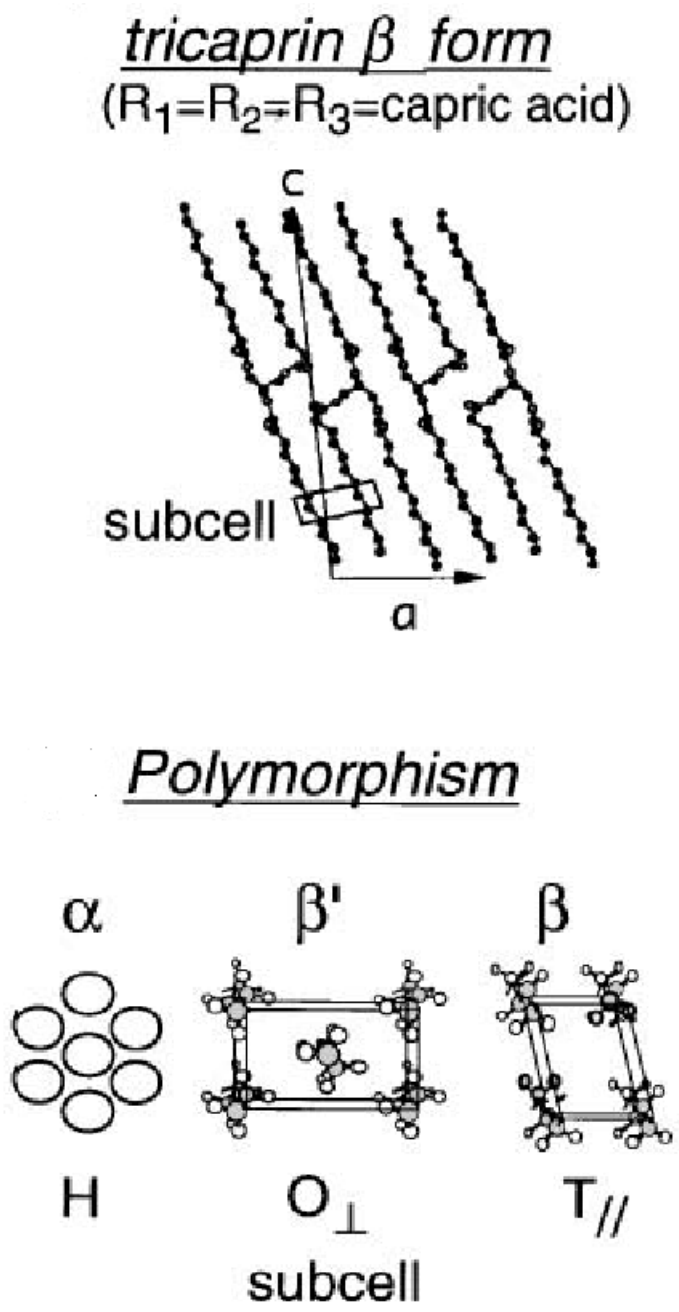

Figure 2.3: Polymorphic forms of a subshell. Reprinted from Chemical Engineering Science, Vol. 56/Issue 7, K. Sato, Crystallization behaviour of fats and lipids -- a review, pg 2255-2265, 2001 with permission from Elsevier.

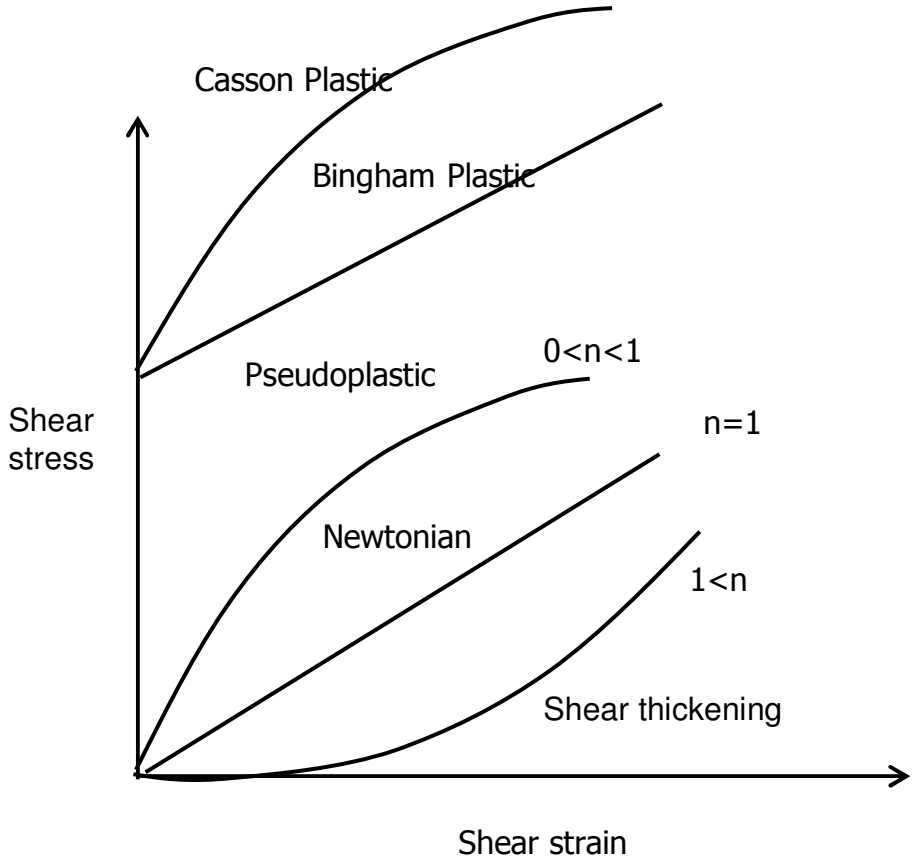

Figure 2.4: Stress and strain relationship of different fluids

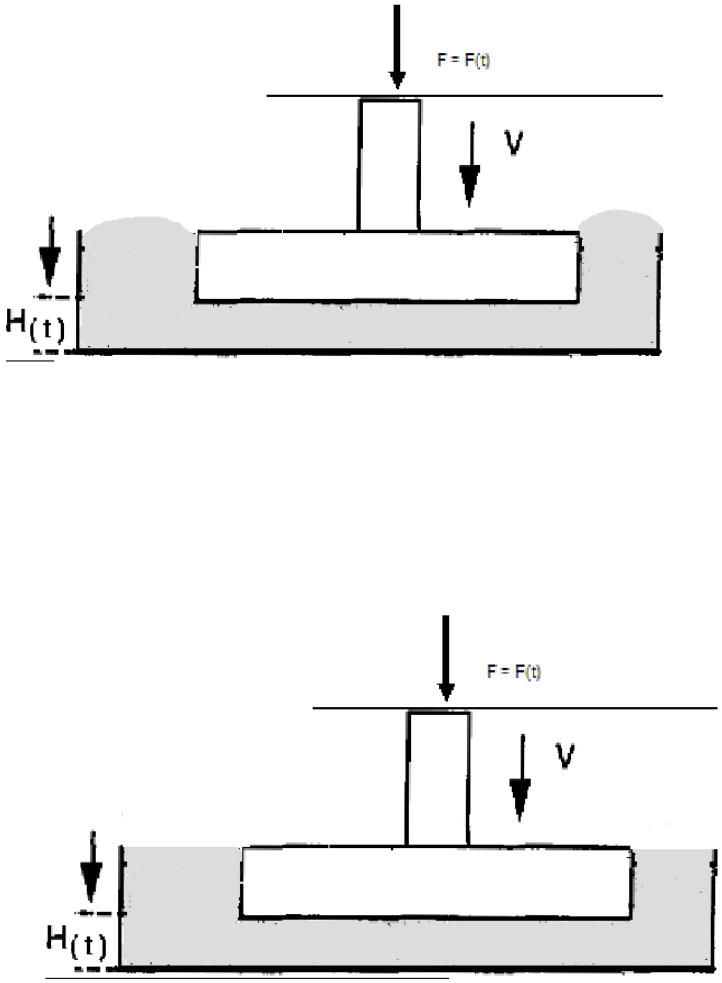

Figure 2.5. Exit flow behavior of fluid upon compression. Frictional flow due to boundary conditions created (Top). Lubricated flow no boundary conditions (Bottom). Reprinted from Journal of Texture Studies, Vol. 28, E. Damrau and M. Peleg, Imperfect squeezing flow viscosimetry of newtonian liquids-theoretical and practical considerations, pg 187-204, 1997 with permission from John Wiley and sons.

CHAPTER 3: TRIACYLGLYCEROL ANALYSIS OF HIGH, MEDIUM AND NORMAL OLEIC PEANUT OIL USING MATRIX-ASSISTED LASER DESORPTION/IONIZATION TIME OF FLIGHT MASS SPECTROMETRY

Abstract

Triacylglycerols (TAG) are large molecular weight compounds that compose 95-98% of most fats. Triacylglycerol composition greatly affects the physical properties of fats. Triacylglycerol composition of peanut oils was determined to examine their role in fat bloom crystal formation in chocolates. In this study, triacylglycerol composition of high, medium and normal oleic peanuts was examined using matrix assisted laser desorption/ionization time of flight mass spectrometry (MALDI-TOF/MS) and gas chromatography (GC). The MALDI-TOF/MS instrument provided rapid analysis and very reproducible results. Identifying peanut oil triacylglycerols by retention time matching with standards was difficult to accomplish using GC. The MALDI-TOF/MS method was able to detect more triacylglycerols species then the GC method. The major triacylglycerol species identified in all oils was triolein (OOO). Trilinoleate (LLL) species was detected in very low concentrations in the normal oleic peanut oils and the presence of LLL was not confirmed in high and medium oleic peanut oils.

Keywords: triacylglycerols, fatty acids, oleic peanut oils, MALDI-TOF/MS

3. 1 Introduction

Triacylglycerols are complex structures that vary in molecular composition because of differences in the fatty acids and positions of fatty acids on the glycerol backbone. When three fatty acids join via an esterification reaction with a glycerol compound a triacylglycerol is formed. The chain length, degree of unsaturation, and position of the fatty acids on the glycerol backbone can affect the triacylglycerol packing arrangement. Fatty acid profile analysis of oils can be easily determined by converting the fatty acids to methyl esters followed by saponification of the esters and analysis using gas chromatography/mass spectrometry. Fatty acid analysis is important to determine oxidative stability and nutritional benefits of food products. Triacylglycerol analysis is important to determine physical properties of the product.

Physical properties of oils include melting temperature, crystallization temperature, viscosity and refractive index. Crystallization of oils is a very important property of triacylglycerols that can affect fat bloom formation on chocolates. Fat bloom is the gray and white discoloration sometimes observed on the surface of chocolates. Fat bloom occurs due to liquid triacylglycerols migrating to the surface, where re-crystallization of dissolved high melting triacylglycerols can occur, causing the original crystals to polymorph into larger crystal structures. The theory behind triacylglycerol migration is often disputed as simple diffusion or migration via porous channels (Rousseau, 2006). These liquid triacylglycerols are low melting fraction triacylglycerols that mainly come from cocoa butter, but other factors such as oil release from nuts or fillings can also contribute to bloom formation. Generally, the higher the degree of unsaturation the lower the melting temperature of the fat. Three main triacylglycerol crystal structures that have been identified are α, β', and β (Larsson, 1966). The α form is considered to be the least stable form, followed by β', with β being the most stable. All crystalline structures

that form are temperature dependent, because melting and cooling causes the triacylglycerols to polymorph. This is well documented in cocoa butter (Wille and Lutton, 1966). Lopez (2006) used x-ray diffraction to record changes in milk fat fractions as triacylglycerol molecules polymorphed into different crystal structures as a function of temperature. Polymorphism is one way that unstable crystal structures transform into larger, more stable crystal structures.

Peanut paste is a popular filling choice for chocolate manufacturers. Research shows that chocolates that contain peanuts or other nut based fillings are very prone to fat bloom formation (McCarthy and McCarthy, 2008; Khan and Rousseau, 2006). This is thought to be due to the release of oil from the nuts into the surrounding chocolate matrix. Khan and Rousseau (2006) documented X-Ray diffraction spectra changes and surface topography changes using atomic force microscopy (AFM) as a result of oil release from hazelnut filling into the chocolate matrix.

Triacylglycerol analysis can be conducted using a variety of chromatographic techniques such as high performance liquid chromatography (HPLC), gas chromatography (GC), and thin layer chromatography (TLC). The HPLC and GC instruments can be equipped with a mass spectrometer. Generally an HPLC requires a evaporative light scattering detector or refractive index detector because triacylglycerols lack chromophores. The GC requires a high temperature column. However, at very high temperatures, unsaturated triacylglycerols may be lost (Buchgraber et al., 2000). Singleton and Pattee (1987) characterized triacylglycerol composition of normal oleic peanuts using HPLC for fractionation of triacylglycerols, followed by GC analysis of triacylglycerols using retention time matching with standards, and electron impact mass spectrometry of the triacylglycerol fractions. An increasingly popular mass spectrometry instrument for triacylglycerols analysis is matrix assisted laser desorption/ionization time of flight mass spectrometry (MALDI-TOF/MS).

Advantages of MALDI include soft ionization allowing analysis of intact biomolecules and synthetic polymers, broad mass range allowing analysis of a wide range of biomolecules, rapid data acquisition, and easy instrument maintenance (Glish and Vachet, 2003). Limitations of MALDI include analysis of volatile and low molecular weight compounds. The matrix used for MALDI produces a lot of low mass peaks which may often mask the signal of the molecules of interest. This is not an issue of concern in triacylglycerol analysis as the molecules of interest are above the mass range where matrix peaks can be an issue.

MALDI-TOF/MS requires the sample to be mixed with a highly absorbing matrix compound and spotted onto a special MALDI plate. The matrix is selected based on type of the sample (Ex: proteins, carbohydrates, polymers). For triacylglycerols 2,5-dihydroxybenzoic acid (DHB) has proved to be a better matrix than other matrixes such as dithranol and potassium ferrocyanide ($K_4[Fe(CN)_6]$/glycerol) (Asbury and others 1999; Wiesman and Chapagain, 2009). Once the solvent has evaporated, the mixed matrix and sample produce a crystalline structure. The MALDI-TOF/MS utilizes a nitrogen laser at 337 nm radiation. The ionization mechanism involves the laser being pulsed onto the sample and the transfer of energy (protons) from the matrix causing desorption and ionization of the analyte molecules (Duncan et al., 2008). Difference in samples may require different laser intensities to ionize the analytes. High voltage is applied to the plate to accelerate ions from the ion source into the flight tube. The vaporized molecules travel down a flight tube to the detector. Smaller molecules reach the detector faster than larger molecules as they have smaller mass to charge to charge ratio *(m/z)* (Glish and Vachet, 2003). The detector records the time of flight (TOF) which is use to calculate the *(m/z)* ratio according to the following equation:

$$(m/z) = 2t^2K/L^2$$

Equation (1)

t is the drift time, *L* is the drift length, *K* is the kinetic energy of ion, m is the mass of ion, z is number of charges on ion

TAG analysis of various oleic peanut cultivars was performed to determine differences in triacylglycerol composition of the high, medium, and normal oleic peanut varieties, and determine the role the triacylglycerols may play in fat bloom formation. Triacylglycerol analysis was primarily determined by MALDI-TOF/MS. This study also discusses triacylglycerol analysis conducted using gas chromatography and the challenge experienced.

3.2 Materials and Methods

3.2.1 Peanut oil extraction

Raw (A) medium oleic peanuts and (B) normal oleic peanuts were received as gift from the Golden Peanut Company (Alpharetta, GA). Raw high oleic peanut and (B) medium oleic and (A) normal oleic peanuts were received as a gift from Maria Balota of Tidewater Agricultural Research and Extension Center (Holland, VA). Roasted peanuts were also removed from Hershey's® Mr. Goodbar chocolates. The raw peanuts were roasted in metal pans in an electric oven at 188 °C to a Hunter lab lightness value of 50$\pm$2 as measured by a colorimeter (Minolta CHROMA METER CR-200 Osaka, Japan). Approximately 25 g of peanuts were blended (Waring Commercial Blendor, New Hartford, Connecticut) with 75 mL chloroform for 1- 2 minutes. The mixture was then filtered slowly with Whatman No. 4 paper. Approximately 50 g anhydrous sodium sulfate was added to the solvent mixture, and this was allowed to stand for 15 min. The mixture was filtered with Whatman No. 4 paper and rinsed with 10 mL chloroform.

The solvent mixture was transferred to a round bottom flask and the solvent was evaporated in a rotary evaporator (Buchi, Rotavapor R-3000, Switzerland) at 60 °C. The samples were stored at -70 °C prior to use.

3.2.2 Fatty acid analysis of peanut oils

One drop of oil (20 mg) was dissolved in 2 mL iso-octane in a 10 mL glass centrifuge tube with a Teflon-lined cap. To each sample, 100 µL of 2N KOH in methanol was added. The sample was vortexed for 60 seconds followed by several minutes rest to allow phase separation. The bottom layer was discarded, and this step was repeated with 0.5 mL saturated ammonium acetate *(aq)*. The bottom layer was discarded, and this step was repeated with 1.0 mL deionized water. The bottom layer was discarded and 0.5 g sodium sulfate was added for 5 minutes. The supernatant was then removed and placed in GC vials (Maxwell and Marmer, 1983). 1 µL of each sample was directly injected into a Shimadzu GC-17A gas chromatograph (Kyoto, Japan) coupled to a QCMS-QP5050A mass spectrometer with a split ratio of 1:20. A Supelco SP2560 (100 m x 0.25 mm i.d. x 0.25 µm film thickness) column (Bellefonte, PA) was used. The injection temperature was 270 °C, interface temperature was 230°C, and the oven was ramped from 175 °C to 240 °C at 2°C per minute and held for 20 minutes. Helium was used as the carrier gas at 1.4 mL/min. The mass spectrometer was set in scan mode for 50 m/z to 650 m/z and recorded data from 7.72 minutes to 25 minutes at a scan speed of 2000. The fatty acid analysis data are presented in Table 3.1.

3.2.3 Triacylglycerol analysis using MALDI TOF/MS

Oil samples were dissolved in hexane at approximately 1mg/mL. The matrix used in this study was 2,5-dihydroxybenzoic acid (DHB), dissolved in acetone to a concentration of 20 mg/mL. The MALDI TOF/TOF instrument (4800 series, Applied Biosystems, Foster City, CA) was calibrated using an internal standard of 250 pmoles tridecanoic acid (C13:0) (Sigma Aldrich, Germany). The oil sample was spotted on the plate, followed by the internal standard and the DHB matrix was spotted last. Each sample type (A medium, B medium, A normal, B normal, high, and Mr. Goodbar) was spotted in replicates. The plate was allowed to dry (5s) prior to analysis. The MALDI TOF/ TOF was operated in positive reflectron mode. The nitrogen laser was set at 337 nm radiations with an accelerating voltage of 20 kV. Each spectrum was internally calibrated using the internal standard peak and the spectra produced were the result of an average of 2000 laser shots.

3.2.4 MALDI-TOF/MS Spectra Analysis

Each spectrum was analyzed by deisotoping the sodium abduct using applied biosystems software. The major fatty acids of the peanut oils listed in Table 3.1 are taken into consideration to calculate the different combinations of triacylglycerols. The theoretic molecular mass of each corresponding triacylglycerol composition, given in Table 3.2, was determined by the following equation:

$$\text{Theoretical Mass} = [\text{Exact Mass}_{TAG} + Na]+$$

The mass of the sodium adduct is 22.98977 minus the mass of a proton 1.00783.

The spectra shown in Figures 3.1-3.4 show a *(m/z)* range of 850-1060, as the most prominent triacylglycerols have a mass to charge ratio within this range. Quantification of data

was performed using Excel (Microsoft, Seattle, WA). Percent compositions (calculated using relative intensity values) are expressed as the percentage of peak intensities of three measurements comprising of 2000 laser shots each of total detected TAG in the range of m/z 850-1060 of MALDI mass spectra after isotopic correction of the peaks. Data analysis was performed using one way Anova and Tukey's HSD test using JMP (JMP 8.0, 2008, SAS Institute, New Jersey, USA).

3.2.5 Triacylglycerol analysis using gas chromatography

A 1 µL sample of 0.1 % (w/v) solution of the medium and normal oil samples was dissolved in hexane (HPLC) and was injected into the gas chromatograph (Hewlett Packard 5890 series II plus). The gas chromatograph was equipped with a DB5-HT column (0.32mm x 30m x 0.1 µm) (Agilent Technologies). The injector temperature was 325 °C and the GC was run in split mode of 50:1. The oven was ramped from 150 °C to 380 °C at 20 °C /min with a hold time for 10 minutes. The total run time was 21.50 min. Standards of tritridecanoin (C13:0), trinonadecanoin (C19:0) tripalmitate (C16:0) triolein (C18:1ω9), trilinoleate (C18:2ω6), were purchased from Sigma Aldrich (St.Louis, Missouri). Peak identification was performed by matching retention time of peaks in the oil samples with the retention time of peaks from the standards. The retention time of the standards are given in Table 3.4. The GC chromatographs of the peanut oil samples are given in Figure 3.3.

3.3 Results and Discussion

3.3.1 Fatty acid analysis

The fatty acid profiling of the oil samples allows for theoretical molecular mass calculation of different triacylglycerol compositions that may be found in the actual oil samples. Peanuts that have 74-84% oleic fatty acid are considered as high oleic peanuts (Knauft et al., 1987; Davis et al., 2008; Reed and others 2000). High oleic peanuts have increased oxidative stability compared to normal oleic peanuts. The fatty acid analysis shows high oleic peanut as having approximately 76% oleic fatty acid, and medium oleic peanuts as having approximately 68- 70% oleic. Both the high and medium oleic peanut oils had oleic fatty acid contents significantly higher than normal oleic peanuts which had 53-55% oleic fatty acid content. The fatty analysis of Mr. Goodbar peanut oil revealed the peanuts to be medium oleic with a fatty acid percentage of 68%. Though the normal oleic peanuts had between 20-25% linoleic fatty acid, which is higher than the 8-13% linoleic fatty acid content of medium oleic peanuts, the A normal and B normal oleic peanuts had significantly different concentrations of linoleic fatty acid. The B medium oleic peanut oil and the high oleic peanut oil were also significantly different in linoleic fatty acid content compared to all the other peanut oil samples. The Mr. Goodbar peanuts were similar in linoleic fatty acid content to the A medium oleic peanuts. The percent of palmitic fatty acid was significantly higher in normal oleic peanuts and Mr. Goodbar peanuts as compared to the high and medium oleic peanuts. The A medium oleic peanuts are considered medium based on oleic fatty acid content however analysis of the other fatty acids present categorizes them close to being high oleic.

3.3.2 MALDI-TOF/MS analysis

In Table 3.3, the most abundant triacylglycerol concentrations are given. The generally low standard deviation of the mean percentages reported for each composition from 3 replicate samples indicates the high reproducibility of MALDI-TOF/MS. The major triacylglycerol found in all oils was OOO. As expected from the fatty acid analysis, oil from high oleic nuts, medium oleic nuts, and Mr. Goodbar nuts had a significantly higher percentage of triolein in comparison with normal nuts. There was no significant difference in the triolein content of oils from high, medium and Mr. Goodbar peanuts. Previous work by Singleton and Pattee (1987) also examined triacylglycerol composition of normal oleic peanuts. They reported an OOO content of 4.48% which is much lower than what is reported in this study, and surprisingly low considering the fatty acid analysis showed high amount (20-60%) of oleic fatty acid in various fractions. Singleton and Pattee (1987) identified the major triacylglycerols (without stereospecific analysis) in normal oleic peanuts as being OLL, OOL, POL and PLL. With the exception of PLL, we also found similar triacylglycerols in oils from both normal and medium oleic peanuts.

Normal oleic peanut oils had a linoleic fatty acid content between 20-25%, however trilinoleate was present in very small concentration and not found in detectable amounts in high and medium oleic peanut oils. The very low concentration of trilinoleate is consistent with the findings of Krist and others (2006) who found trilinoleate to be detected at 1.4% in high oleic sunflower oil. Singleton and Pattee (1987) reported a higher value of 5.82% trilinoleate in their TAG analysis of normal peanut oil. A molecular weight of 905.76 which corresponds to LLS/ OOL triacylglycerol species was found to be significantly higher in oils from normal oleic nuts compared with high and medium oleic nuts. The LLS/OOL triacylglycerol was found to be higher in normal oleic peanut oils in comparison with high, medium, and Mr. Goodbar oleic peanut oils, most probably because of the higher concentration of linoleic acid in the normal

peanuts. The medium oleic peanut oils had a significantly higher concentration of LLS/OOL as compared to the high oleic peanut oils. Mr. Goodbar peanut oil was similar to medium and high oleic peanuts, but significantly different than normal oleic peanuts.

The major triacylglycerols found in cocoa butter, the main fat in chocolate, are POP (17 %), POS (36.6 %), and SOS (27.3%) (Loisel et al., 1998). One study shows that these three symmetrical triacylglycerols, POP, POS and SOS, compose 85% of the triacylglycerol profile of cocoa butter (Lipp and others 2001). These three triacylglycerols were not reported in our study because the triacylglycerols concentration was not detectable or detected in extremely low abundances. The triacylglycerols reported in this study may not be directly associated with the fat bloom crystals observed in chocolates, but maybe part of the liquid phase that contributes to triacylglycerol migration from the center to the surface of chocolate. Studies have shown that fat bloom formation occurs as a result of phase separation and a bloomed chocolate has a higher concentration of POS and PPO, whereas the concentration of OOO decreases only slightly (Loisel et al., 1998; Kinta and Hattia, 2005). In these previous studies, the OOO acid was a component of cocoa butter and not released from nuts in the chocolate. Thus, not seeing differences in the level of OOO in bloomed and unbloomed chocolates studied by Loisel and others (1998) and Kinta and Hattia (2005) was expected. Khan and Rousseau (2006) showed OOO/POS concentration increasing as the oil migrated into the dark chocolate as a function of time and temperature. This study suggests that the monounsaturated and polyunsaturated concentration of triacylglycerols in peanut oils are in considerable concentrations as low melting fraction triacylglycerols, and thus may be a critically important factor contributing to increased softness and oil migration in peanut chocolates that initiates fat bloom formation.

3.3.3 Gas chromatography analysis

The trioleic and trilinoleate standards were of particular interest in this study as the fatty acid analysis of the peanut oils revealed differences in oleic and linoleic acid content. The GC method applied separated the standards well (Table 3.4). The oleic and linoleic fatty acids are structurally similar and since their carbon number (CN=54) is the same, the elution time of the two standards was expected to be close. Under the same GC settings, the medium and normal oleic peanut oil samples were run and the two prominent peaks in each chromatograph occurred at 12.160 min and 12.660 min. The prominent peaks are most likely triacylglycerol mixtures composed of oleic and linoleic fatty acid such as OOL and OLL. Clear peaks for triolein and trilinoleate were not identifiable on the GC chromatographs (Figure 3.5). Buchgraber and others (2004) found similar challenges in identifying triacylglycerols in soybean oil as vegetable oils that contain a high degree of polyunsaturated triacylglycerols with the same carbon number.

Conclusions

MALDI-MS/TOF was effective in providing rapid and reproducible analysis of triacylglycerols from high, medium and normal oleic peanuts. The MALDI method detected a far greater number of triacylglycerols as compared to the GC method. The results identified similar triacylglycerols compositions in the oils from the three cultivars, but differences in the concentration of each triacylglycerol species. The triacylglycerols identified and quantified in this study differed from the triacylglycerols analyzed in previous studies on cocoa butter and fat bloom in chocolates suggesting the role of the triacylglycerols released from peanut oils as only contributing to oil migration of liquid triacylglycerols from cocoa butter. Gas Chromatography

analysis showed the majority of TAG to be polyunsaturated mixtures of oleic and linoleic fatty acids.

Acknowledgements

We acknowledge Golden Peanut Company (Alpharetta, GA and Ashburn GA) and Tidewater Agricultural Research and Extension Center (Holland, VA) for the gift of peanuts. We extend thanks to Dr. W. Keith Ray at the Virginia Tech Mass Spectrometry Incubator for assistance with the MALDI-TOF/MS analysis. We thank Macromolecular Interfaces with Life Sciences (MILES) Integrative Graduate Education and Research Traineeship (IGERT) through NSF for funding support under Agreement No. DGE-0333378.

References

Asbury GR, Al-Saad K, Siems WF, Hannan RM & Herbert H. Hill J. 1999. Analysis of triacylglycerols and whole oils by matrix-assisted laser desorption/ionization time of flight mass spectrometry. Journal of the American Society for Mass Spectrometry 1999(10):983-991.

Buchgraber M, Ulberth F & Anklam E. 2000. Comparison of HPLC and GLC techniques for the determination of the triglyceride profile of cocoa butter. Journal of Agricultural and Food Chemistry 2000(48):3359-3363.

Buchgraber M, Ulberth F, Emons H & Anklam E. 2004. Triacylglycerol profiling by using chromatographic techniques. European Journal of Lipid Science and Technology 106(9):621-648

Davis JP, Dean LO, Faircloth WH & Sanders TH. 2008. Physical and chemical characterizations of normal and high oleic oils from nine commercial cultivars of peanuts. Journal of The American Oil Chemist Society 85:235-243.

Duncan MW, Roder H & Hunscuker SW. 2008. Quantitative matrix-assisted laser/desorption/ionization mass spectrometry. Briefings in Functional Genomics and Proteomics 7(5):355-370.

Glish GL & Vachet RW. 2003. The basics of mass spectrometry in the twenty-first century. Nature 2(1 February):140-150.

Khan RS & Rousseau D. 2006. Hazelnut oil migration in dark chocolate - kinetic, thermodynamic and structural considerations. European Journal of Lipid Science and Technology 108(5):434-443.

Kinta Y & Hattia T. 2005. Composition and structure of fat bloom in untempered chocolate. Journal of Food Science 70(7):S450-S452.

Knauft DA, Gorbet DW, Norden AJ & Norden CK, inventors; University of Florida Research Foundation, Inc., Gainsville, Fla., assignee. 1987. Peanut Oil From Enhanced Peanut Products. USA patent.

Krist S, Stuebiger G, Bail S & Unterweger H. 2006. Detection of adulteration of poppy seed oil with sunflower oil based on volatiles and triacylglycerol composition. Journal of Agricultural and Food Chemistry 54(17):6385-6389.

Larsson K. 1966. Classification of glyceride crystal forms. Acta Chemica Scandinavia 20:2255–2260.

Lipp M, Simoneau C, Ulberth F, Anklam E, Crews C, Brereton P, de Greyt W, Schwack W & Wiedmaier C. 2001. Composition of genuine cocoa butter and cocoa butter equivalents. Journal of Food Composition and Analysis 14(4):399-408.

Loisel C, Keller G, Lecq G, Bourgaux C & Ollivon M. 1998. Phase transitions and polymorphism of cocoa butter. Journal of the American Oil Chemists' Society 75(4):425-439.

Lopez C, Bourgaux C, Lesieur P, Riaublanc A & Ollivon M. 2006. Milk fat and primary fractions obtained by dry fractionation: 1. Chemical composition and crystallization properties. Chemistry and Physics of Lipids 144(1):17-33.

Maxwell R & Marmer W. 1983. Fatty acid analysis: Phospholipid-rich analysis. Lipids 18(7):453-459.

McCarthy KL & McCarthy MJ. 2008. Oil Migration in chocolate-peanut butter paste confectionary as a function of chocolate formulation. Journal of Food Science 73(6):E266-273.

Reed K, Gorbet D & O'Keefe S. 2000. Effect of chocolate coating on oxidative stability of normal and high oleic peanuts. Journal of Food Lipids 7(1):31-38.

Rousseau D. 2006. On the porous mesostructure of milk chocolate viewed with atomic force microscopy. LWT 39:852–860.

Singleton J & Pattee H. 1987. Characterization of peanut oil tricacyglycerols by HPLC, GLC and EIMS. Journal of the American Oil Chemists' Society 64(4):534-538.

Wiesman Z & Chapagain BP. 2009. Determination of fatty acid profiles and TAGs in vegetable oils by MALDI-TOF/MS fingerprinting. Methods in Molecular Biology 579:315-336.

Wille R & Lutton E. 1966. Polymorphism of cocoa butter. Journal of the American Oil Chemists' Society 43(8):491-496.

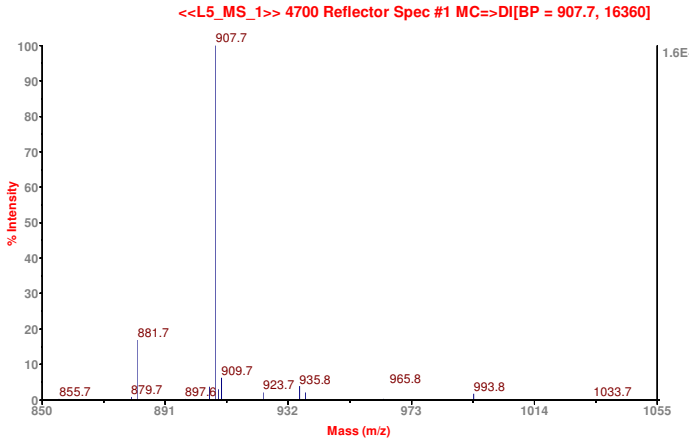

Figure 3.1. MALDI-TOF/MS spectrum of high oleic peanuts

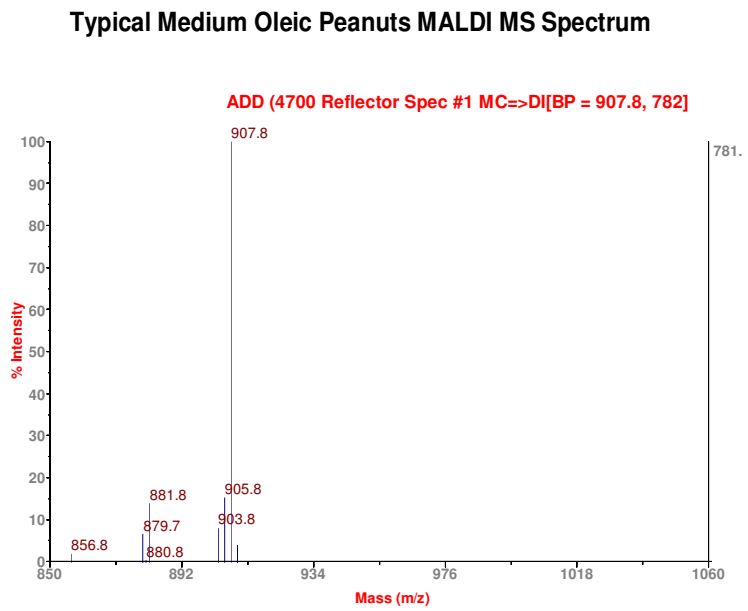

Figure 3.2. MALDI-TOF/MS spectrum of medium oleic peanuts

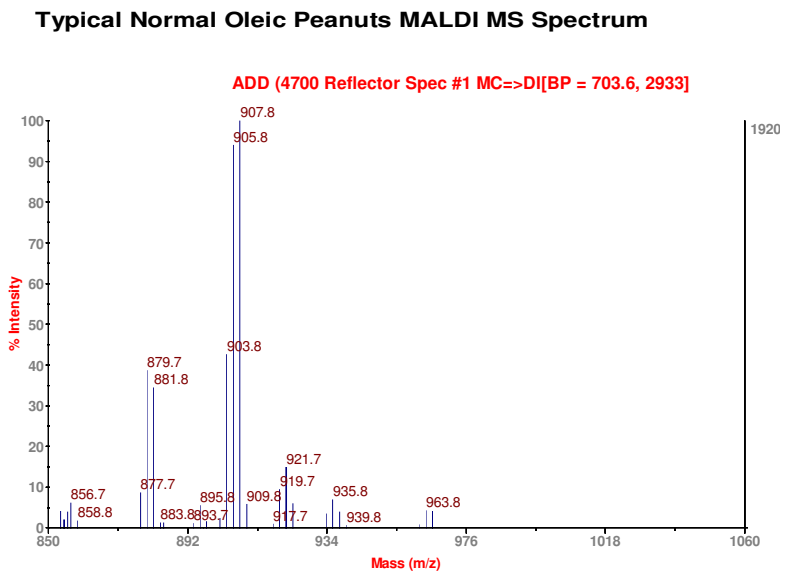

Figure 3.3. MALDI-TOF/MS spectrum of normal oleic peanuts

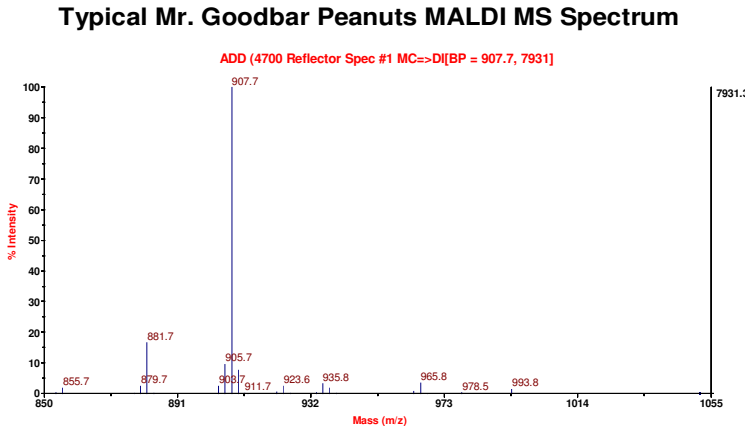

Figure 3.4. MALDI-TOF/MS spectrum of medium oleic peanuts from Hershey's® Mr. Goodbar

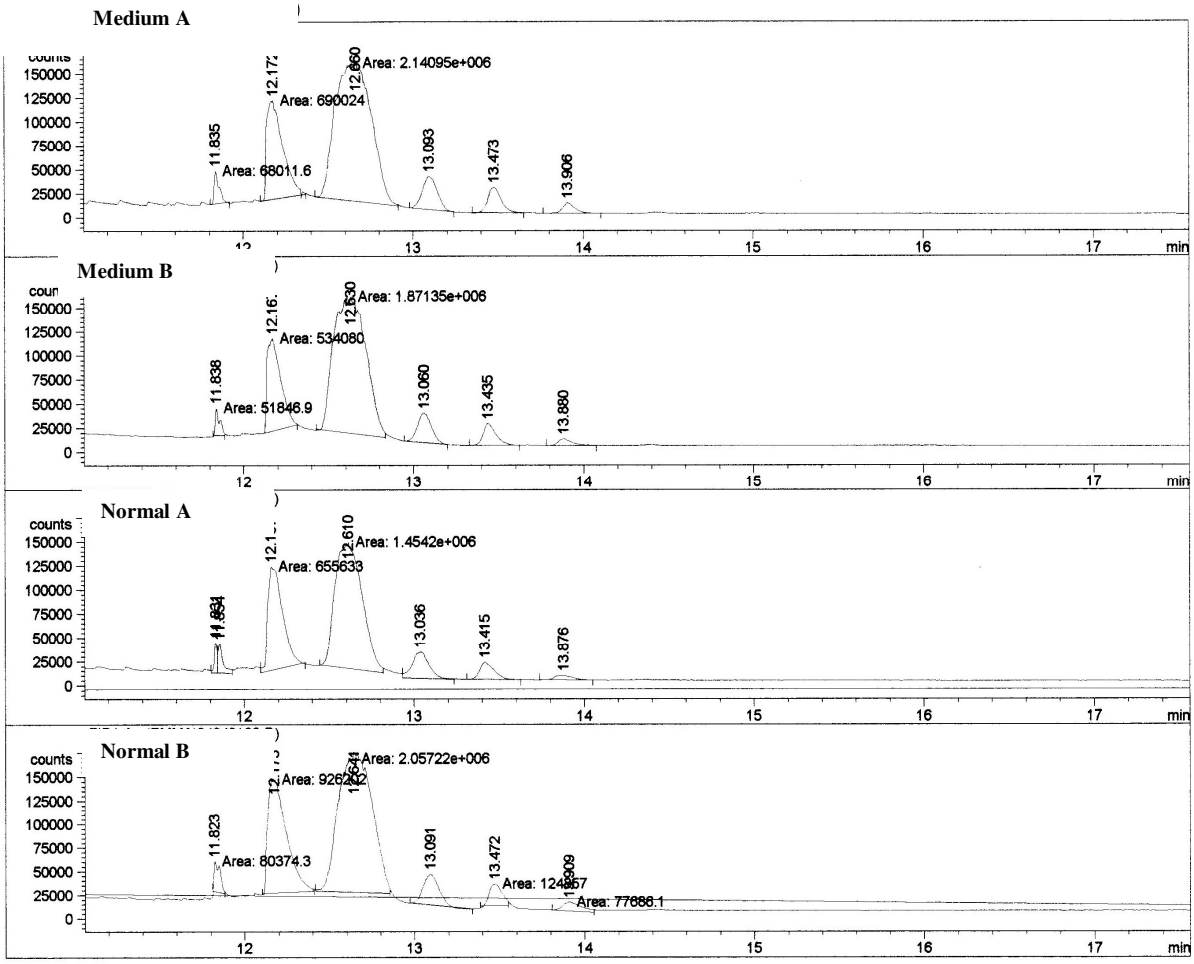

Figure 3.5. Gas chromatographs of medium and normal oleic peanut oils

Table 3.1. Mean fatty acid percentage in the different peanut cultivars[1]

Fatty Acid Name	**High Oleic ±SD**	**A Normal Oleic ±SD**	**B Normal Oleic ±SD**	**A Medium Oleic ±SD**	**B Medium Oleic ±SD**	**Hershey's ® Mr. Goodbar ±SD**
Palmitic C16:0	6.5% ±0.39	9.7% ±0.44	9.5% ±0.78	6.2% ±0.11	7.5% ±0.11	8.6% ±0.46
Steric C18:0	2.4% ±0.79	2.8% ±0.28	2.8% ±0.133	2.2% ±0.07	3.4% ±0.09	3.7% ±0.22
Oleic C18:1 ω-9	75.9% ±0.345	51.2% ±1.67	55.8% ±1.37	73.4% ±3.07	67.3% ±2.42	68.3% ±2.53
Linoleic C18:2 ω - 6	2.3% ±0.16	26.3% ±0.81	21.8% ±1.80	6.4% ±1.97	14.3% ±1.38	7.5% ±0.28
Arachidic C20:0	1.2% ±0.05	1.4% ±0.17	1.3% ±0.14	1.0% ±0.05	1.3% ±0.23	1.3% ±0.06
Gondoic C20:1 ω - 9	1.8% ±0.15	1.2% ±0.17	1.1% ±0.19	1.7% ±0.01	1.1% ±0.17	1.8% ±0.18
Behenic C22:0	2.9% ±0.1322	3.2% ±0.35	2.7% ±0.54	2.6% ±0.20	2.0% ±0.83	3.0% ±0.12
Lignoceric C24:0	2.2% ±0.78	1.4% ±0.17	1.2% ±0.41	1.5 % ±0.31	0.7% ±0.58	1.7% ±0.14

[1]Three replications for all samples

Table 3.2. Calculated molecular mass of expected triacylglycerol compositions

TAG Abbreviation	ECN	Mass	$[M+H]^+$	$[M+Na]^+$
OOPo	46	856.75	857.76	879.74
POL	46	856.75	857.76	879.74
OOP	48	858.77	859.78	881.76
PSL	48	858.77	859.78	881.76
LLL	42	878.74	879.74	901.72
LLO	44	880.75	881.76	903.74
OOLn	44	880.75	881.76	903.74
SLLn	44	880.75	881.76	903.74
LLS	46	882.77	883.78	905.76
OOL	46	882.77	883.78	905.76
SOL	48	884.78	885.79	907.77
OOO	48	884.78	885.79	907.77
OOS	50	886.80	887.81	909.79
SSL	50	886.80	887.81	909.79
PLA	50	886.80	887.81	909.79
OLA	50	912.81	913.82	935.8
OOG	50	912.81	913.82	935.8
SLA	50	912.81	913.82	935.8

O=oleic fatty acid, L=linoleic acid, S=steric acid, P=palmitic acid, A= arachidic acid, G=gondoic acid, Po=palmitoleic

Table 3.3. Relative triacylglycerol composition of different peanut oils analyzed by MALDI-TOF/MS[1]

TAG Abbreviation	High Peanut Oil ±SD	A Normal Peanut Oil ±SD	B Normal Peanut Oil ±SD	A Medium Peanut Oil ±SD	A Medium Peanut Oil ±SD	Hershey's ® Mr. Goodbar Peanut Oil ±SD
OOPo/POL	0.4 ± 0.05	9.3 ± 0.18	9.5 ± 0.61	4.0 ± 0.53	4.2 ± 0.18	1.8 ± 0.22
OOP/ PSL	11.2 ± 0.59	9.2 ± 1.29	11.8 ± 1.91	10.3 ± 0.92	8.9 ± 3.39	10.5 ± 0.93
LLL	N/A	1.2 ± 0.80	0.5 ± 0.33	N/A	N/A	N/A
LLO	N/A	10.8 ± 0.50	8.2 ± 1.27	4.7 ± 0.87	4.6 ± 0.83	1.6 ± 0.14
LLS/ OOL	2.3 ± 0.28	24.4 ± 3.55	21.7 ± 0.63	8.2 ± 3.10	9.6 ± 1.74	6.4 ± 0.68
LOS/OOO	71.2 ± 3.72	25.8 ± 2.34	31.6 ± 3.39	56.7 ± 9.73	55.3 ± 8.82	69.3 ± 0.59
PLA/LSS/ OOS	3.9 ± 0.445	1.6 ± 0.97	1.9 ± 0.50	4.0 ± 1.37	4.1 ± 1.49	4.1 ± 1.25
SLA/LOA/ OOG	2.6 ± 0.36	1.4 ± 0.25	1.4 ± 0.18	0.9 ± 0.18	1.5 ± 0.19	1.7 ± 0.41

[1]Three replications for all samples

N/A not available

O=oleic fatty acid, L=linoleic acid, S=steric acid, P=palmitic acid, A= arachidic acid, G=gondoic acid, Po=palmitoleic

Table 3.4. Retention time of triacylglycerol standards by gas chromatography

TAG Abbreviation	Retention Time (min)
Tritridecanoin (C13:0)	10.053
Tripalmitate (C16:0)	11.487
Trioleate (C18:1)	12.513
Trilinoleate (C18:2)	12.417
Trinonadecanoin (C19:0)	12.952

CHAPTER 4: RHEOLOGICAL PROPERTIES OF HIGH, MEDIUM, AND NORMAL OLEIC PEANUT PASTES USING THE IMPERFECT SQUEEZING FLOW METHOD

Abstract

This study examined the yield stress and flow index behavior of high oleic, medium oleic and normal oleic peanut paste using the imperfect squeezing flow method. Lubricated squeezing flow using Teflon plates compressed the peanut pastes to generate force and height displacement plots. The apparent yield stress τ_o was calculated from force vs. time plots and the flow index *n* was calculated from the log force vs. log displacement plots. The testing conditions were determined using 60,000 cp silicone fluid and the reliability of the test was determined by measuring the yield stress and flow index behavior of previously tested products such as commercial ketchup and commercial peanut butter. The study found significant difference between the apparent yield stress of high oleic peanut paste and medium oleic peanut paste. The flow indices of the high, medium and normal oleic peanut pastes were significantly different from one another. The normal oleic peanut paste had a higher shear thinning behavior compared to the high and medium oleic peanut pastes. The high oleic peanut paste had the lowest shear thinning behavior with a absolute flow index value of 1, indicating possible friction with the use of Teflon plates.

Keywords: peanut paste, squeeze flow, flow index behavior, yield stress

4.1 Introduction

Peanut paste is a popular filling choice for chocolate manufacturers. Research shows that chocolates that contain peanuts or other nut based fillings are very prone to fat bloom formation (McCarthy and McCarthy, 2008; Khan and Rousseau, 2006). This is due to the release of oil from the nuts into the surrounding chocolate matrix. Fat bloom is the gray and white discoloration sometimes seen on the surface of chocolates. Fat bloom occurs due to liquid triacylglycerols that migrate from the center to the surface where re-crystallization may occur causing the original crystals to polymorph into larger crystal structures. These liquid triacylglycerols mainly come from cocoa butter, but other factors such as release of oils from nuts or fillings can also contribute to bloom formation. Fat bloom formation can be triggered due to temperature fluctuations, incompatible fats, and improper tempering. Finding a filling that may hinder oil migration can provide a simple and rapid solution to delaying migration of low melting fraction triacylglycerols. High oleic peanut paste has a high oleic fatty acid content and is less unsaturated compared to medium and normal oleic peanut pastes, so it may have a higher flow index and yield stress. Normal oleic peanut paste is expected to have the lowest flow index and yield stress as the oleic fatty acid content is not very high compared to high and medium oleic peanuts. Normal oleic peanut paste also has a higher concentration of linoleic fatty acid, a polyunsaturated fatty acid, compared to high and medium oleic peanut pastes.

The rheological properties of peanut paste have previously been characterized using a rheometer and parallel plate set up for oscillatory measurements. Traditional rheometers using parallel plates shear the internal structure of the specimen which can lead to inconsistency upon replication. Due to the high amount of fat in peanut paste the sample is prone to slippage between the plates and at a greater risk for inaccurate measurements. Damrau and Peleg (1997)

describe slip as the tendency of suspended particles to migrate to the sheared layer's center leaving the viscometer surface in contact with a liquid film that acts like a lubricant. Citerne and others (2001) tried to overcome the problem of slippage with the use of sand paper to roughen the plates. The rheological properties of semi-liquid foods such as peanut pastes may also be determined using squeezing flow viscometry. Squeezing flow viscometry produces lateral flow as a result of uniaxial compression between parallel plates (Campanella and Peleg, 2002; Campanella and Peleg, 1987a; Campanella and Peleg, 1987b). There are two main types of squeezing flow tests. The first test is one with a constant displacement rate with the generation of force vs. height (displacement) curves and the second test is a constant load (creep) test with the generation of height vs. time curves (Campanella and Peleg, 2002; Campanella and Peleg, 1987b). In our study the constant displacement test was performed at a velocity of 0.10 mm/s. This velocity was chosen based on recommendations in previous studies by Suwonsichon and Peleg (1999) who showed that increasing the velocity from 0.1 mm second to 0.2 mm/s can increase the force generated, possibly affecting the deformation and rate dependent components of the product causing intensive structural damage.

There are two types of flows that can be generated by squeezing flow viscosity: lubricated and frictional flow. Lubricated flow can also be generated when plates are lubricated with oil or are composed of a material with a low coefficient of friction such as Teflon. Non lubricated flow can be generated using intentionally roughened plates such as ones with grooves or by attaching sand paper. The flow pattern can be distinguished based on the shape of the fluid exit flow upon compression shown in Figure 4.1, reprinted from Journal of Texture Studies, Vol. 28, E. Damrau and M. Peleg, Imperfect squeezing flow viscosimetry of newtonian liquids-

theoretical and practical considerations, pg 187-204, 1997 with permission from John Wiley and sons.

The term slope used in this study is calculated from the squeezing flow region from the log force vs. log displacement plot (Figure 4.4). The squeezing flow region is the region where the actual compression of the sample is free from entrance effects and instrument geometry effects that the transient region consists of.

Flow between parallel plates for Newtonian fluids is calculated by the Stefan's Equation when the diameter of the upper plate and the gap height ratio is greater than 10. Newtonian fluids do not exhibit slip. For Newtonian fluids, during non-lubricated frictional compression the force height relationship with a constant displacement rate is governed by the following equation (Campanella and Peleg, 2002; Terpstra et al., 2007; Damrau and Peleg, 1997):

$$F(t)=\frac{3\pi R^4 V(t)\mu}{2H(t)^3}$$

Equation (1)

F is the momentary force, *H* is the specimen's momentary height, R is the radius of the upper plate, V is compression speed and μ is the fluid shear viscosity

For Newtonian fluids, during lubricated compression the force height relationship with a constant displacement rate is governed by the following equation (Damrau and Peleg, 1997):

$$F(t)=\frac{3\pi R^2 V(t)\mu}{H(t)}$$

Equation (2)

F is the momentary force, *H* is the specimen's momentary height, R is the radius of the upper plate, V is compression speed, and μ is the fluid shear viscosity

For Newtonian fluids under lubricated testing conditions, the slope of the log force vs. log displacement plot indicates the flow index behavior and this should be equal to -1. Under

non lubricated conditions the slope for Newtonian fluids should be equal to -3 (Hoffner et al., 1997; Terpstra et al., 2007; Damrau and Peleg, 1997; Suwonsichon and Peleg, 1998).

For Non-Newtonian fluids, during non-lubricated frictional flow the force height relationship with a constant displacement rate is governed by the following equation (Campanella and Peleg, 2002; Terpstra et al., 2007):

$$F(t)=[2\pi KR^{(n+3)}/\ (n+3)][(2n+1)/n)^n V^n/H(t)^{\,2n+1}]$$

Equation (3)

F is the momentary force, *H* is the specimen's momentary height, *K* and n are the specimen's consistency and flow index, respectively, R is the radius of the upper plate, *V* is the compression speed

For Non-Newtonian fluids, during lubricated flow the force height relationship with a constant displacement rate is governed by the following equation (Campanella and Peleg, 2002; Terpstra et al., 2007):

$$F(t)=3^{(n+1/2)}\pi KR^2(V/H(t))^n$$

Equation (4)

F is the momentary force, *H* is the specimen's momentary height, *K* and n are the specimen's consistency and flow index, respectively, R is the radius of the upper plate, *V* is the linear velocity

For Non-Newtonian fluids during the non-lubricated condition, the slope is equal to -(2*n*+1) and for the lubricated condition the slope is equal to –*n*. The absolute value of the slope should be greater than 1 under non-lubricated flow and less than 1 under lubricated flow. Lubrication of the plates intentionally produces slip, and slip is calculated in the results (Campanella and Peleg, 1987b; Suwonsichon and Peleg, 1998). Slip can only occur during non-lubricated conditions.

When the behavior of the fluid is unknown, and if the absolute slope of the log F(t) and log H (t) is less than one, the conclusion can be the flow is lubricated. If the absolute value of slope of the log F(t) and log H (t) in the squeezing flow region is between 1.0 and 3.0 the flow

can be frictional or slip (Terpstra et al., 2007). Campanella and Peleg (1987) used lubricated squeezing flow viscometry to determine the rheological characteristics of commercial peanut butter.

Imperfect squeezing flow viscometry differs from perfect squeezing flow viscometry due to the specimen being placed in a shallow container such as a petri dish (compared to plates with no boundaries) (Campanella and Peleg, 2002; Damrau and Peleg, 1997; Suwonsichon and Peleg, 1998). The use of plates made from materials with a high coefficient of friction can result in friction and lead to error. An important point to note is the measured forces of squeezing flow are also influenced by buoyancy. Buoyancy or hydrostatic pressure is the upward force exerted by the fluid as the fluid displaces. This force can cause significant errors if proper care is not taken to reduce this force. The error can be reduced if the specimen is pressed to a very small height in a plate with a large width (Damrau and Peleg, 1997). In this study the buoyancy force was calculated and the force was correct by subtracting the buoyancy force from the actual measured forced. The buoyancy force was calculated according to the following equation (Terpstra et al., 2007):

$$B(t) = \frac{[H_{ini} - H_{(t)}]\, R^2_{dish}\, R^2_{plate}\, \pi \rho g}{R^2_{dish} - R^2_{plate}}$$

Equation (5)

H_{ini} is the specimen's initial height, $H_{(t)}$ is the specimen's momentary height, $R_{container}$ is the radius of the dish/container, R_{plate} is the radius of the upper plate ρ is the density of the fluid, and g is the gravitational acceleration

Yield stress is the applied stress needed to initiate shear flow. The apparent yield stress τ_o can be determined from squeezing flow viscometry performed at constant displacement from the residual apparent stress of the fluid at a given height after the fluid has been allowed to relax for a given time (Suwonsichon and Peleg, 1998). Campanella and Peleg (1987a) found yield

stress values experimentally derived from squeezing flow tests to be in agreement with the yield stress values determined using a coaxial viscometer (Campanella and Peleg, 1987a). Campanella and Peleg (1987a) concluded that the yield stress is mostly independent of testing conditions. For a Newtonian fluid, the residual stress level would reduce to the level of the buoyancy effect. Apparent yield stress is calculated with the following equation:

$$\tau_o = F_{@time} / \pi R^2$$

Equation (6)

F is the force at time (t=2 min), B is the buoyancy force at 1 mm R is the radius of the upper plate

Apparent yield stress is considered as a measure of consistency and structure. The higher the yield stress value the more solid the specimen's structure (Suwonsichon and Peleg, 1999; Corradini and Peleg, 2005).

The objective of this study was to determine the rheological properties of flow index *n*, and the apparent yield stress τ_o of peanut pastes made from high, medium, and normal oleic peanuts. Our study also selected previously tested products such as silicone fluid, commercial ketchup and commercial peanut butter to ensure the testing procedure gave reliable results. This study also used the silicone fluid to determine how the flow index and apparent stress changed with the use of a smooth acrylic upper plate with a petri dish container, the use of a Teflon upper plate with a petri dish container, and the use of a Teflon upper plate and a Teflon container. Rheological differences in the peanut paste made from the different peanuts may indicate which peanut variety would be most likely help hindering migrate of liquid triacylglycerols at room temperature. This information can be very useful to chocolate manufacturers trying to determine ways to slow down fat bloom formation in chocolates.

4.2 Materials and Methods

Raw high oleic, medium oleic, and normal oleic peanuts were received as a gift from Tidewater Agricultural Research and Extension Center (Holland, VA). The raw peanuts were roasted in metal pans in a pizza oven at 188 °C to a Hunter lab lightness value of 2± 50 as measured by colorimeter (Minolta CHROMA METER CR-200 Osaka, Japan). The peanuts were roasted under similar conditions at different times resulting in different batches. The peanuts were stored in a dark cabinet at room temperature prior to use. The peanuts were grounded in a Black & Decker Quick 'N Easy food processor (Towson, MD) until a creamy texture was observed. The peanut paste was then processed through a Speco Model 2.5 colloid mill (Beverly, MA) with a stainless steel grinding wheel. The peanut pastes were stored at -4 °C until usage. Silicone fluid was purchase from Brookfield Engineering (Middleboro, MA). The shear viscosity of the fluid was received certified at 58560 centipose. Heinz ketchup and Jif's all natural peanut butter were purchased locally. The Brix (°Bx) value of the ketchup was measured using a digital refractometer (Model Reichert Jung Abbe Mark II, Leica Co., Buffalo, NY) and found to be 33.3°Bx.

4.2.1 Particle size analysis

Peanut butter was defatted using chloroform followed by vacuum filtration. The solid particles were allowed to dry at 50 °C for 24-28 hr. The particle size distribution for each sample was measured using a using a laser diffraction particle size analyzer (Horiba LA-700, Horiba Instruments Inc, Irvine, CA) with water as a dispersant. The particles were sonnicated in solution prior to taking measurements.

4.2.2 Fatty acid analysis of peanut oils

Approximately 25 g of peanuts were blended (Waring Commercial Blendor, New Hartford, Conneticut) with 75 mL chloroform for 1- 2 minutes on low speed. The mixture was then filtered slowly with Whatman No. 4 paper. Approximately 50 g anhydrous sodium sulfate was added and the solvent mixture was allowed to stand for 15 min. The mixture was filtered with Whatman No. 4 paper and rinsed with 10 mL chloroform. The solvent mixture was transferred to a round bottom flask and the solvent was evaporated in a rotary evaporator (Buchi, Rotavapor R-3000, Switzerland) at 60 °C. The samples were stored at -70 °C prior to use. One drop of oil (20 mg) was dissolved in 2 mL iso-octane in a 10 mL glass centrifuge tube with a Teflon-lined cap. To each sample, 100 µL of 2N KOH in methanol was added. The sample was vortexed for 60 seconds followed by several minutes of standby as the phases separated. The bottom layer was discarded, and this step was repeated with 0.5 mL saturated ammonium acetate (aq). The bottom layer was discarded, and this step was repeated with 1.0 mL deionized water. The bottom layer was discarded and 0.5 g sodium sulfate was added for 5 minutes. The supernatant was then removed and placed in GC vials (Maxwell and Marmer, 1983). 1 µL of each sample was directly injected into a Shimadzu GC-17A gas chromatograph (Kyoto, Japan) coupled to a QCMS-QP5050A mass spectrometer with a split ratio of 1:20. A Supelco SP2560 (100 m x 0.25 mm i.d. x 0.25 µm film thickness) column (Bellefonte, PA) was used. The injection temperature was 270 °C, interface temperature was 230°C, and the oven was ramped from 175 °C to 240 °C at 2°C per minute and held for 20 minutes. Helium was used as the carrier gas at 1.4 mL/min. The mass spectrometer was set in scan mode for 50 m/z to 650 m/z and recorded data 35 cm/sec from 7.72 minutes to 25 minutes at a scan speed of 2000. The fatty acids analysis data are presented in Table 4.1.

4.2.3 Squeezing flow tests

A texture analyzer (TA.TX 2, Texture Technologies Corp., Scarsdale, NY) was used for the compression tests. The upper plate acted as the plunger for compressing the sample and each plate was smooth finished and circular. The upper plates used in the test were acrylic and Teflon plate (McMaster Carr Supply, Chicago, IL). The containers used were a polystyrene petri dish (Becton Dickinson Labware, Franklin lakes NJ) and a custom made Teflon dish (material from McMaster Carr Supply, Chicago, IL). The set up of the squeezing flow experiment is shown in Figure 4.2. Each sample was compressed to final height of 0.5 mm. The relaxation time following compression was 2 min before the upper plate was released. Each sample was tested three times. The instrument force and height were calibrated prior to each test. The density measurement of each sample was repeated three times using a 1.98 mL pycnometer. The density calculation is given in Appendix A. The buoyancy force was calculated using the equation five (Appendix B). The yield stress was calculated using equation 6 (Appendix C). The calculated shear viscosity μ_s of the silicone fluid from the log force vs. log displacement plot under lubricated conditions is shown in Appendix D. Linear regression was use to calculate the slope of the log force vs. log height displacement plots.

4.2.4 Statistics

Data analysis was performed using one way Anova and Tukey's HSD tests using JMP (JMP 8.0, 2008, SAS Institute, New Jersey, USA).

4.3 Results and Discussion

The fatty acid analysis of the peanuts confirmed that the samples received were high, medium, and normal in oleic fatty acid content. The median particle size of the peanut pastes ranged from 20.6-24.6 μm. The particle size was measured to eliminate any differences in rheological property measurements due to particle size discrepancies.

4.3.1 Silicone fluid

Figure 4.3 shows the force and distance plots of silicone fluid tested using the different plates and dishes. The force plotted was corrected for the buoyancy effect. The start time for each sample is different due to a difference in sample depth. The apparent yield stress values are given in Table 4.2. The expected yield stress for a Newtonian fluid should be equal to zero. In Figure 4.5, the box regions represent the transient effects. For all plots, the transient region can be easily distinguished from the squeezing flow regime by plotting the log force and log height displacement curves (Figure 4.4). The box region indicates the transient region. The flow index behavior for each curve was calculated from the slope of the squeezing flow region. For a Newtonian fluid the absolute value of slope should equal 1 under fully lubricated conditions and 3 for non-lubricated conditions. The flow index values given in Table 4.3 for the 76.60 mm Teflon plate/ 86 mm petri dish and 76.60 mm acrylic plate/ 86 mm petri dish show that using the polystyrene petri dish as the bottom container resulted in a flow index greater than 1 which indicates friction as the silicone fluid is Newtonian and would not exhibit slip. The calculated shear viscosity of the silicone fluid using the Teflon upper plate and Teflon dish was incorrect (Appendix D). This may be explained by the low sensitivity of the texture analyzer and/or error in the sample depth determination. Damrau and Peleg (1997) showed that if the sample depth

decreases the error in the depth measurement becomes higher and thus the sample depth becomes a limiting factor. In this study the initial sample depth H_0 was determine when the measured force became steadily positive. As Damrau and Peleg (1997) also concluded that measuring the exact initial specimen height is difficult to accomplish due to a lack of measurement techniques.

As evident from Figure 4.3 the force after 2 minutes of relaxation returned below the starting force indicating a zero yield stress as expected. The use of the 65 mm Teflon plate and 68 mm Teflon dish gave the expected Newtonian flow index behavior of approximately 1. The yield stress τ_o calculated has little dependence on testing conditions and is especially useful if making comparison between products (Campanella and Peleg, 1987a; Kampf and Peleg, 2002). Campanella and Peleg (2002) state that flow index calculated is useful for comparing formulation differences or handling differences of pseudoplastic materials. The use of a Teflon upper plate and Teflon bottom dish gave the expected yield stress of zero (and values lower than 0 due to buoyancy effects see Figure 4.3 and Table 4.2) and a flow index of approximately one for silicone fluid and thus this set up was chosen to continue testing the other samples used in this study.

4.3.2 Commercial ketchup and peanut butter

The force vs. time and log force vs. log displacement plots of the ketchup and peanut butter are shown in Figure 4.5 and Figure 4.6, respectively. The yield stress and flow index values are given in Table 4.4 and Table 4.5, respectively. The yield stress of ketchup was less than the buoyancy force. The yield stress was determined to be near 0 and this small value was expected as the consistency of the product is watery in nature compared to a food item like peanut butter. The force measured during the test was also very low. The absolute value of the

flow index behavior for the ketchup was 0.36 ± 0.03, indicating shear thinning behavior. The yield stress of the ketchup found in this study was lower than values reported by Campanella and Peleg (1987a), Lorenzo and others 1997) and Corradini and Peleg (2005). Campanella and Peleg (1987a) reported a yield stress of 0.030-0.018 kPa and Corradini and Peleg (2005) reported values between 1.0-0.9 kPa. However, in both studies the buoyancy force was not taken into consideration. The ketchup used by Corradini and Peleg (2005) had 32°Bx and the measurement was taken after two minutes of relaxation. Lorenzo and others (1997) used ketchup with a 32.5°Bx and the measurement was also taken after two minutes. Campanella and Peleg (1987a) did not report the Brix value and used the force at a given height for their measurement. The Brix value is a good assessment of the measure of solids in the product and large differences in Brix may explain discrepancies in results. The flow index of ketchup (0.36 ± 0.03) reported in this study was very close to the values previously reported by Lorenzo and others (1997) whose ketchup samples absolute value of flow indices were in the range of 0.39-0.52. The flow index of the commercial peanut butter was previously examined by Campanella and Peleg (1987b). The absolute value of the flow index of peanut butter in this study was 0.76 ± 0.10 which is very similar to values reported by Campanella and Peleg (1987b) who determined the flow index range of commercial peanut butter to be 0.53-0.72. The yield stress of commercial peanut butter was 10.61 kPa ± 3.04. The higher yield stress value was expected as the product was very thick and solid. Both the commercial ketchup and peanut butter were self lubricating systems. Ketchup has a high amount of water and peanut butter a high amount of oil that would help lubricate the system. Lorenzo and others (1997) found the flow index for ketchup determined by both the use of smooth and roughened metal plates were in agreement due to the self-lubricating nature of the product. Discrepancies in values reported in this study from previous studies may lay in how the

sample was prepared prior to the test. If the sample was stirred or disrupted the yield stress would be low as the sample has already been sheared. Pre-caution was taken in this study to ensure that the sample in the testing container was allowed to rest for 3-5 minutes immediately after being placed transferred into the container and prior to starting the compression test.

4.3.3 High, medium and normal oleic peanut pastes

Figures 4.7, 4.8, and 4.9 show the force vs. time and log force vs. log displacement plots for the high, medium, and normal oleic peanut pastes, respectively. The yield stress and flow index values are given in Table 4.6 and Table 4.7, respectively. From the shape of the force vs. time plot the force during relaxation does not drop close to the starting force indicating a minimum yield stress for all samples. The yield stress was small and the measure forces were also low. There was a significant difference in the mean yield stress of the high oleic peanut paste compared to the mean yield stress of medium oleic peanut paste. There was no significant difference between the mean yield stress of the high oleic peanut paste and the normal oleic peanut paste and no significant difference between the mean yield stress of the medium oleic peanut paste and normal oleic peanut paste. The high yield stress value of high and normal oleic peanut pastes shows the pastes to have stronger consistency than the medium oleic paste. The consistency or solidity of the high and medium oleic peanut pastes was expected to be higher than the normal oleic pastes due to the higher monounsaturated oleic fatty acid content and very low polyunsaturated linoleic fatty acid content. Normal oleic peanut paste did have a higher concentration of palmitic acid (C16:0), a saturated fatty acid with a shorter aliphatic chain compared to oleic and linoleic (18 carbon) acids, which could explain the product's stronger consistency than the medium oleic peanut paste. The differences in rheological properties of the

high, medium, and normal oleic peanut pastes cannot be solely due to chain length, but maybe more so different due to degree of unsaturation. Fasina and others (2006) reported positive correlation between the mass fraction of polyunsaturated or monounsaturated fatty acid in the oil and the melting characteristics of vegetable oils. However, in this study the normal oleic peanut paste which had the highest concentration of linoleic fatty acid did not show the weakest consistency.

The difference in yield stress values maybe due to factors such as total oil content and particle-particle interaction. The total oil content can affect the suspension of the particles in the peanut paste as peanut paste is a suspension of non-colloidal peanut particles in peanut oil (Citerne et al., 2001). The absence of a stabilizer such as palm kernel oil can also affect the particles suspension in the matrix. The particle-particle interaction can depend on factors such as the shape and surface roughness of the particles which can lead to slip or friction. However, in an intentionally lubricated system with the use of Teflon plates, the slip factor is taken into consideration in calculating the rheological properties (Damrau and Peleg, 1997).

The flow index behavior for all peanut paste samples was pseudoplastic and the calculated flow index behavior was significantly different for each sample. According to the flow index values in this study the normal oleic paste was the most shear thinning, followed by the medium oleic peanut paste, and high oleic peanut paste, respectively. The difference in flow index behavior may be due to the high concentration of linoleic fatty acid in the normal oleic peanut paste as compared to the high and medium oleic peanut pastes. The borderline value of the high oleic peanut paste of 1 is an important factor that indicates that even with the use of a Teflon upper plate and Teflon bottom container friction may not be completely eliminated from the set up. Terpstra and others (2007) applied a lubricant to a Teflon geometry set up and showed

a decrease in the calculated viscosity of low fat mayonnaise compared to the values measured in the setup without the applied lubricant.

Conclusions

All peanut pastes samples had a minimum yield stress. The difference in yield stress values may be attributed to differences in fatty acid content due to differences in the degree of unsaturation and higher concentration of palmitic fatty acid which has a shorter aliphatic chain. The difference in flow indices of the pseudoplastic materials served useful in comparing high, medium, and normal oleic peanut pastes. The difference in flow index behavior of the high, medium, and normal oleic peanut pastes may be attributed to the difference in the polyunsaturated fatty acid content. Further examination of the microstructure of the samples and addition of a stabilizer to the pastes, may give better insight to explain the results found in this study.

References

Campanella OH & Peleg M. 1987a. Determination of the yield Stress of semi-liquid foods from squeezing flow data. Journal of Food Science 52(1):214-215.

Campanella OH & Peleg M. 1987b. Squeezing flow viscosimetry of peanut butter. Journal of Food Science 52(1):180-184.

Campanella OH & Peleg M. 2002. Squeezing flow viscosimetry for nonelastic semiliquid foods-theory and application. Critical Reviews in Food Science and Nutrition 42(3):241-264.

Citerne GP, Carreau PJ & Moan M. 2001. Rheological properties of peanut butter. Rheologica Acta 40(1):86-96.

Corradini MG & Peleg M. 2005. Consistency of dispersed food systems and its evaluation by squeezing flow viscometry. Journal of Texture Studies 36(5-6):605-629.

Damrau E & Peleg M. 1997. Imperfect squeezing flow of visosimetry of Newtonian liquids-theoretical and practical considerations. Journal of Texture Studies 28(1997):187-204.

Fasina O, Hallman H, Craig-Schmidt M & Clements C. 2006. Predicting temperature-dependence viscosity of vegetable oils from fatty acid composition. Journal of the American Oil Chemists' Society 83(10):899-903.

Hoffner B, Gerhards C & Peleg M. 1997. Imperfect lubricated squeezing flow viscometry for foods. Rheologica Acta 36(6):686-693.

Kampf N & Peleg M. 2002. Characterization of chick pea (Cicer arietum L) pastes using squeezing flow viscometry. Rheologica Acta 41(6):549-556.

Khan RS & Rousseau D. 2006. Hazelnut oil migration in dark chocolate - kinetic, thermodynamic and structural considerations. European Journal of Lipid Science and Technology 108(5):434-443.

McCarthy KL & McCarthy MJ. 2008. Oil Migration in chocolate-peanut butter paste confectionary as a function of chocolate formulation. Journal of Food Science 73(6):E266-273.

Suwonsichon T & Peleg M. 1999. Rheological characterization of almost intact and stirred yogurt by imperfect squeezing flow viscometry. Journal of the Science of Food and Agriculture 79(6):911-921.

Suwonsichon T & Peleg M. 1998. Imperfect squeezing flow viscometry of mustards with suspended particulates. Journal of Food Engineering 39:217-226.

Terpstra MEJ, Janssen AM & Linden Evd. 2007. Exploring Imperfect Squeezing Flow Measurements in a Teflon Geometry for Semisolid Foods. Journal of Food Science 72(9):E492-E502.

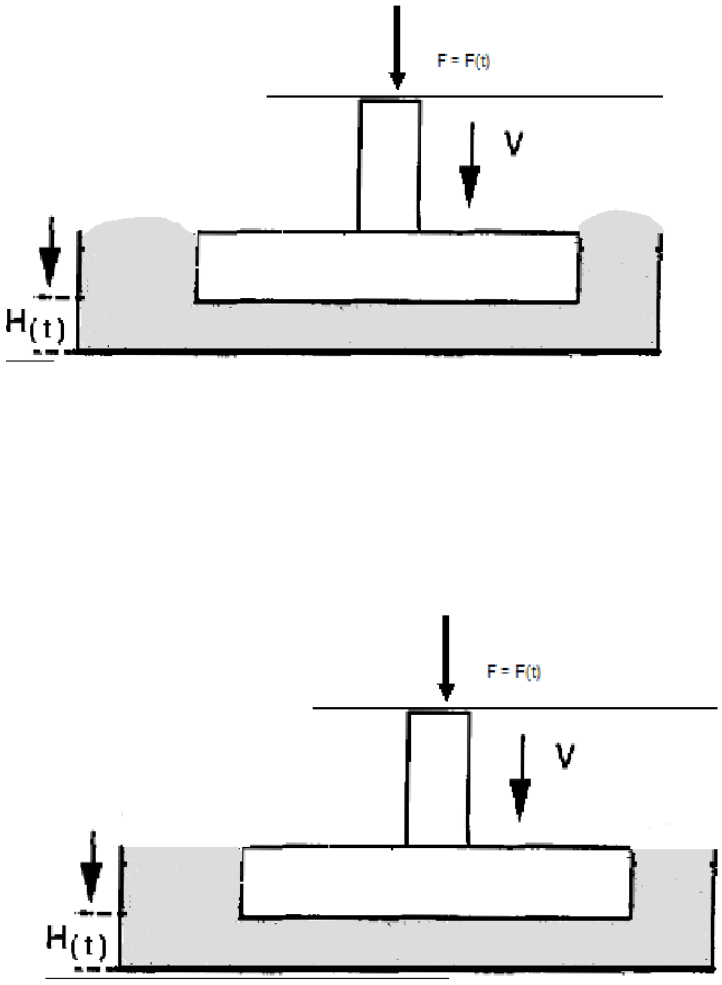

Figure 4.1. Exit flow behavior of fluid upon compression. Frictional flow due to boundary conditions created (Top). Lubricated flow no boundary conditions (Bottom). Reprinted from Journal of Texture Studies, Vol. 28, E. Damrau and M. Peleg, Imperfect squeezing flow viscosimetry of newtonian liquids-theoretical and practical considerations, pg 187-204, 1997 with permission from John Wiley and sons.

Figure 4.2. Squeeze flow test set-up using telfon plates

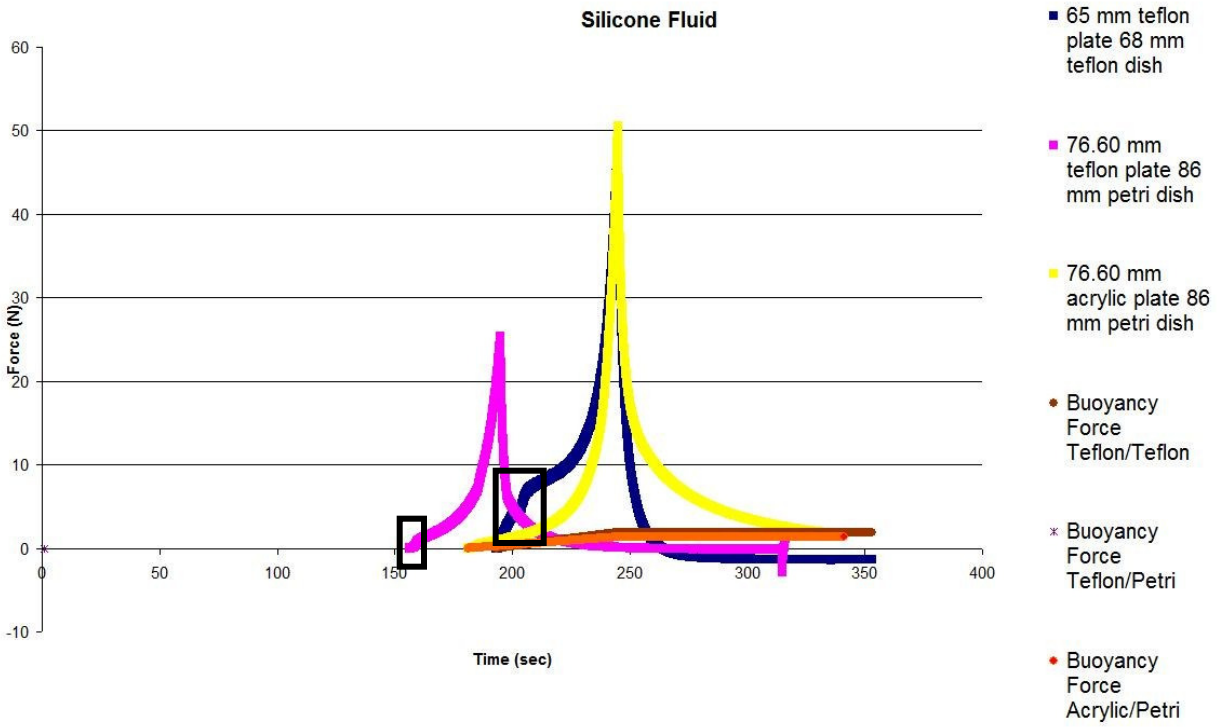

Figure 4.3. Force vs. time plot for silicone fluid. Box indicates transient region.

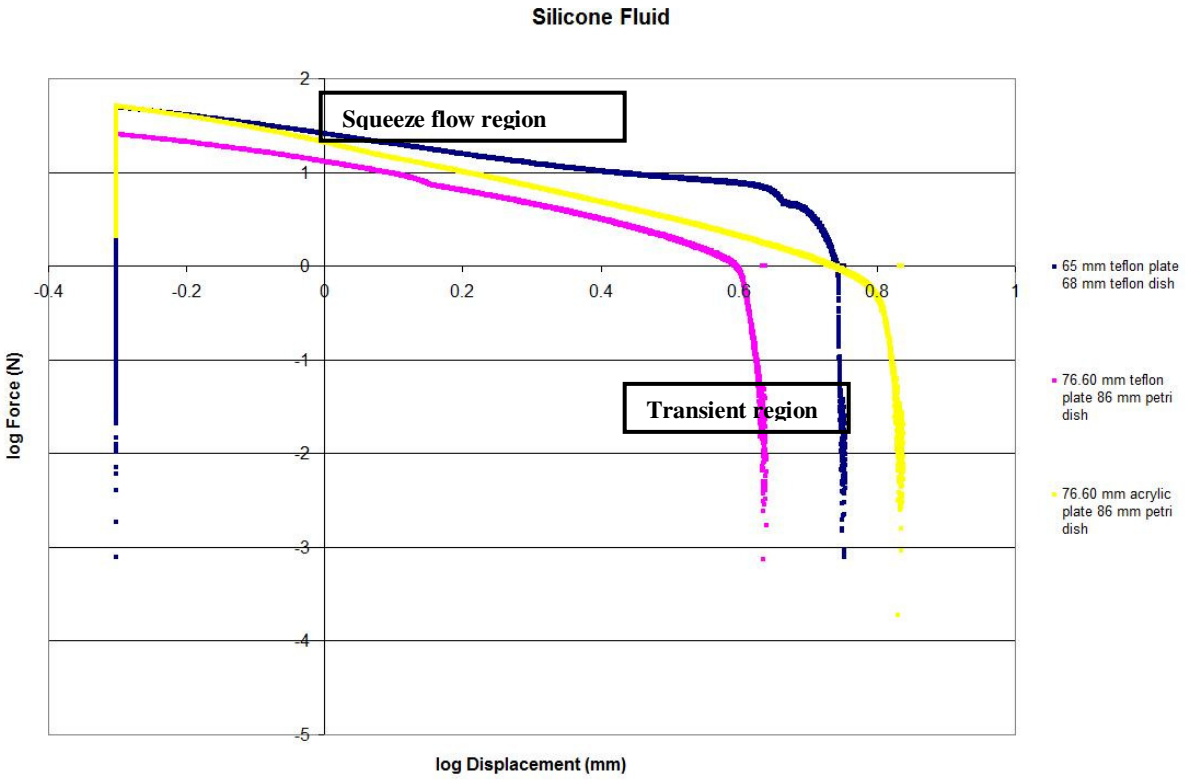

Figure 4.4. log Force vs. log Displacement plot for silicone fluid. From the slope of the squeeze flow region the flow index behavior is calculated.

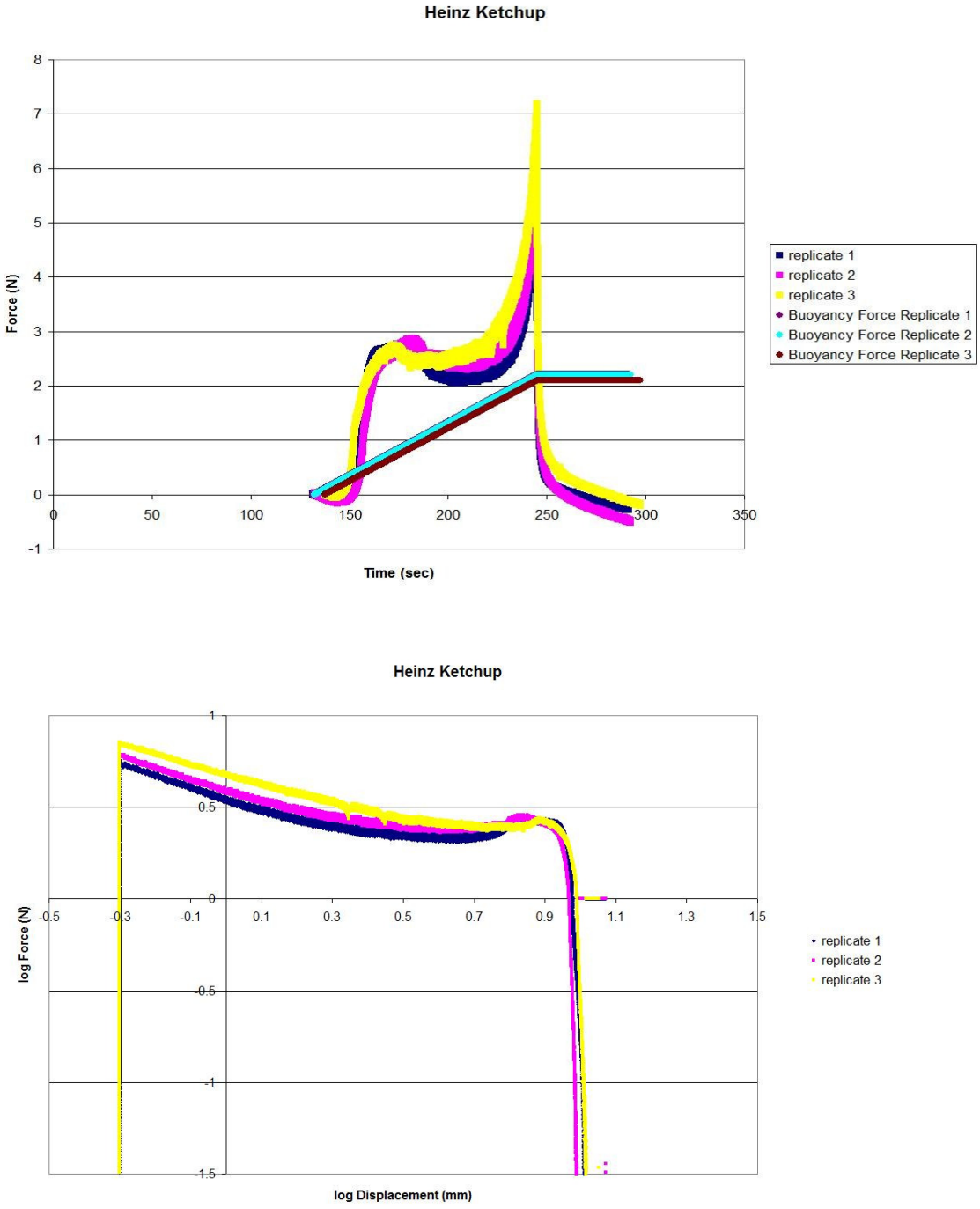

Figure 4.5. Force vs. time plot for ketchup (top), log Force vs. log Displacement plot for ketchup (bottom). The apparent yield stress is calculated from the measured force after two minutes relaxation as seen in the force vs. time plot. The flow index behavior is calculated from the squeezing region in log Force vs. log Displacement plot.

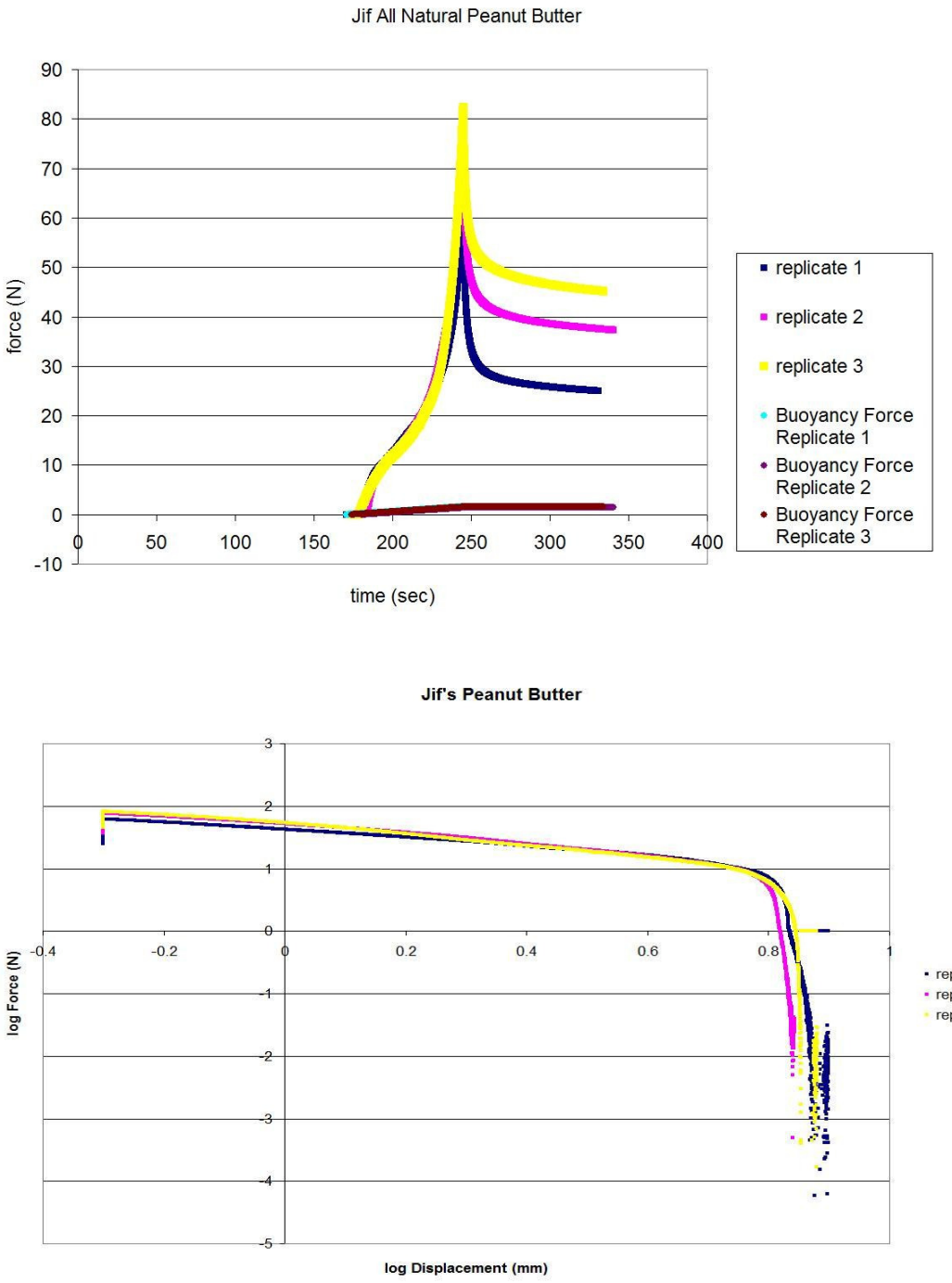

Figure 4.6. Force vs. time plot for peanut butter (top), log Force vs. log Displacement plot for peanut butter (bottom). The apparent yield stress is calculated from the measured force after two minutes relaxation as seen in the force vs. time plot. The flow index behavior is calculated from the squeezing region in log Force vs. log Displacement plot.

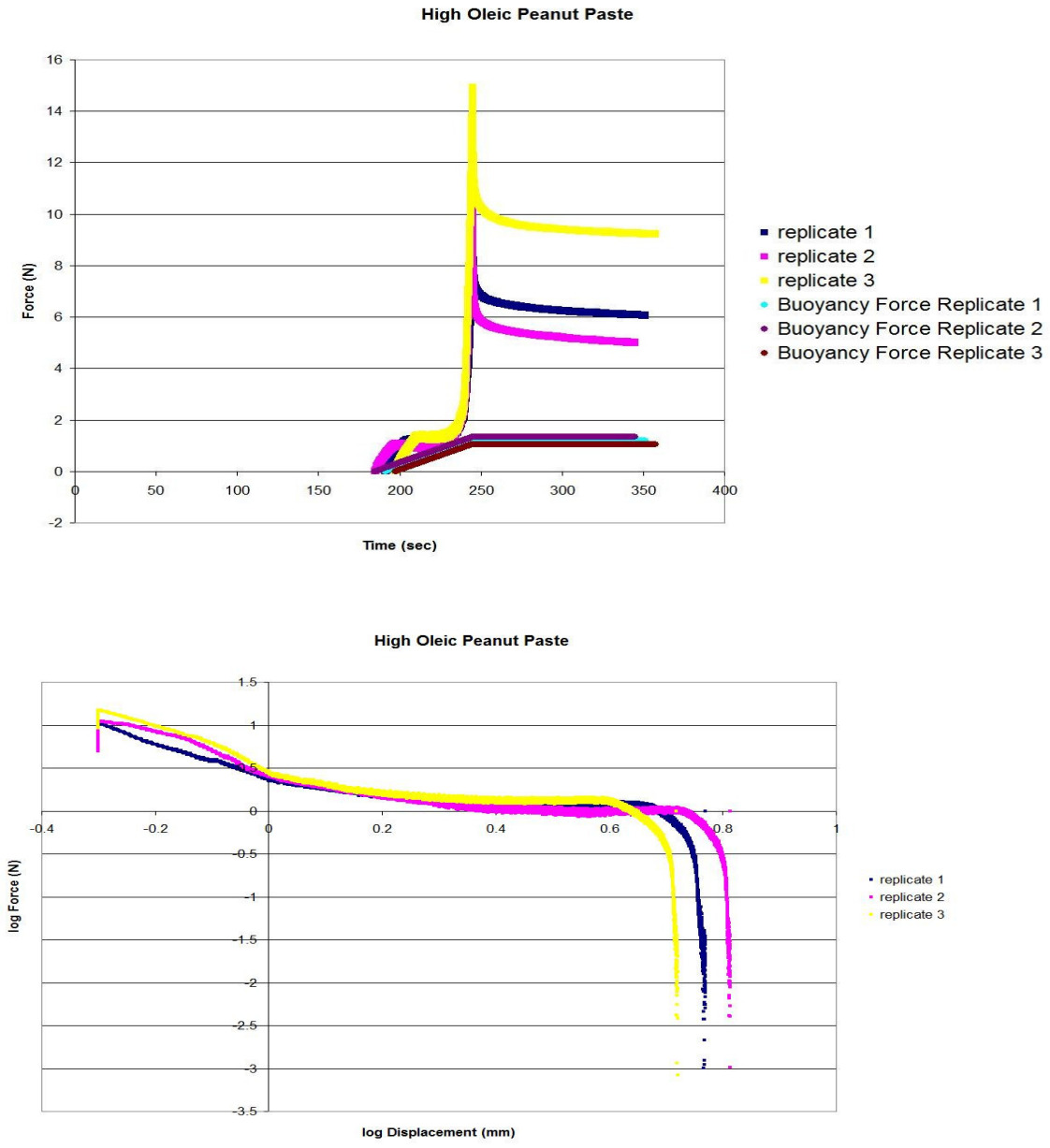

Figure 4.7. Force vs. time plot for high oleic peanut paste (top), log Force vs. log Displacement plot for high oleic peanut paste (bottom). The apparent yield stress is calculated from the measured force after two minutes relaxation as seen in the force vs. time plot. The flow index behavior is calculated from the squeezing region in log Force vs. log Displacement plot.

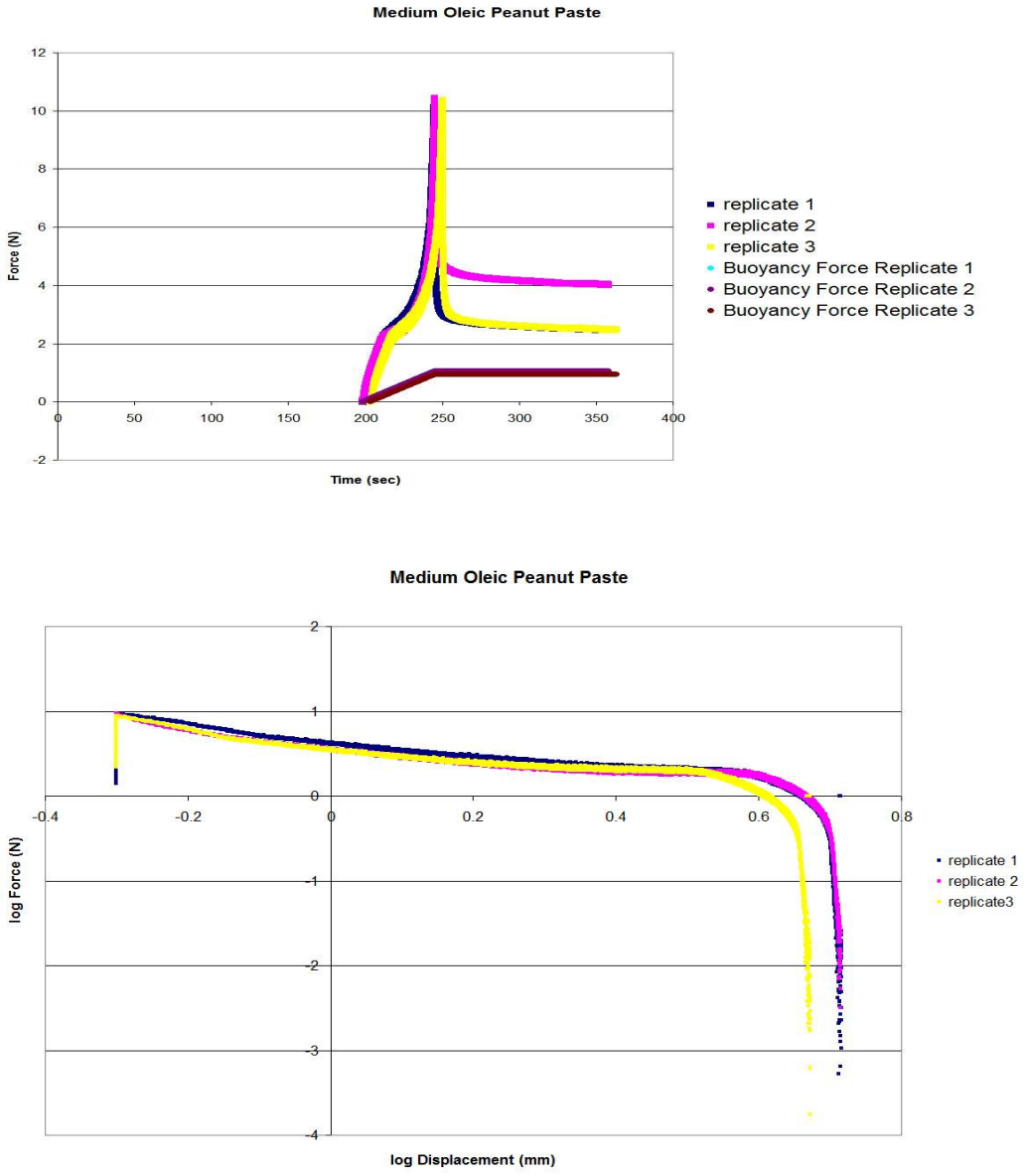

Figure 4.8. Force vs. time plot for medium oleic peanut paste (top), log Force vs. log Displacement plot for medium oleic peanut paste (bottom). The apparent yield stress is calculated from the measured force after two minutes relaxation as seen in the force vs. time plot. The flow index behavior is calculated from the squeezing region in log Force vs. log Displacement plot.

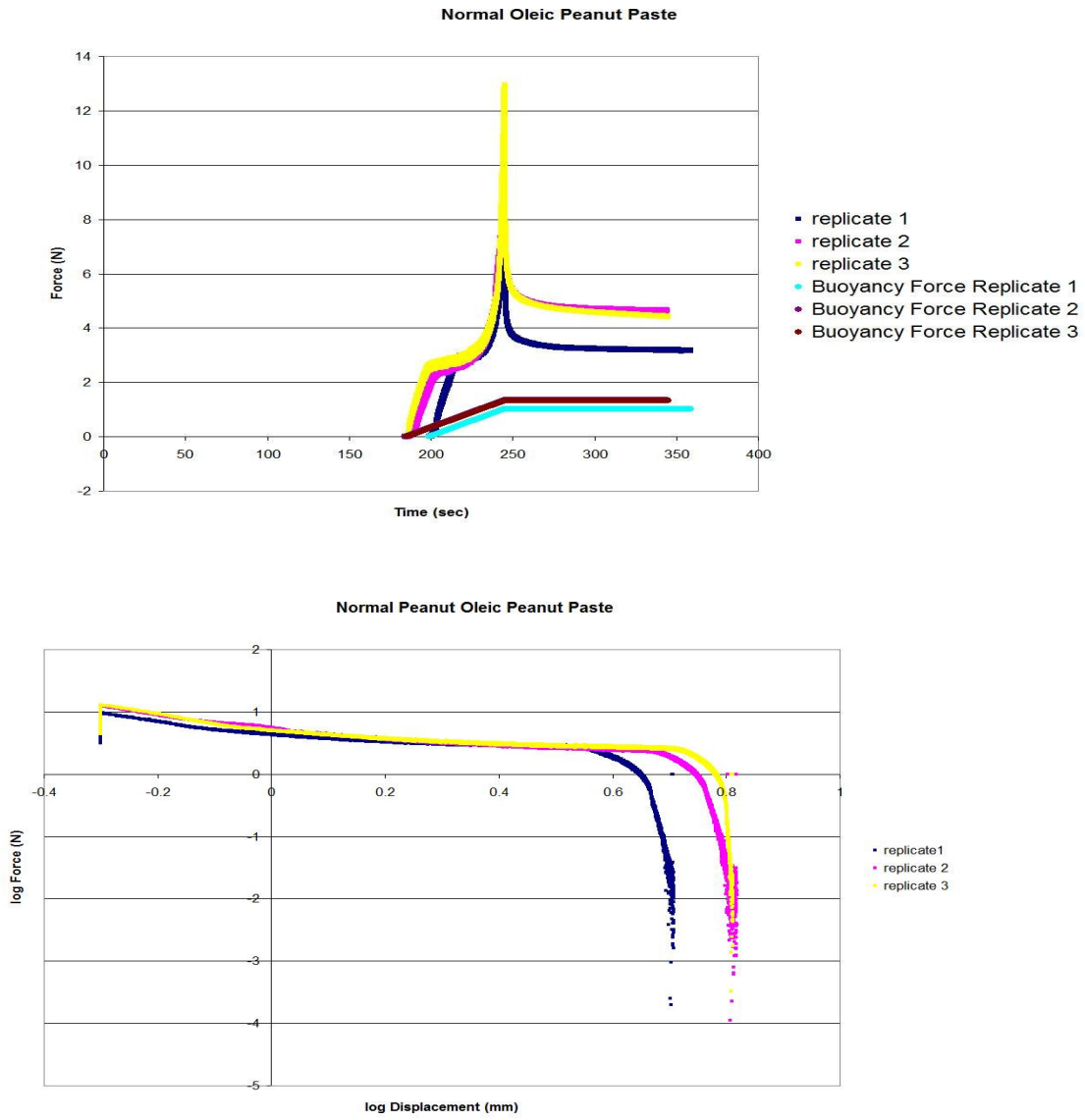

Figure 4.9. Force vs. time plot for normal oleic peanut paste (top), log Force vs. log Displacement plot for normal oleic peanut paste (bottom). The apparent yield stress is calculated from the measured force after two minutes relaxation as seen in the force vs. time plot. The flow index behavior is calculated from the squeezing region in log Force vs. log Displacement plot.

Table 4.1: Fatty acid analysis of peanut pastes

Sample	C16:0	C18:0	C18:1	C18:2	C20:0	C20:1	C22:0	C24:0
High Oleic	6.5 ±0.39	2.4 ±0.079	75.9 ±0.35	2.3 ±0.17	1.2 ±0.053	1.8 ±0.15	2.9 ±0.13	2.2 ±0.78
Medium Oleic	6.2 ±0.11	2.2 ±0.07	73.4 ±3.07	6.4 ±1.97	1.0 ±0.05	1.7 ±0.01	2.6 ±0.20	1.5 ±0.31
Normal Oleic	9.7 ±0.44	2.8 ±0.28	51.2 ±1.67	26.3 ±0.81	1.4 ±0.17	1.2 ±0.17	3.2 ±0.35	1.4 ±0.17

Mean Percent fatty acid ± standard deviation

Table 4.2. Apparent yield stress silicone fluid

Sample	**τ=k•Pa**
65 mm Teflon plate 68 mm Teflon dish	-0.3973 ± 0.028
76.60 mm Teflon plate 86 mm petri dish	-0.09076 ± 0.00
76.60 mm acrylic plate 86 mm petri dish	0.2477 ± 0.16

τ =yield stress, S.D =standard deviation

Table 4.3 Flow index behavior silicone fluid

Sample	***n*** ± S.D
65 mm Teflon plate 68 mm Teflon dish	0.91 ± 0.033
76.60 mm Teflon plate 86 mm petri dish	1.57 ± 0.07
76.60 mm acrylic plate 86 mm petri dish	1.54 ± 0.022

n= absolute value flow index, S.D =standard deviation

Table 4.4. Apparent yield stress of commercial ketchup and commercial peanut butter

Sample	**τ=k•Pa**
Ketchup	-0.2590 ± 0.09
Peanut Butter	10.61 ± 3.04

τ =yield stress, S.D =standard deviation

Table 4.5. Flow index behavior of commercial ketchup and commercial peanut butter

Sample	***n*** ± S.D
Ketchup	0.36 ± 0.03
Peanut Butter	0.76 ± 0.10

n= absolute value flow index, S.D =standard deviation

Table 4.6. Apparent yield stress of high, medium, normal oleic peanut pastes

Sample	**τ=k•Pa**
High Oleic Peanut Paste	2.023 ± 0.66
Medium Oleic Peanut Paste	0.5833 ± 0.24
Normal Oleic Peanut Paste	1.1705 ± 0.022

τ =yield stress, S.D =standard deviation

Table 4.7. Flow index behavior of high, medium, normal oleic peanut pastes

Sample	***n*** ± S.D
High Oleic Peanut Paste	1.04 ± 0.05
Medium Oleic Peanut Paste	0.79 ± 0.019
Normal Oleic Peanut Paste	0.65 ± 0.031

n=absolute value flow index, S.D =standard deviation

CHAPTER 5: SENSORY EVALUATION AND OPTICAL MICROSCOPY CHARACTERIZATION OF FAT BLOOMED PEANUT CHOCOLATES

Abstract

Fat bloom is the formation of a crystal network on the surface of the chocolate. The crystal network formed from triacylglycerol polymorphism gives the chocolates a dull off -white appearance. An online sensory survey was conducted to evaluate the visual and textural properties of unbloomed and bloomed commercial peanut chocolates. The unbloomed and bloomed chocolates were characterized using optical microscopy and a colorimeter. The rate of bloom formation was determined by the number of temperature cycles between 26-29°C needed for visual differences in color. Sensory evaluation among chocolate consumers found the unbloomed chocolate candy bar to have a similar mean glossiness rating as one of the bloomed chocolate candy bar's but different from the other bloomed candy bar. The sensory results showed the surface texture of the unbloomed chocolate candy bar was found to be smoother in comparison to the two bloomed chocolate candy bars. Characterization of fat bloomed chocolates showed a lighter color and more coarse surface as compared to the unbloomed chocolates. There was significant difference between whiteness values of unbloomed and bloomed chocolates.

5.1 Introduction

Chocolate is undoubtedly one of the most popular confectionary products in the world. The satisfaction that the rich creamy and sweet taste that chocolate gives to consumers is often considered irreplaceable by other sweets. Chocolate contains a minimum 18% cocoa butter, which is the main fat responsible for fat bloom formation (Lonchampt and Hartel, 2004). Fat bloom is the formation of large imperfect fat crystals on the surface of the confectionary. The crystal network scatters light giving the chocolates a gray to off-white discoloration. The low melting fractions of triacylglycerols in cocoa butter can polymorph from small to large crystals giving rise to fat bloom. The discoloration may vary from partial to full coverage, which leads to highly debated questions regarding the mechanism (porous or simple diffusion) behind bloom formation. There are three main ways to trigger bloom formation, and these include lack of tempering, incompatible fats, and temperature fluctuations. Temperature fluctuations may be the most important factor that affects the chocolates quality stability as bloom formation can occur often during storage and handling by consumers. Slight increases in temperature increase the volume of liquid triacylglycerols in the chocolate forcing the migration of the triacylglycerols to the surface (Lonchampt and Hartel, 2004). The re-crystallization step which occurs upon cooling results in polymorphic transition of the crystals from the βV to the βVI structure. Depending on if the crystals form as spikes or layers affects the appearance of visual bloom as spiky crystals are needed to reflect light (Bricknell and Hartel, 1998; Lonchampt and Hartel, 2004).

Previous studies using analytical instruments such as atomic force microscopy (AFM) and environmental scanning electron microscopy (ESEM) have well documented the visual

textural (roughness) effects of fat bloom on the quality of the confectionery (Rousseau and Smith, 2008; James and Smith, 2009; Hodge and Rousseau, 2002). The surface roughness is the statistical deviation from the average height, but this may not give information of height distribution over the surface. The visual effect is easily discernible using instruments such as a colorimeter, optical microscopy or simple documentation with a camera.

Few studies have examined sensory aspects of fat bloom formation in commercial chocolates. Most sensory studies have focused on accelerating bloom on dark chocolates made in the lab followed by evaluation with a trained descriptive panel (Ali et al., 2001; Andrae-Nightingale et al., 2009). Fat bloom formation on dark chocolates makes detection of the characteristic white discoloration very obvious. Milk chocolates take a longer time to bloom as increasing milk fractions have been shown to delay bloom formation (Sonwai and Rousseau, 2010). Sensory evaluation of chocolates includes five critical senses described by Voltz and Beckett (1997). The five critical senses include sight, touch, smell, and taste (the most important sensory quality) (Voltz and Beckett, 1997). If the chocolates lack gloss or appear bloomed the chocolates will be less likely to be purchased (Voltz and Beckett, 1997). Touch, described by Voltz and Beckett is the snap of the chocolates when the bar is bitten into. This property is also termed as texture and can be further defined as the mechanical and geometric properties of the product (Meilgaard and others 2007). The mechanical properties include hardness, cohesiveness, adhesiveness, denseness, and springiness. The geometric properties include perception of size, shape and orientation such as smoothness of the product.

The objective of this study was to visually characterize the glossiness and surface texture properties of unbloomed and bloomed commercial peanut chocolates. The characterization techniques included an online sensory evaluation composed of untrained panelists who represent

the average consumer and characterization of the geometric properties of surface roughness and height distribution of the chocolate surface using optical microscopy.

5.2 Materials and Methods

Large Hershey's ® Mr. Goodbar chocolates were purchased locally. The chocolates were broken into squares (dimensions) and were subjected to accelerated fat bloom formation by temperature cycling between 26 °C and 29 °C every 26 hours. The chocolate squares were visually examined and observations were noted once daily. After 45 day of temperature cycling the bloomed chocolate microstructure was examined using digital optical microscopy (KH-7700 unit, lens model MX 5040Z and MX(G)-10C-OL 700(II) Hirox, Tokyo, Japan). Pictures were taken under normal resolution 50X magnification (Figure 5.1) and under high resolution at 700x-1400x magnification (Figure 5.2). The L*,a*, and b* values for color of the chocolates was measured using a colorimeter (Minolta CHROMA METER CR-200 Osaka, Japan). The whiteness index (WI) was calculated according to the following equation:

$$WI = 100 - [(100-L^*)^2 + a^{*2} + b^{*2}]^{1/2}$$

A visual sensory evaluation of unbloomed and bloomed chocolates was done to determine differences in color glossiness and surface texture attributes of the chocolates. Sensory evaluation was conducted using survey.vt.edu. The only requirements to participate were being at least 18 years old and possessing the ability to distinguish color differences. Panelists (n=57) were presented with three coded chocolate candy bar samples; a fresh chocolate candy piece (#580) and two chocolate candy pieces (#294, #313) removed after 45 days of storage under temperature cycling from 26-29 °C approximately every 26 hours. Panelists were asked to visually evaluate and rate the glossiness and surface texture attributes using the provided scale

(Appendix E). Panelists personal information and contact information were not collected. Following completion of the questionnaire, subjects were asked to complete a demographics survey (Appendix E). Approval from the Institutional Review Board (IRB) for research involving human subjects was received (IRB # 06-619) prior to conducting the sensory tests (Appendix F).

Data analysis was performed using one way Anova tests to determine the *F* statistic and Tukey's HSD using JMP (JMP 8.0, 2008, SAS Institute, New Jersey, USA). For the sensory survey tests the null hypothesis (H_0)= no significant difference between glossiness and surface texture of unbloomed and bloomed chocolates and the alternate hypothesis (H_A)=significant difference between glossiness and surface texture of bloomed and unbloomed chocolates. Each rating was assigned a corresponding numeric values; very shiny or very smooth=1, shiny and smooth =2, dull and rough =3, very dull and very rough =4.

5.3 Results and Discussion

Our observations noted that after 5 days, there was an increase in the number of holes or cracks forming on the surface of the chocolate. This effect may be due to the dry air environment of the incubator. After 16 days the glossiness of the chocolates appeared duller as compared to chocolates at day 0. The dullness in the chocolate gloss is characteristic of bloom as reported in other studies (Bricknell and Hartel, 1998). After 45 days, the colorimeter readings also indicated significant difference in the whiteness values of unbloomed (WI=32. 38) being darker than the bloomed (WI=35. 91) chocolates as previously reported (Sonwai and Rousseau, 2010; Lohman and Hartel, 1994). The optical microscopy results of this study indicate that after 45 days of temperature cycling the bloomed chocolates had considerable surface roughness and appeared

duller in color as compared to the unbloomed chocolate (Figure 5.1 and Figure 5.2). The spiky crystals are not evident in these pictures. Rousseau and Smith were able to document formation of the spiky crystals using environmental scanning microscopy (ESEM) and Hodge and Rousseau (2002) and Khan and Rousseau (2006) both used atomic force microscopy (AFM) to show increased coarseness of the surface consistent with the findings in this study. Our initial attempt to search for these structures using AFM was unsuccessful. The switch to optical microscopy was a valid approach though as the size of the bloomed crystal structures is greater than 5 μm, which is the height limitation of using AFM (Khan and Rousseau, 2006). A 3-d image analysis of the surface topography of the chocolates indicated differences in the height distribution of the unbloomed and bloomed chocolates. The dullness and incomplete coverage of the characteristic white haze indicated that the fat bloom was still progressing or the chocolate crystals formed in layers rather than sharp spikes as Lonchampt and Hartel (2004) hypothesized. Khan and Rousseau reported advanced signs of bloom formation with large crystal formation evident on hazelnut filled chocolates stored at 26 °C after 14 days. This rapid formation of spiky crystal was not evident in our chocolates most likely due to a difference in composition or more time needed for fat bloom to form significant crystals. Khan and Rousseau made their confectionery with dark chocolate and 40 wt% hazelnut oil filling. Chocolates with fillings generally have a greater amount of saturated fat that can directly contribute to fat bloom crystal formation.

The height distribution of unbloomed chocolates determined using optical microscopy ranged from 5.83 μm to 8.15 μm with the average height being 6.81 ± 0.58 μm. This height measurement is larger than height measurements reported by Khan and Rousseau (2006) for unbloomed plain chocolates. The height distribution of bloomed chocolates using optical

microscopy ranging from 7.61 μm to 15.02 μm with the average height being 10.68 ± 1.70 μm. The height distribution at the surface of the chocolates reported in this study may have been affected by the proximity of the peanuts embedded in the chocolates to the surface.

For the glossiness attribute the calculated *F* statistic was greater than the critical value of *F*, so the null hypothesis was rejected in favor of the alternate hypothesis. Sensory analysis revealed that panelists were not able to distinguish differences in the glossiness of the unbloomed and one of the two bloomed chocolates. The unbloomed chocolate bar coded #580 (center position) was not significantly different in glossiness from bloomed chocolate bar #294 (left position) but significantly different from bloomed chocolate bar #313 (right position). The unbloomed chocolate bar #580 had a mean glossiness rating value of 2.28 and the bloomed chocolate bar #294 (left position) a mean glossiness rating value of 2.26 indicating both chocolates had a generally shiny characteristic. The bloomed chocolate bar # 313 (right position) had a mean glossiness rating value of 2.80 indicating the chocolate was generally considered dull. The sensory results for glossiness confirm the assumption that the chocolates were still undergoing bloom and visual coverage of bloom was incomplete.

Other possible explanations for the panelists to consider the unbloomed chocolate bar #580 (center) and bloomed chocolate bar # 294 (left position) as having similar shininess maybe due to differences in the variability of the contrast and brightness ratios of individual liquid crystal display (LCD) screens and the presentation order of the samples. Differences in screen variability are independent factors that can make panelists unable to accurately identify the glossiness attribute. All three samples were presented at the same, which may have increased the tendency of the panelists to compare the samples (contrast effect) rather than view each sample independently (Meilgaard et al., 2007).

For the texture attribute the calculated *F* statistic was greater than the critical value of *F*, so the null hypothesis was rejected in favor of the alternate hypothesis. All three samples had a mean surface texture rating significantly different from each other. The unbloomed chocolate bar #580 had a mean surface texture rating value of 2.23 indicating a smooth surface. The bloomed chocolate bar #294 (left position) had a mean surface texture rating value of 2.54 and the bloomed chocolate bar # 313 (right position) had a mean surface texture rating value of 2.83 indicating the bloomed chocolates were more rough than the unbloomed chocolates. The sensory results for the surface texture attribute are in agreement with the rough/coarse surface texture of bloomed chocolates observed using digital optical microscopy (Figure 5.2).

The demographics survey indicated that the respondents were 43% female and 57% male. The majority of respondents fell in the category of consuming chocolates regularly (once a week), occasionally (2 or 3 times a month), or frequently (2 to 6 times a week). The demographics survey was vital to show that among chocolate consumers 67% of respondents had previously seen whitish discoloration on the surface of the chocolate, but most chocolate consumers did not know that the discoloration on the surface of the chocolates was a result of fat bloom formation. Majority (40%) of the respondents thought the discoloration was because the chocolates had gone old. The demographics survey also brings added attention that fat bloom is a problem that needs to be addressed even more in dark chocolates with a nut based filling. The demographics survey also showed that dark chocolates were slightly more preferred than milk chocolates and nut or nut cream filling chocolates are the most popular filling choice in chocolates. Chocolates with nut filling are more prone to fat bloom formation as compared to plain chocolates.

Conclusions

The optical microscopy scans showed differences in glossiness and surface texture of unbloomed and bloomed chocolates. The visual sensory study results did not show the unbloomed chocolates as having the shiniest gloss. The surface texture results from the visual sensory survey study did show the bloomed chocolates as being rough in comparison to unbloomed chocolates. Both the optical microscopy and visual sensory survey results indicated fat bloom was still progressing in the chocolates candies examined in this study. Fat bloom in chocolates is a quality problem that still requires ways to reduce the discoloration as most consumers that have seen white discoloration on the surface of the chocolate think the color change is because the chocolate has grown old.

References

Ali A, Selamat J, CheMan YB & Suria AM. 2001. Effect of storage temperature on texture, polymorphic structure, bloom formation and sensory attributes of filled dark chocolate. Food Chemistry 72(4):491-497.

Andrae-Nightingale LM, Lee S-Y & Engeseth NJ. 2009. Textural changes in chocolate characterized by instrumental and sensory techniques. Journal of Texture Studies 40:427-444.

Bricknell J & Hartel R. 1998. Relation of fat bloom in chocolate to polymorphic transition of cocoa butter. Journal of the American Oil Chemists' Society 75(11):1609-1615.

Hodge S & Rousseau D. 2002. Fat bloom formation and characterization in milk chocolate observed by atomic force microscopy. Journal of the American Oil Chemists' Society 79(11):1115-1121.

James BJ & Smith BG. 2009. Surface structure and composition of fresh and bloomed chocolate analysed using X-ray photoelectron spectroscopy, cryo-scanning electron microscopy and environmental scanning electron microscopy. LWT - Food Science and Technology 42(5):929-937.

Khan RS & Rousseau D. 2006. Hazelnut oil migration in dark chocolate - kinetic, thermodynamic and structural considerations. European Journal of Lipid Science and Technology 108(5):434-443.

Lohman M & Hartel R. 1994. Effect of milk fat fractions on fat bloom in dark chocolate. Journal of the American Oil Chemists' Society 71(3):267-276.

Lonchampt P & Hartel RW. 2004. Fat bloom in chocolate and compound coatings. European Journal of Lipid Science and Technology 106(4):241-274.

Meilgaard MC, Civille GV & Carr BT. 2007. Sensory Evaluation Techniques. Boca Raton: CRC press. p. 9-10, 341-343.

Rousseau D & Smith P. 2008. Microstructure of fat bloom development in plain and filled chocolate confections. The Royal Society of Chemistry Soft Matter 4:1706-1712.

Sonwai S & Rousseau D. 2010. Controlling fat bloom formation in chocolate - Impact of milk fat on microstructure and fat phase crystallization. Food Chemistry 119(1):286-297.

Voltz M & Beckett ST. 1997. Sensory of chocolate. The Manufacturing Confectioner February 49.

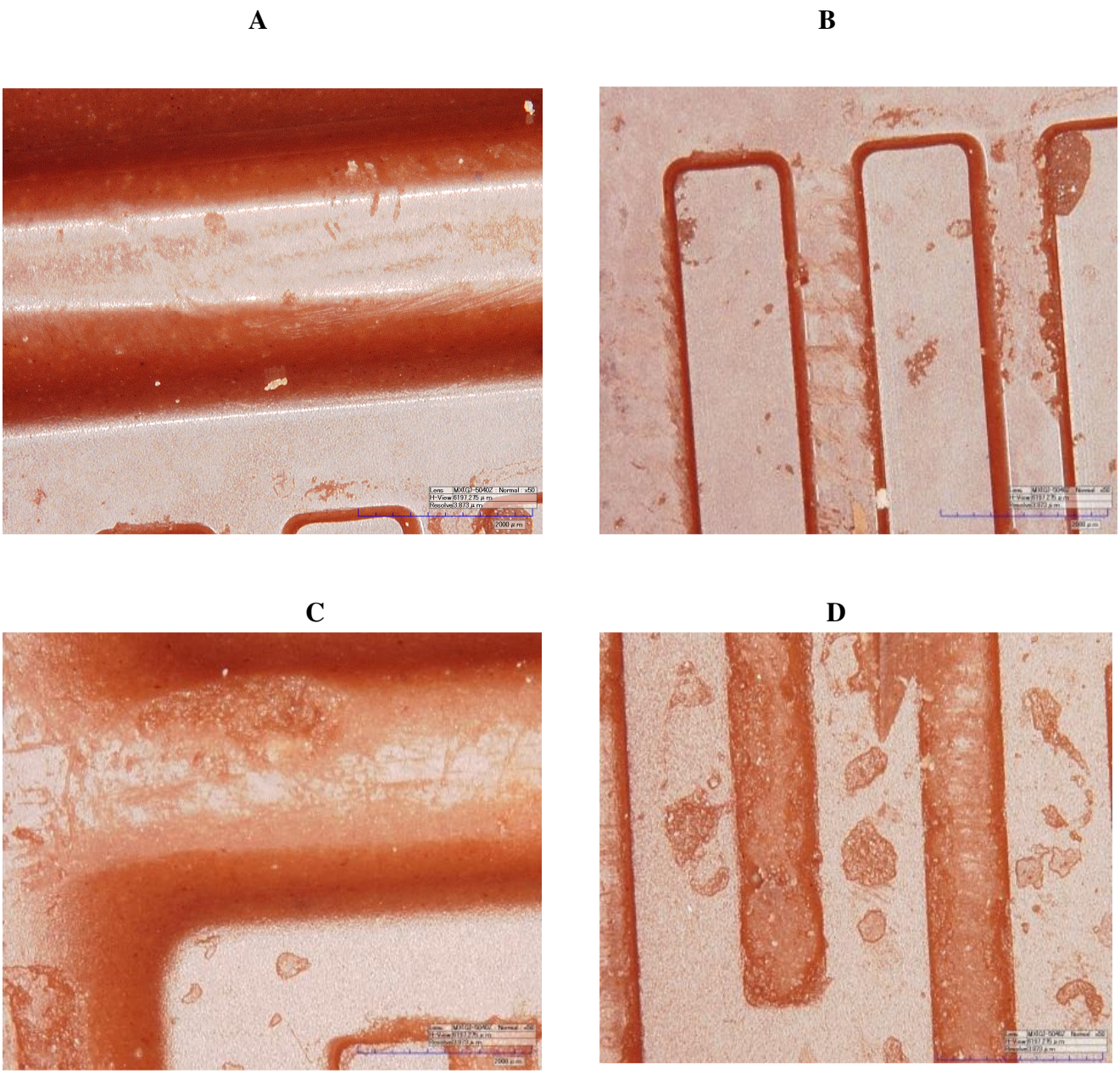

Figure 5.1: Chocolates examined under 50X magnification using a digital optical microscope. A & B unbloomed chocolates (top), C & D bloomed chocolates (bottom).

A **B**

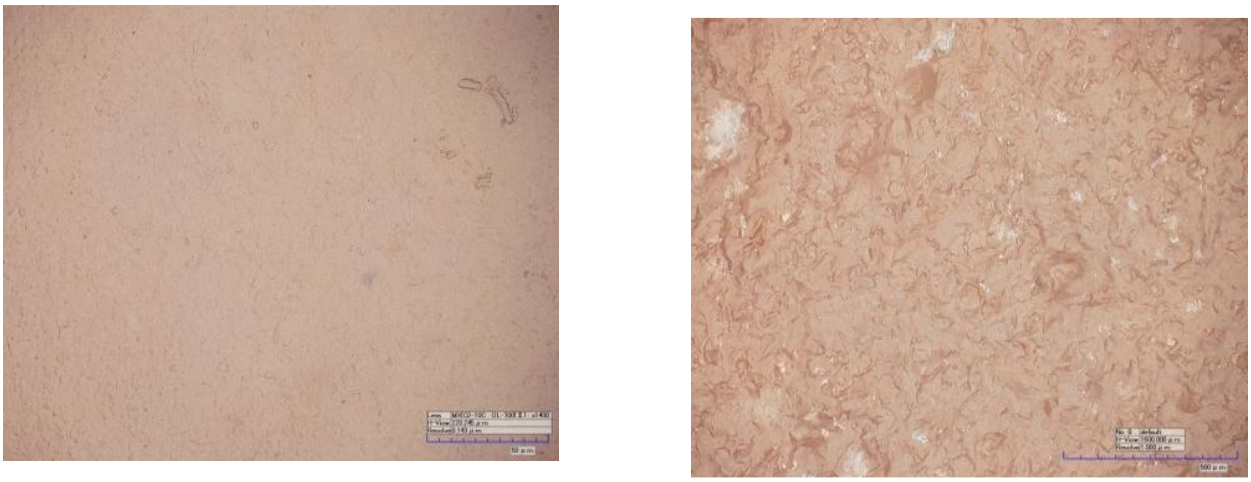

Figure 5.2: Chocolates examined under high magnification using a digital optical microscope. A) unbloomed chocolates under 1400x magnification (left), B) bloomed chocolates under 700x magnification (right).

CHAPTER 6 CONCLUSIONS

The triacylglycerol composition of oils from high oleic, medium oleic, and normal oleic oils were successfully analyzed using MALDI-MS/TOF. When comparing the MALDI-MS/TOF to the GC method for triacylglycerol analysis, the MALDI-MS/TOF method proved to be more effective in detecting and providing rapid and reproducible analysis of the peanut oils. All peanut oils had similar triacylglycerol compositions, however the concentration of each triacylglycerol species varied, thus making the decision of which peanut variety maybe least likely to contribute to fat bloom formation difficult to predict. The main triacylglycerol species in the peanut oils was triolein. The triacylglycerols composition of peanut oils was not similar to cocoa butter eliminating any direct link of polymorphism of triacylglycerols in peanut oils to fat bloom formation in peanut chocolate confectionery.

The imperfect squeezing flow set up was used to study the yield stress and flow behavior of high oleic, medium oleic, and normal oleic peanut pastes. All peanut pastes samples had a minimum yield stress and the difference in yield stress may be attributed to differences in fatty acid content due to differences in the degree of unsaturation and chain length. All three peanut paste varieties showed differences in flow behavior and this may be attributed to differences in polyunsaturated fatty acid content. The close to 1 flow index value of high oleic peanut pastes strongly suggests that friction was not eliminated even with the use of Teflon plates with a low coefficient of friction.

Optical microscopy proved sensitive enough to evaluate difference in surface texture of unbloomed and bloomed peanut chocolates. There are no previous studies reported for use of optical microscopy for evaluating fat bloom in chocolates. The rate of fat bloom formation in peanut chocolate confectionery was approximately 45 days with temperature cycling between 26

°C and 29 °C approximately every 26 hours. The microscopy results showed dullness of the chocolates and a roughened surface, both traits being characteristic of fat bloom formation. The sensory results gave mixed review of glossiness and surface texture evaluation as determined by an online visual survey using photos of bloomed and unbloomed chocolates. The results suggest that the use of virtual online surveys for evaluation of fat bloom in chocolates may not be very accurate and representative of ratings as compared to an in-person onsite sensory evaluation.

Future studies should focus on improving the rheological measurements recorded in this study. This may be accomplished by using a more sensitive instrument such as the Instron and examining the product using both roughened and smooth plates. This may also require further examination of the micro-structural properties of particles in the peanut paste specifically looking at the geometric properties of the particle shapes and interaction of various additives in the peanut pastes. The results from demographics survey respondents in this study serve as a reminder to manufacturers and researchers that consumers are well aware of discoloration in chocolates and novel methods to reduce bloom formation in nut fill confectionary still need to be developed.

APPENDIX A

Density Calculation

Density ρ =mass/volume

Where:
Mass=Mass of the empty pycnometer (kg)- Mass of filled pycnometer (kg)
Volume of pycnometer=1.98 mL= 1.98×10^{-6} m^3

For silicone fluid ρ =specific gravity from fluid certificate*density of water at 25 °Celsius

$$\frac{0.97 * .997 g/cm^3}{1000g * 1 \times 10^{-6} m^3}$$

Sample	Density kg/m^3	Standard Deviation
Silicone Fluid	967.1	N/A
Ketchup	577.61	1.84826
Jif's	579.01	0.737665
high peanut paste	589.74	1.234157
medium peanut paste	591.03	0.974088
normal peanut paste	587.89	2.320257

N/A=not available

APPENDIX B

Buoyancy Force Calculation

$$B(t)=\frac{[H_0-H_t]\ R^2_{dish}*R^2_{plate}*g*\rho*\pi}{R^2_{dish}-R^2_{plate}}$$

Where:
R^2_{dish}=radius of the dish (m^2)
R^2_{plate}=radius of the upper plate (m^2)
g=gravitational acceleration=9.81 m/s^2
ρ=density (kg/m^3)
$[H_0-H_t]$=Initial Height (m)-Final Height (m)

Silicone Fluid

Teflon upper plate/Teflon dish
Diameter Upper plate =65 mm
Diameter Teflon dish= 68 mm
g=9.81 m/s^2
ρ= density of silicone fluid =967.1 kg/m^3
$B(t)=(H_0-H_t)*364.83\ kg/s^2$

Ketchup

Teflon upper plate/Teflon dish
Diameter Upper plate =65 mm
Diameter Teflon dish= 68 mm
g=9.81 m/s^2
ρ= density of Ketchup =577.61 kg/m^3
$B(t)=(H_0-H_t)*195.07\ kg/s^2$

Peanut Butter

Teflon upper plate/Teflon dish
Diameter Upper plate =65 mm
Diameter Teflon dish= 68 mm
g=9.81 m/s^2
ρ= density of peanut butter =579.01 kg/m^3
$B(t)=(H_0-H_t)*218.43\ kg/s^2$

High Oleic Paste

Teflon upper plate/Teflon dish
Diameter Upper plate =65 mm
Diameter Teflon dish= 68 mm
g=9.81 m/s^2
ρ= density of high oleic peanut paste =589.74 kg/m^3
$B(t)=(H_0-H_t)*222.48$ kg/s^2

Medium Oleic Paste

Teflon upper plate/Teflon dish
Diameter Upper plate =65 mm
Diameter Teflon dish= 68 mm
g=9.81 m/s^2
ρ= density of medium oleic peanut paste =591.03 kg/m^3
$B(t)=(H_0-H_t)*222.97$ kg/s^2

Normal Oleic Paste

Teflon upper plate/Teflon dish
Diameter Upper plate =65 mm
Diameter Teflon dish= 68 mm
g=9.81 m/s^2
ρ= density of normal oleic peanut paste =587.89 kg/m^3
$B(t)=(H_0-H_t)*221.78$ kg/s^2

APPENDIX C

Apparent Yield Stress Calculation

$\tau_o = F_{@time} / \pi R^2$

Where:
$F_{@time}$ =Force after 2 minutes
π=approximately 3.14
R^2=radius of upper plate =.00105625 m^2

APPENDIX D

Shear Viscosity Calculation

Shear Viscosity under lubricated conditions

$$\mu_s = \frac{(Force_{height\ A} - Force_{heightB})}{(3\pi R^2_{plate} Velocity[1/H_{eightA} - 1/H_{eightB}])}$$

Where:

$F_{height\ A}$ =the force at a given height from point A chosen in the squeeze flow region

$F_{height\ B}$= the force at a given height from a point B chosen in the squeeze flow region

R^2_{plate}=radius of upper plate =.00105625 m^2

Velocity= 0.0001 m

$1/ H_{eightA}$= the reciprocal of the height from point A chosen in the squeeze flow region

$1/ H_{eightB}$= the reciprocal of the height from point B chosen in the squeeze flow region

APPENDIX E

Online Survey Questionnaire

This is an online survey for visual sensory evaluation of chocolates candies followed by a brief demographic questionnaire. The emotional risks associated with this survey are very minimal. No personal information or contact information will be collected from this study. If you do not want to complete the survey you are not obligated to do so. You are free to withdraw at anytime (by closing the window). By clicking on the agree button below you acknowledge that you are at least 18 years old, that you do not have any problems visually distinguishing color, and that you understand the risks associated with this study are minimal. Thank you for your participation.

I agree

I disagree (please close this window)

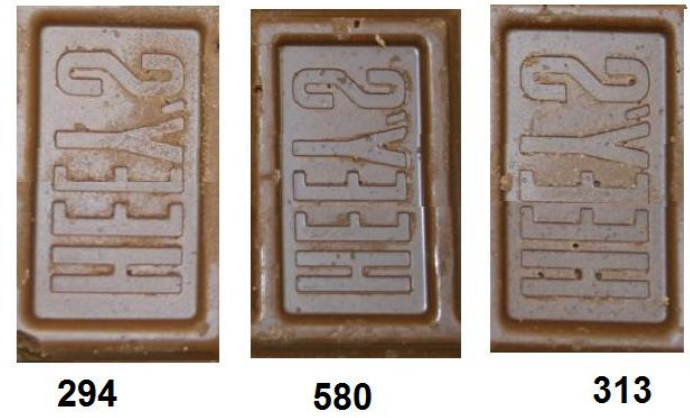

Rate the glossiness for chocolate candy bar # 294 (on the far left)
very shiny
shiny
dull
very dull

Rate the surface texture intensity for chocolate candy bar # 294 (on the far left)
very smooth
smooth
rough
very rough

Rate the glossiness for chocolate candy bar # 580 (center)
very shiny
shiny
dull
very dull

Rate the surface texture intensity for chocolate candy bar # 580 (center)
very smooth
smooth
rough

very rough

Rate the glossiness for chocolate candy bar # 313 (on the far right)
very shiny
shiny
dull
very dull

Rate the surface texture intensity for chocolate candy bar # 313 (on the far right)
very smooth
smooth
rough
very rough

Please indicate your gender
male
female

How often do you consume chocolate?
daily (at least once a day)
frequently (2 to 6 times a week)
regularly (once a week)
occasionally (once or twice a month)
rarely (once a month)
never (less than 6 times a years)

Do you prefer dark chocolate or milk chocolate candy ?
dark chocolate
milk chocolate
equally prefer both types of chocolates
do not prefer either type of chocolates

Which is your most favorite filling inside a chocolate?
fruit filling
vanilla
coconut
caramel
nut (almond, peanut, hazelnut) or a nut cream filling such as peanut butter

Have you ever noticed a white discoloration on the surface of chocolate candy as seen below?

no
yes

If you answered yes to the above question please comment on what causes the white discoloration of chocolate? (check all that apply)
mold growth
the chocolate has grown old
sugar sprinkled on the surface
I don't know
other:

APPENDIX F

IRB Approval letter for Sensory Online Survey

MEMORANDUM

DATE: March 26, 2010
TO: Susan E. Duncan, Vinodini Buck, Sean F. O'Keefe

FROM: Virginia Tech Institutional Review Board (FWA00000572, expires June 13, 2011)

PROTOCOL TITLE: Sensory Evaluation of Peanut Chocolates

IRB NUMBER: 10-112
As of March 26, 2010, the Virginia Tech IRB Chair, Dr. David M. Moore, approved the new protocol for the above-mentioned research protocol. This approval provides permission to begin the human subject activities outlined in the IRB-approved protocol and supporting documents. Plans to deviate from the approved protocol and/or supporting documents must be submitted to the IRB as an amendment request and approved by the IRB prior to the implementation of any changes, regardless of how minor, except where necessary to eliminate apparent immediate hazards to the subjects. Report promptly to the IRB any injuries or other unanticipated or adverse events involving risks or harms to human research subjects or others.
All investigators (listed above) are required to comply with the researcher requirements outlined at http://www.irb.vt.edu/pages/responsibilities.htm (please review before the commencement of your research).

PROTOCOL INFORMATION:
Approved as: **Exempt, under 45 CFR 46.101(b) category(ies) 6**
Protocol Approval Date: **3/26/2010**
Protocol Expiration Date: **NA**
Continuing Review Due Date*: **NA**
*Date a Continuing Review application is due to the IRB office if human subject activities covered under this protocol, including data analysis, are to continue beyond the Protocol Expiration Date.

FEDERALLY FUNDED RESEARCH REQUIREMENTS:
Per federally regulations, 45 CFR 46.103(f), the IRB is required to compare all federally funded grant proposals / work statements to the IRB protocol(s) which cover the human research activities included in the proposal / work statement before funds are released. Note that this requirement does not apply to Exempt and Interim IRB protocols, or grants for which VT is not the primary awardee.
The table on the following page indicates whether grant proposals are related to this IRB protocol, and which of the listed proposals, if any, have been compared to this IRB protocol, if required.

Date* OSP Number Sponsor Grant Comparison Conducted?
If this IRB protocol is to cover any other grant proposals, please contact the IRB office (irbadmin@vt.edu) immediately.
*Date this proposal number was compared, assessed as not requiring comparison, or comparison information was revised.

Institutional Review Board
2000 Kraft Drive, Suite 2000 (0497)
Blacksburg, Virginia 24060
540/231-4606 Fax 540/231-0959
e-mail irb@vt.edu
Website: www.irb.vt.edu

APPENDIX G

Permission to Reproduce Figure from Damrau & Peleg (1997)

This is a License Agreement between Vinodini Buck ("You") and John Wiley and Sons ("John Wiley and Sons") provided by Copyright Clearance Center ("CCC"). The license consists of your order details, the terms and conditions provided by John Wiley and Sons, and the payment terms and conditions.

All payments must be made in full to CCC. For payment instructions, please see information listed at the bottom of this form.

License Number 2391130572235
License date Mar 16, 2010
Licensed content publisher John Wiley and Sons
Licensed content publication Journal of Texture Studies
Licensed content title IMPERFECT SQUEEZING FLOW VISCOSIMETRY OF NEWTONIAN LIQUIDS – THEORETICAL AND PRACTICAL CONSIDERATIONS
Licensed content author DAMRAU EVI, PELEG MICHA
Licensed content date Jan 30, 2007
Type of use Dissertation/Thesis
Requestor type University/Academic
Format Print and electronic
Portion Figure/table
Number of figures/tables 1
Original Wiley figure/table number(s)
Figure 3
Will you be translating? No
Order reference number
Total 0.00 USD
Terms and Conditions

TERMS AND CONDITIONS

This copyrighted material is owned by or exclusively licensed to John Wiley & Sons, Inc. or one if its group companies (each a "Wiley Company") or a society for whom a Wiley Company has exclusive publishing rights in relation to a particular journal (collectively "WILEY"). By clicking "accept" in connection with completing this licensing transaction, you agree that the following terms and conditions apply to this transaction (along with the billing and payment terms and conditions established by the Copyright Clearance Center Inc., ("CCC's Billing and Payment terms and conditions"), at the time that you opened your Rightslink account (these are available at any time at http://myaccount.copyright.com).

Terms and Conditions

1. The materials you have requested permission to reproduce (the "Materials") are protected by copyright.
2. You are hereby granted a personal, non-exclusive, non-sublicensable, non-transferable, worldwide, limited license to reproduce the Materials for the purpose specified in the licensing Rightslink Printable License https://s100.copyright.com/App/PrintableLicenseFrame.jsp?publisherID=... 1 of 3 3/16/2010 11:37 PM process. This license is for a one-time use only with a maximum distribution equal to the number that you identified in the licensing process. Any form of republication granted by this licence mustbe completed within two years of the date of the grant of this licence (although copies prepared before may be distributed thereafter). Any electronic posting of the Materials is limited to one year from the date permission is granted and is on the condition that a link is placed to the journal homepage on Wiley's online journals publication platform at www.interscience.wiley.com. The Materials shall not be used in any other manner or for any other purpose. Permission is granted subject to an appropriate acknowledgement given to the author, title of the material/book/journal and the publisher and on the understanding that nowhere in the text is a previously published source acknowledged for all or part of this Material. Any third party material is expressly excluded from this permission.
3. With respect to the Materials, all rights are reserved. No part of the Materials may be copied, modified, adapted, translated, reproduced, transferred or distributed, in any form or by any

means, and no derivative works may be made based on the Materials without the prior permission of the respective copyright owner. You may not alter, remove or suppress in any manner any copyright, trademark or other notices displayed by the Materials. You may not license, rent, sell, loan, lease, pledge, offer as security, transfer or assign the Materials, or any of the rights granted to you hereunder to any other person.
4. The Materials and all of the intellectual property rights therein shall at all times remain the exclusive property of John Wiley & Sons Inc or one of its related companies (WILEY) or their respective licensors, and your interest therein is only that of having possession of and the right to reproduce the Materials pursuant to Section 2 herein during the continuance of this Agreement. You agree that you own no right, title or interest in or to the Materials or any of the intellectual property rights therein. You shall have no rights hereunder other than the license as provided for above in Section 2. No right, license or interest to any trademark, trade name, service mark or other branding ("Marks") of WILEY or its licensors is granted hereunder, and you agree that you shall not assert any such right, license or interest with respect thereto.
5. WILEY DOES NOT MAKE ANY WARRANTY OR REPRESENTATION OF ANY KIND TO YOU OR ANY THIRD PARTY, EXPRESS, IMPLIED OR STATUTORY, WITH RESPECT TO THE MATERIALS OR THE ACCURACY OF ANY INFORMATION CONTAINED IN THE MATERIALS, INCLUDING, WITHOUT LIMITATION, ANY IMPLIED WARRANTY OF MERCHANTABILITY, ACCURACY, SATISFACTORY QUALITY, FITNESS FOR A PARTICULAR PURPOSE, USABILITY, INTEGRATION OR NON-INFRINGEMENT AND ALL SUCH WARRANTIES ARE HEREBY EXCLUDED BY WILEY AND
WAIVED BY YOU.
6. WILEY shall have the right to terminate this Agreement immediately upon breach of this Agreement by you.
7. You shall indemnify, defend and hold harmless WILEY, its directors, officers, agents and employees, from and against any actual or threatened claims, demands, causes of action or proceedings arising from any breach of this Agreement by you.
8. IN NO EVENT SHALL WILEY BE LIABLE TO YOU OR ANY OTHER PARTY OR ANY OTHER PERSON OR ENTITY FOR ANY SPECIAL, CONSEQUENTIAL, INCIDENTAL, INDIRECT, EXEMPLARY OR PUNITIVE DAMAGES, HOWEVER CAUSED, ARISING OUT OF OR IN CONNECTION WITH THE DOWNLOADING, PROVISIONING, VIEWING OR USE OF THE MATERIALS REGARDLESS OF THE FORM OF ACTION, WHETHER FOR BREACH OF CONTRACT, BREACH OF WARRANTY, TORT, NEGLIGENCE, INFRINGEMENT OR OTHERWISE (INCLUDING, WITHOUT LIMITATION, DAMAGES BASED ON LOSS OF PROFITS, DATA, FILES, USE, BUSINESS OPPORTUNITY OR CLAIMS OF THIRD PARTIES), AND WHETHER OR NOT THE PARTY HAS BEEN ADVISED OF THE POSSIBILITY OF SUCH DAMAGES. THIS LIMITATION SHALL APPLY NOTWITHSTANDING ANY FAILURE OF ESSENTIAL
PURPOSE OF ANY LIMITED REMEDY PROVIDED HEREIN.
9. Should any provision of this Agreement be held by a court of competent jurisdiction to be illegal, invalid, or unenforceable, that provision shall be deemed amended to achieve as nearly as possible the same economic effect as the original provision, and the legality, validity and enforceability of the remaining provisions of this Agreement shall not be affected or impaired thereby.
10. The failure of either party to enforce any term or condition of this Agreement shall not constitute a waiver of either party's right to enforce each and every term and condition of this

Agreement. No breach under this agreement shall be deemed waived or excused by either party unless such waiver or consent is in writing signed by the party granting such waiver or consent. The waiver by or consent of a party to a breach of any provision of this Agreement shall not operate or be construed as a waiver of or consent to any other or subsequent breach by such other party.
11. This Agreement may not be assigned (including by operation of law or otherwise) by you without WILEY's prior written consent.
12. These terms and conditions together with CCC’s Billing and Payment terms and conditions (which are incorporated herein) form the entire agreement between you and WILEY concerning this licensing transaction and (in the absence of fraud) supersedes all prior agreements and representations of the parties, oral or written. This Agreement may not be amended except in a writing signed by both parties. This Agreement shall be binding upon and inure to the benefit of the parties' successors, legal representatives, and authorized assigns.

13. In the event of any conflict between your obligations established by these terms and conditions and those established by CCC's Billing and Payment terms and conditions, these terms and conditions shall prevail.
14. WILEY expressly reserves all rights not specifically granted in the combination of (i) the license details provided by you and accepted in the course of this licensing transaction, (ii) these terms and conditions and (iii) CCC's Billing and Payment terms and conditions.
15. This Agreement shall be governed by and construed in accordance with the laws of England and you agree to submit to the exclusive jurisdiction of the English courts.
BY CLICKING ON THE "I ACCEPT" BUTTON, YOU ACKNOWLEDGE THAT YOU HAVE READ AND FULLY UNDERSTAND EACH OF THE SECTIONS OF AND PROVISIONS SET FORTH IN THIS AGREEMENT AND THAT YOU ARE IN AGREEMENT WITH AND ARE WILLING TO ACCEPT ALL OF YOUR OBLIGATIONS AS SET FORTH IN THIS AGREEMENT.
V1.2
Gratis licenses (referencing $0 in the Total field) are free. Please retain this printable license for your reference. No payment is required.
If you would like to pay for this license now, please remit this license along with your payment made payable to "COPYRIGHT CLEARANCE CENTER" otherwise you will be invoiced within 48 hours of the license date. Payment should be in the form of a check or money order referencing your account number and this invoice number RLNK10752161.
Once you receive your invoice for this order, you may pay your invoice by credit card. Please follow instructions provided at that time.
Make Payment To:
Copyright Clearance Center
Dept 001
P.O. Box 843006
Boston, MA 02284-3006
If you find copyrighted material related to this license will not be used and wish to cancel, please contact us referencing this license number 2391130572235 and noting the reason for cancellation.
Questions? customercare@copyright.com or +1-877-622-5543 (toll free in the US) or +1-978-646-2777.

APPENDIX H

Permission to Reproduce Figure from Sato (2001)

ELSEVIER LICENSE
TERMS AND CONDITIONS

Mar 06, 2010
This is a License Agreement between Vinodini Buck ("You") and Elsevier ("Elsevier") provided by Copyright Clearance Center ("CCC"). The license consists of your order details, the terms and conditions provided by Elsevier, and the payment terms and conditions.

All payments must be made in full to CCC. For payment instructions, please see information listed at the bottom of this form.

Supplier

Elsevier Limited
The Boulevard,Langford Lane
Kidlington,Oxford,OX5 1GB,UK

Registered Company Number 1982084

Customer name Vinodini Buck

Customer address 1102 Ascot Lane, Blacksburg, VA 24060

License Number 2383230069761

License date Mar 06, 2010

Licensed content publisher Elsevier

Licensed content publication Chemical Engineering Science

Licensed content title Crystallization behaviour of fats and lipids — a review

Licensed content author Kiyotaka Sato

Licensed content date April 2001

Volume number 56

Issue number 7

Pages 11

Type of Use Thesis / Dissertation

Portion Figures/tables/illustrations

Number of Figures/tables/illustrations 1

Format Both print and electronic

You are an author of the Elsevier article No

Are you translating? No

Order Reference Number

Expected publication date May 2010

Elsevier VAT number GB 494 6272 12

Permissions price 0.00 USD

Value added tax 0.0%

0.00 USD Total

0.00 USD

Terms and Conditions

INTRODUCTION

1. The publisher for this copyrighted material is Elsevier. By clicking "accept" in connection with completing this licensing transaction, you agree that the following terms and conditions apply to this transaction (along with the Billing and Payment terms and conditions established by Copyright Clearance Center, Inc. ("CCC"), at the time that you opened your Rightslink account and that are available at any time at http://myaccount.copyright.com).

GENERAL TERMS

2. Elsevier hereby grants you permission to reproduce the aforementioned material subject to the terms and conditions indicated.

3. Acknowledgement: If any part of the material to be used (for example, figures) has appeared in our publication with credit or acknowledgement to another source, permission must also be sought from that source. If such permission is not obtained then that material may not be included in your publication/copies. Suitable acknowledgement to the source must be made, either as a footnote or in a reference list at the end of your publication, as follows:

"Reprinted from Publication title, Vol /edition number, Author(s), Title of article / title of chapter, Pages No., Copyright (Year), with permission from Elsevier [OR APPLICABLE SOCIETY COPYRIGHT OWNER]." Also Lancet special credit - "Reprinted from The Lancet, Vol. number, Author(s), Title of article, Pages No., Copyright (Year), with permission from Elsevier."

4. Reproduction of this material is confined to the purpose and/or media for which permission is hereby given.

5. Altering/Modifying Material: Not Permitted. However figures and illustrations may be altered/adapted minimally to serve your work. Any other abbreviations, additions, deletions and/or any other alterations shall be made only with prior written authorization of Elsevier Ltd. (Please contact Elsevier at permissions@elsevier.com)

6. If the permission fee for the requested use of our material is waived in this instance, please be advised that your future requests for Elsevier materials may attract a fee.

7. Reservation of Rights: Publisher reserves all rights not specifically granted in the combination of (i) the license details provided by you and accepted in the course of this licensing transaction, (ii) these terms and conditions and (iii) CCC's Billing and Payment terms and conditions.

8. License Contingent Upon Payment: While you may exercise the rights licensed immediately upon issuance of the license at the end of the licensing process for the transaction, provided that you have disclosed complete and accurate details of your proposed use, no license is finally effective unless and until full payment is received from you (either by publisher or by CCC) as provided in CCC's Billing and Payment terms and conditions. If full payment is not received on a timely basis, then any license preliminarily granted shall be deemed automatically revoked and shall be void as if never granted. Further, in the event that you breach any of these terms and conditions or any of CCC's Billing and Payment terms and conditions, the license is automatically revoked and shall be void as if never granted. Use of materials as described in a revoked license, as well as any use of the materials beyond the scope of an unrevoked license, may constitute copyright infringement and publisher reserves the right to take any and all action to protect its copyright in the materials.

9. Warranties: Publisher makes no representations or warranties with respect to the licensed material.

10. Indemnity: You hereby indemnify and agree to hold harmless publisher and CCC, and their respective officers, directors, employees and agents, from and against any and all claims arising out of your use of the licensed material other than as specifically authorized pursuant to this license.

11. No Transfer of License: This license is personal to you and may not be sublicensed, assigned, or transferred by you to any other person without publisher's written permission.

12. No Amendment Except in Writing: This license may not be amended except in a writing signed by both parties (or, in the case of publisher, by CCC on publisher's behalf).

13. Objection to Contrary Terms: Publisher hereby objects to any terms contained in any purchase order, acknowledgment, check endorsement or other writing prepared by you, which terms are inconsistent with these terms and conditions or CCC's Billing and Payment terms and conditions. These terms and conditions, together with CCC's Billing and Payment terms and conditions (which are incorporated herein), comprise the entire agreement between you and publisher (and CCC) concerning this licensing transaction. In the event of any conflict between your obligations established by these terms and conditions and those established by CCC's Billing and Payment terms and conditions, these terms and conditions shall control.

14. Revocation: Elsevier or Copyright Clearance Center may deny the permissions described in this License at their sole discretion, for any reason or no reason, with a full refund payable to you. Notice of such denial will be made using the contact information provided by you. Failure to receive such notice will not alter or invalidate the denial. In no event will Elsevier or Copyright Clearance Center be responsible or liable for any costs, expenses or damage incurred by you as a result of a denial of your permission request, other than a refund of the amount(s) paid by you to Elsevier and/or Copyright Clearance Center for denied permissions.

LIMITED LICENSE

The following terms and conditions apply only to specific license types:

15. **Translation**: This permission is granted for non-exclusive world **English** rights only unless your license was granted for translation rights. If you licensed translation rights you may only translate this content into the languages you requested. A professional translator must perform all translations and reproduce the content word for word preserving the integrity of the article. If this license is to re-use 1 or 2 figures then permission is granted for non-exclusive world rights in all languages.

16. **Website**: The following terms and conditions apply to electronic reserve and author websites:
Electronic reserve: If licensed material is to be posted to website, the web site is to be password-protected and made available only to bona fide students registered on a relevant course if:
This license was made in connection with a course,
This permission is granted for 1 year only. You may obtain a license for future website posting,
All content posted to the web site must maintain the copyright information line on the bottom of each image,
A hyper-text must be included to the Homepage of the journal from which you are licensing at http://www.sciencedirect.com/science/journal/xxxxx or the Elsevier homepage for books at http://www.elsevier.com , and
Central Storage: This license does not include permission for a scanned version of the material to be stored in a central repository such as that provided by Heron/XanEdu.

17. **Author website** for journals with the following additional clauses:

All content posted to the web site must maintain the copyright information line on the bottom of each image, and
he permission granted is limited to the personal version of your paper. You are not allowed to download and post the published electronic version of your article (whether PDF or HTML, proof or final version), nor may you scan the printed edition to create an electronic version,
A hyper-text must be included to the Homepage of the journal from which you are licensing at http://www.sciencedirect.com/science/journal/xxxxx , As part of our normal production process, you will receive an e-mail notice when your article appears on Elsevier's online service ScienceDirect (www.sciencedirect.com). That e-mail will include the article's Digital Object Identifier (DOI). This number provides the electronic link to the published article and should be included in the posting of your personal version. We ask that you wait until you receive this e-mail and have the DOI to do any posting.
Central Storage: This license does not include permission for a scanned version of the material to be stored in a central repository such as that provided by Heron/XanEdu.

18. **Author website** for books with the following additional clauses:
Authors are permitted to place a brief summary of their work online only.
A hyper-text must be included to the Elsevier homepage at http://www.elsevier.com

All content posted to the web site must maintain the copyright information line on the bottom of each image
You are not allowed to download and post the published electronic version of your chapter, nor may you scan the printed edition to create an electronic version.
Central Storage: This license does not include permission for a scanned version of the material to be stored in a central repository such as that provided by Heron/XanEdu.

19. **Website** (regular and for author): A hyper-text must be included to the Homepage of the journal from which you are licensing at http://www.sciencedirect.com/science/journal/xxxxx. or for books to the Elsevier homepage at http://www.elsevier.com

20. **Thesis/Dissertation**: If your license is for use in a thesis/dissertation your thesis may be submitted to your institution in either print or electronic form. Should your thesis be published commercially, please reapply for permission. These requirements include permission for the Library and Archives of Canada to supply single copies, on demand, of the complete thesis and include permission for UMI to supply single copies, on demand, of the complete thesis. Should your thesis be published commercially, please reapply for permission.

21. **Other Conditions**: None

v1.6

Gratis licenses (referencing $0 in the Total field) are free. Please retain this printable license for your reference. No payment is required.

If you would like to pay for this license now, please remit this license along with your payment made payable to "COPYRIGHT CLEARANCE CENTER" otherwise you will be invoiced within 48 hours of the license date. Payment should be in the form of a check or money order referencing your account number and this invoice number RLNK10746080.
Once you receive your invoice for this order, you may pay your invoice by credit card. Please follow instructions provided at that time.

Make Payment To:
Copyright Clearance Center
Dept 001
P.O. Box 843006
Boston, MA 02284-3006

If you find copyrighted material related to this license will not be used and wish to cancel, please contact us referencing this license number 2383230069761 and noting the reason for cancellation.

Questions? **customercare@copyright.com** or +1-877-622-5543 (toll free in the US) or +1-978-646-2777.